DEGREE SUBCOMPLEXES OF AUTER SPACE AND RIBBON GRAPH COMPLEXES

A Dissertation

Presented to the Faculty of the Graduate School

of Cornell University

in Partial Fulfillment of the Requirements for the Degree of

Doctor of Philosophy

by

Bradley Todd Forrest

May 2009

DEGREE SUBCOMPLEXES OF AUTER SPACE AND RIBBON GRAPH COMPLEXES

Bradley Todd Forrest, Ph.D.

Cornell University 2009

The group $Aut(F_n)$ of automorphisms of a finitely generated free group acts properly and cocompactly on a simply-connected simplicial complex known as the degree 2 subcomplex of the spine of Auter space. In the first part of this thesis, we show that the degree 2 subcomplex contains a proper, invariant, simply-connected subcomplex κ, and use κ to simplify a finite presentation of $Aut(F_n)$ given by Armstrong, Forrest, and Vogtmann. Further, we prove that κ is contained in every $Aut(F_n)$-invariant simply-connected subcomplex of the degree 2 subcomplex.

The mapping class group $MCG_u^{\pm}(\Sigma)$ of an orientable, basepointed, punctured surface (Σ, u) acts properly and cocompactly on a simplicial complex known as $\mathfrak{R}_{(\Sigma,u)}$ the ribbon graph complex of (Σ, u). We define a filtration $\mathfrak{J}_0 \subset \mathfrak{J}_1 \subset \mathfrak{J}_2 \ldots$ on $\mathfrak{R}_{(\Sigma,u)}$ and prove that $\mathfrak{J}_i$ is i-dimensional and $(i-1)$-connected.

BIOGRAPHICAL SKETCH

Bradley Todd Forrest was born on September 12, 1980 in Falls Church, Virginia. He attended Harvey Mudd College in Claremont, California from August 1998 to May 2002, when he was awarded a B.S. in Mathematics and Physics. He entered the graduate program in Mathematics at Cornell University in August 2002. He married Melissa Kennish on April, 26, 2008. Bradley completed his Ph.D. in 2009 under the supervision of Dr. Karen Vogtmann.

This thesis is dedicated to my mother Joyce and father Richard, whose guidance and encouragement helped instill in me a life long love of learning, and my wife Melissa whose patience and support made this thesis possible.

ACKNOWLEDGEMENTS

First I would like to thank and acknowledge my advisor Karen Vogtmann for her guidance throughout my graduate studies. She patiently helped me learn about Geometric Group Theory, Auter space, and Outer space. Her ideas not only form the mathematical foundations of this thesis, but were also vital to solving specific challenges that arose in my research. Her suggestions were crucial in improving the mathematical language of this work. Without her this thesis would not have been possible.

I would also like to acknowledge my committee members Allen Hatcher and Ken Brown. Discussing the degree theorem with Allen made learning it a much easier task and Allen's textbook *Algebraic Topology* was a boon to my studies of the subject. Ken's leadership as the Chair of the Mathematics Department for my first few years at Cornell University helped provide stability for my graduate education, and later in my time at Cornell Ken gave me the opportunity to speak in the Topology and Geometric Group Theory Seminar for which he was the organizer.

My graduate education has not only focused on learning research level mathematics, but also on learning how to communicate mathematics. Maria Terrell played an essential role in helping me learn to communicate as an instructor. I thank and acknowledge Maria for the many enlightening and supportive conversations we had. I am grateful for my friend and mentor James Belk who not only assisted me in learning to verbally communicate mathematics in collaborative efforts but also helped me navigate the academic job market.

My friends have each played a unique role in keeping my morale high and helping me grow as a person. I would particularly like to thank Lance Curry and Michael Luther, Lance for his willingness to listen and wit and Michael for his humble perspective and kind heart. I would also like to thank Heather Armstrong,

Tim Goldberg, and Jonathan Needleman for their sympathetic ears.

Lastly and certainly not least I must thank my family. My parents Joyce and Richard have been steadfastly supportive of my educational goals for as long as I can remember, my debt to them for this is beyond measure. I would like to thank my siblings Brenda, Jeff, and Kelly for their loving support. My wife Melissa has been with me in every step of my graduate education, her caring and understanding have been crucial in helping me navigate the highs and lows of life as a graduate student. To her I humbly offer my gratitude.

TABLE OF CONTENTS

LIST OF FIGURES

CHAPTER 1

INTRODUCTION

Studying groups through examining their actions on well-chosen topological spaces is a classical technique that has helped to answer many challenging questions in group theory. This thesis focuses on two pairs of groups and topological spaces.

Chapters 2 through 8 investigate $Aut(F_n)$ the automorphism group of a finitely generated free group and its action on Auter space. More specifically, these chapters study the action of $Aut(F_n)$ on a simply-connected simplicial complex contained in Auter space called the degree 2 subcomplex. The degree subcomplexes were defined by Hatcher and Vogtmann in [7] and used to study the rational homology of $Aut(F_n)$. These subcomplexes are indexed by degree, let K_i be the degree i subcomplex. The degree subcomplexes act like "skeleta" for the spine of Auter space in that they form a filtration $K_0 \subset K_1 \subset \ldots \subset K_{2n-2} = K$ with K_i i-dimensional and $(i-1)$-connected for all i. $Aut(F_n)$ acts on K_i with finite stabilizer groups and a compact quotient that does not change as n increases for $n \geq 4$. In particular, K_2 is 1-connected, and Brown's method [4] can be used to find a presentation for $Aut(F_n)$. This was carried out in [2]. There are only seven 2-simplices in $K_2/Aut(F_n)$ so the resulting presentation has a small number of relations. Since $K_2/Aut(F_n)$ remains constant as n increases for $n \geq 4$, the only alterations to the presentation of $Aut(F_n)$ that occur as n increases in this range come from the increased size of the simplex stabilizers. These change only by the size of the signed symmetric groups W which occur in the stabilizers.

A natural question which arises at this point is whether there is any smaller simply-connected subcomplex of K_2. In chapters 3 through 8 we answer this question as follows. In chapter 3 a subcomplex $\kappa \subset K_2$ that is preserved under the

action of $Aut(F_n)$ is proved to be simply-connected. Applying the methods of [2] to κ gives a presentation with one fewer relation. The redundancy of the relation that was eliminated is proved algebraically in chapter 4. Chapter 5 presents a method to fill loops in K_2 that is used in chapters 6, 7, and 8 to prove that every simply-connected subcomplex of K_2 that is preserved under the action of $Aut(F_n)$ contains κ. In particular, this presentation of $Aut(F_n)$ cannot be simplified further by this method.

Chapters 9 and 10 investigate $MCG_u^{\pm}(\Sigma)$ the basepointed mapping class group of an orientable, punctured surface Σ with basepoint u. $MCG_u^{\pm}(\Sigma)$ is studied via its action on $\mathfrak{T}(\Sigma, u)$ the basepointed Teichmüller space of (Σ, u). The main result of these chapters is an analog of Hatcher and Vogtmann's Degree Theorem [7] for $\mathfrak{T}(\Sigma, u)$. Specifically, chapter 9 defines the degree subcomplexes of $\mathfrak{T}(\Sigma, u)$, which are denoted $\mathfrak{J}_i$ where i is the degree. In chapter 10, we prove that $\mathfrak{J}_i$ is i-dimensional and $(i-1)$-connected. This result is motivated by the results for $Aut(F_n)$ described above. However, applying the methods of Brown [4] to the action of $MCG_u^{\pm}(\Sigma)$ on $\mathfrak{J}_2$ is more challenging than in the $Aut(F_n)$ case as $\mathfrak{J}_2/MCG_u^{\pm}(\Sigma)$ grows arbitrarily large as the genus of Σ increases, and is a potential subject of future work.

CHAPTER 2

AUTER SPACE AND THE DEGREE 2 COMPLEX

In this chapter the definitions of Auter space, the spine of Auter space, and the degree subcomplexes of Auter space are given. Further, the results of Hatcher and Vogtmann in [7] and Armstrong, Forrest, and Vogtmann in [2] are stated briefly, and the relation of these results to this thesis is explained.

2.1 Auter Space and its Spine

Auter space is a contractible topological space on which $Aut(F_n)$ acts properly discontinuously with finite stabilizer groups. Auter space is a close cousin of Outer space, which was first defined by Culler and Vogtmann in [5] though the first definition of Auter space was given by Hatcher and Vogtmann in [7]. For more complete details on the following definitions, see those two sources.

All graphs used in the definitions in this chapter are basepointed, and all graph morphisms in the following definitions must send basepoints to basepoints. For the following definitions, fix a positive integer n.

Definition 1. *Let Γ be a connected finite graph with basepoint w. An isomorphism $g : F_n \to \pi_1(\Gamma, w)$ is called a* marking *of Γ. Two marked graphs Γ_1 and Γ_2 with markings g_1 and g_2 are* equivalent *if there exists a graph isomorphism $h : \Gamma_1 \to \Gamma_2$ with $h_* \circ g_1 = g_2$, where h_* is the map on the fundamental groups of Γ_1 and Γ_2 induced by h.*

Definition 2. *Let (Γ_1, g_1) and (Γ_2, g_2) be a marked graphs. (Γ_2, g_2) is obtained from (Γ_1, g_1) by a* forest collapse *if there exists a quotient map $q : \Gamma_1 \to \Gamma_2$ so that q collapses a forest in Γ_1 to a disjoint union of vertices in Γ_2 and is otherwise the*

identity map on Γ_1*, and* $q_* \circ g_1 = g_2$ *where* q_* *is the map on the fundamental groups of* Γ_1 *and* Γ_2 *induced by* q*.*

The set of equivalence classes of marked graphs is a poset where $(\Gamma_2, g_2) \leq (\Gamma_1, g_1)$ if (Γ_2, g_2) can be obtained from (Γ_1, g_1) by a forest collapse. Auter space is a union of open simplices where each open i-simplex in Auter space is given by an equivalence class of marked graphs with $i + 1$ edges, where all non-basepoint vertices in Γ are required to have valence at least 3 and the basepoint has valence at least 2. These faces glue together by the ordering described above, specifically the simplex corresponding to (Γ_2, g_2) is a face of the simplex corresponding to (Γ_1, g_1) if $(\Gamma_2, g_2) \leq (\Gamma_1, g_1)$. Often, the set of graphs is restricted further to exclude graphs with separating edges; the remaining graphs form a subspace of Auter space known as *reduced Auter space*.

Theorem 2.1.1 (Hatcher, Vogtmann [7]). *Auter space is contractible.*

Removing graphs with separating edges from the poset of marked graphs described above, the *spine of Auter space* is the geometric realization of this poset. Specifically, each vertex in the spine of Auter space corresponds to an open simplex in reduced Auter space. Two vertices are connected by an edge if one of their corresponding simplices is a face of the other, and for vertices v_1, v_2, ..., v_{i+1}, there is an i-simplex spanning these vertices if these vertices are pairwise connected by edges.

The spine of Auter space naturally embeds into Auter space by mapping each vertex in the spine to the barycenter of the corresponding open simplex. For each simplex Δ in the spine of Auter space, there is a unique simplex of minimal dimension in reduced Auter space whose closure contains the images of the 0-

dimensional faces of Δ. Letting the embedding be linear uniquely determines the image of Δ in this simplex of reduced Auter space.

Auter space deformation retracts onto the embedded image of the spine, and so the spine of Auter space is a contractible. $Aut(F_n)$ acts on the spine properly discontinuously, and cocompactly and with finite stabilizers, this action will be given below.

Let (Γ, g) be a marked graph representing an open simplex in reduced Auter space. One can describe the marking g by labeling certain edges of Γ as follows. Choose a maximal tree in Γ. The edges not in this maximal tree give a natural basis for $\pi_1(\Gamma, w)$. Orient each of these edges and label them by the inverse image of the basis element of $\pi_1(\Gamma, w)$ that passes through that edge with the correct orientation. Note that this labeling depends on the choice of maximal tree. For instance, fix generators $a_1, \ldots, a_n$ for the free group F_n with $\bar{a}_i$ the inverse of a_i, and note that the two graphs in figure 2.1 represent the same point in Auter space. In the Figures throughout this thesis the basepoint of a graph will be the bottommost vertex, and will often be darkened.

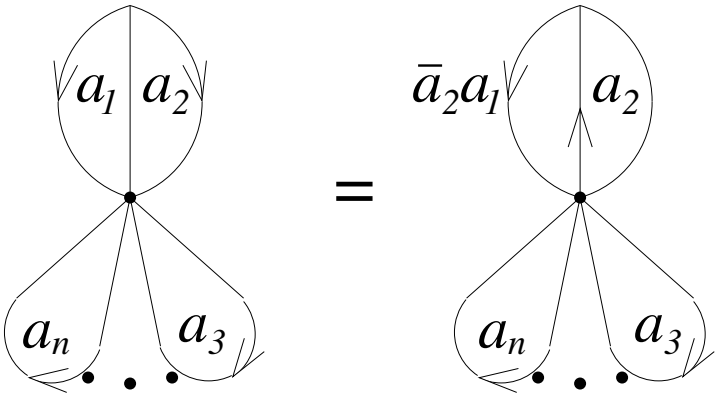

Figure 2.1: Two labelled graphs describing the same point in the spine of Auter space

Convention: Given $\alpha, \beta \in Aut(F_n)$, $\alpha\beta$ is the automorphism obtained by performing α and then by performing β, namely $\beta \circ \alpha$.

With the convention given above, $Aut(F_n)$ acts on Auter space simplicially on the left by $\alpha \cdot (g, \Gamma) = (g \circ \alpha, \Gamma)$. Another way to view this action is that $\alpha \cdot (g, \Gamma)$ is the open simplex corresponding to the labelled graph given by applying α^{-1} to the edges-labels determined by g. This action restricts to an action on the spine of Auter space.

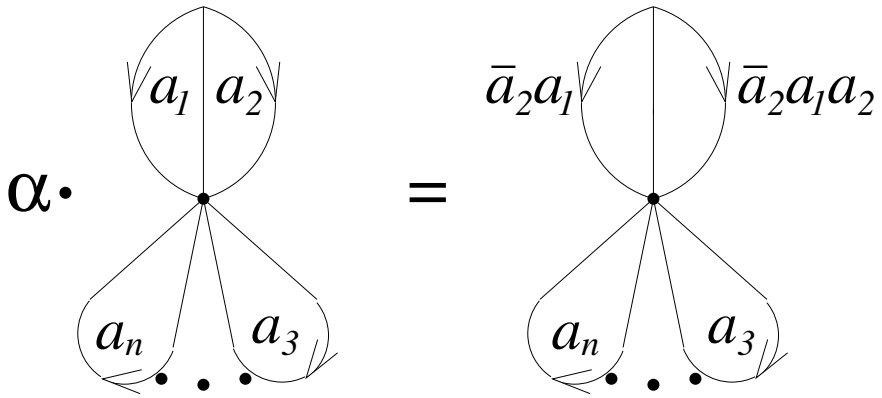

Figure 2.2: Example of the action of $Aut(F_n)$ on the spine of Auter space

Figure 2.2 shows the action of α on the graph from Figure 2.1, where α is the element:

$$\alpha\colon \begin{cases} a_1 \mapsto \bar{a}_1 a_2 a_1 \\ a_2 \mapsto \bar{a}_1 a_2 \\ a_k \mapsto a_k \qquad k > 2 \end{cases}$$

Note that the action of α on a homotopy marked graph alters the edge-labels

by α^{-1}.

$$\alpha^{-1}\colon \begin{cases} a_1 \mapsto \bar{a}_2 a_1 \\ a_2 \mapsto \bar{a}_2 a_1 a_2 \\ a_k \mapsto a_k \qquad k > 2 \end{cases}$$

Definition 3. *The* degree *of a finite connected graph* Γ *with basepoint* w *is*

$$Deg(\Gamma) = \sum_{x \neq w,\, x \in V\Gamma} |x| - 2,$$

where the sum is over all vertices $x \neq w$ *of* Γ *and* $|x|$ *denotes the valence of* x*.*

Graphs with low degree have most of their branching at the basepoint. The only graph of degree 0 is R_n, the graph with one vertex and n edges. R_n is called the *rose with n-petals*. The only graph of degree 1 is the graph with 2 vertices, 3 edges connecting those 2 vertices, and $n-2$ edges that are loops at the basepoint. This graph is called a *Nielsen graph* and the Nielsen graph with fundamental group F_n is denoted θ_n. For example, the underlying graph of the marked graph in Figure 2.1 is θ_4. There are 5 different graphs of degree 2, for $n \geq 4$. In this range, the only difference between the set of graphs of degree 2 or less for rank n and that set for rank $n+1$ is one additional loop that is incident only to the basepoint. A forest collapse cannot increase degree, so the vertices of degree at most i span a subcomplex of the spine.

Definition 4. (Hatcher-Vogtmann [7]) *The subcomplex of the spine of Auter space spanned by vertices of degree at most* i *is the* degree i subcomplex *of Auter space, and is denoted* K_i*.*

2.2 Applications of Degree Subcomplexes

In using the degree subcomplexes to study the rational homology of $Aut(F_n)$, Hatcher and Vogtmann proved that the degree complexes K_i are topologically well-behaved:

Degree Theorem 1. (Hatcher-Vogtmann [7]) *K_i is i-dimensional and $(i-1)$-connected.*

In particular, the degree subcomplexes behave like "skeleta" as $K_i \subset K_j$ for non-negative integers $j > i$. The subcomplex K_2 spanned by graphs of degree at most 2 is a simply-connected 2-dimensional simplicial complex. The quotient of K_2 by $Aut(F_4)$ is shown in Figures 2.3, 2.4, and 2.5. We will use the vertex, edge, and triangle labels given in these figures throughout this thesis. The quotients $K_2/Aut(F_n)$ are homeomorphic for all $n \geq 4$. The only alteration to Figures 2.3, 2.4, and 2.5 that is required to depict $K_2/Aut(F_n)$ for $n > 4$ is the addition of $n-4$ loops to the basepoint of each graph shown. The vertices of $K_2/Aut(F_n)$ are labeled $\mathsf{v}_0, \mathsf{v}_1, \ldots \mathsf{v}_6$, the edges are labeled $\mathsf{e}_0, \mathsf{e}_1, \ldots \mathsf{e}_{12}$, and the faces are labeled $\mathsf{f}_1, \mathsf{f}_2, \ldots, \mathsf{f}_7$. Capitalization denotes a representative in K_2 of a particular simplex in $K_2/Aut(F_n)$, V_i is a representative of v_i, E_i is representative of e_i, and F_i is a representative f_i for all i.

Let κ be the full subcomplex of K_2 spanned by all vertices (Γ, g) where Γ is not the underlying graph of v_2 or v_3. Denote the orbit of a subspace X of K_2 as $orbit(X)$, then κ is defined explicitly as $\kappa = \bigcup_{i=4}^{7} orbit(\mathsf{F}_i)$. The quotient of κ by $Aut(F_n)$ is shown in Figure 2.6.

In chapter 3 the following will be proved:

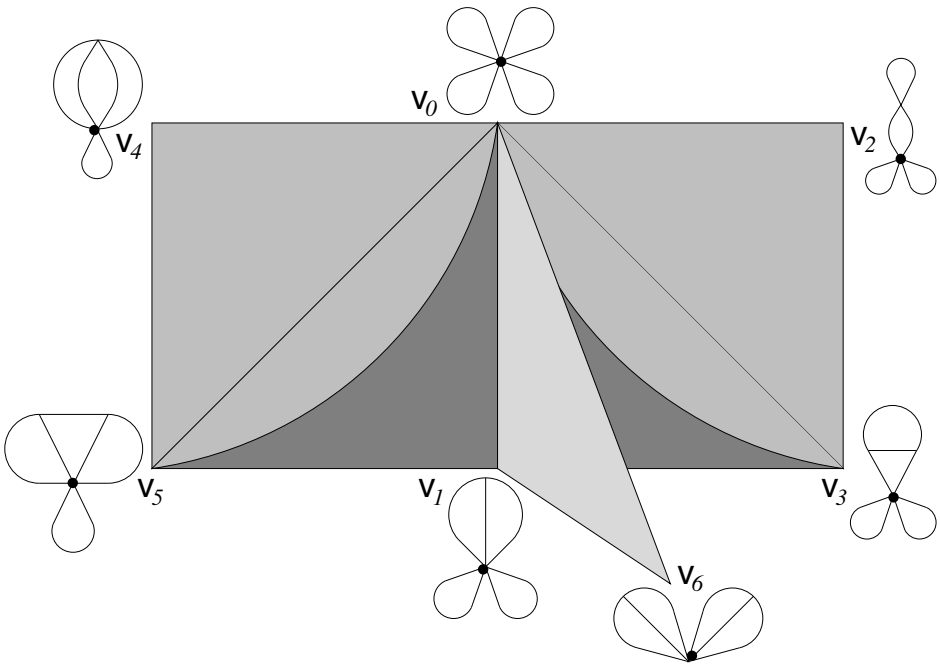

Figure 2.3: Vertices in $K_2/Aut(F_n)$

Theorem 2.2.1. *For $n \geq 3$, κ is simply connected.*

By considering the action of $Aut(F_n)$ on κ and applying the methods used in [2], the presentation given there is simplified by eliminating a relation. To describe the presentation, fix the following notation. Let W_n be the subgroup of $Aut(F_n)$ which permutes and inverts the generators. W_n is generated by the automorphisms τ_i, which inverts a_i and fixes all other a_k, and σ_{ij}, which interchanges a_i and a_j and fixes all other a_k. Let η be the order 2 automorphism shown below:

$$\eta\colon \begin{cases} a_1 \mapsto \bar{a}_2 a_1 \\ a_2 \mapsto \bar{a}_2 \\ a_k \mapsto a_k \qquad k > 2 \end{cases}$$

The only difference between the presentations below and those appearing in [2] is that the relation $((\eta\tau_1)^2\tau_2)^2 = 1$ is missing. This is a stabilizer relation from a

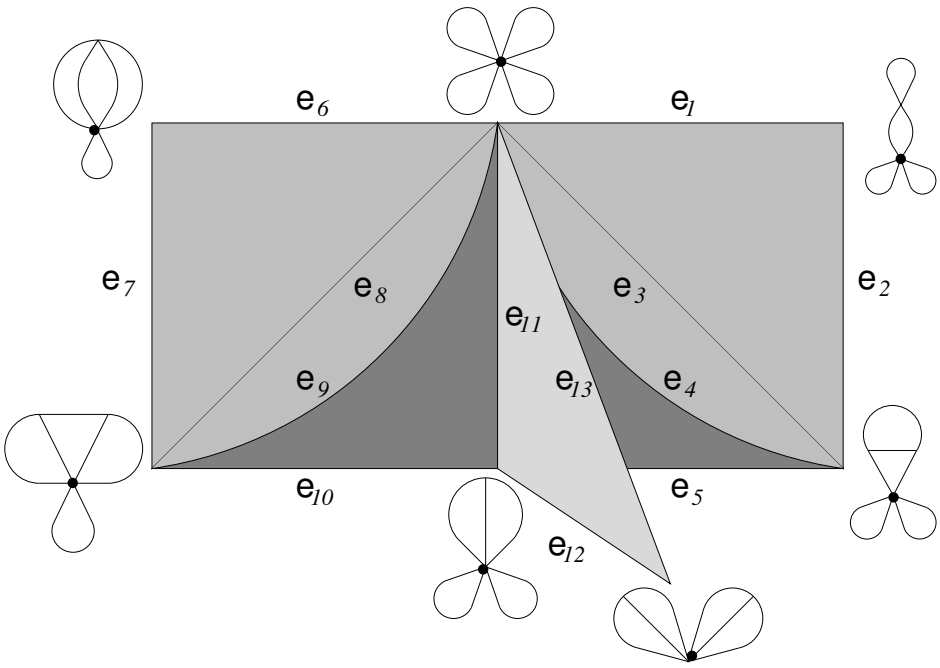

Figure 2.4: Edges in $K_2/Aut(F_n)$

representative of v_3 in K_2. Since κ is being used instead of K_2, representatives of v_3 are no longer considered. Applying the methods of [2] to κ gives the following presentation:

Theorem 2.2.2. *For $n \geq 4$, $Aut(F_n)$ is generated by W_n and η, subject to the following relations:*

1. $\eta^2 = 1$
2. $(\sigma_{12}\eta)^3 = 1$
3. $(\eta\tau_i)^2 = 1$ *for* $i > 2$
4. $(\eta\sigma_{ij})^2 = 1$ *for* $i, j > 2$
5. $(\sigma_{14}\sigma_{23}\eta)^4 = 1$
6. $(\eta\sigma_{13}\tau_2\eta\sigma_{12})^4 = 1$

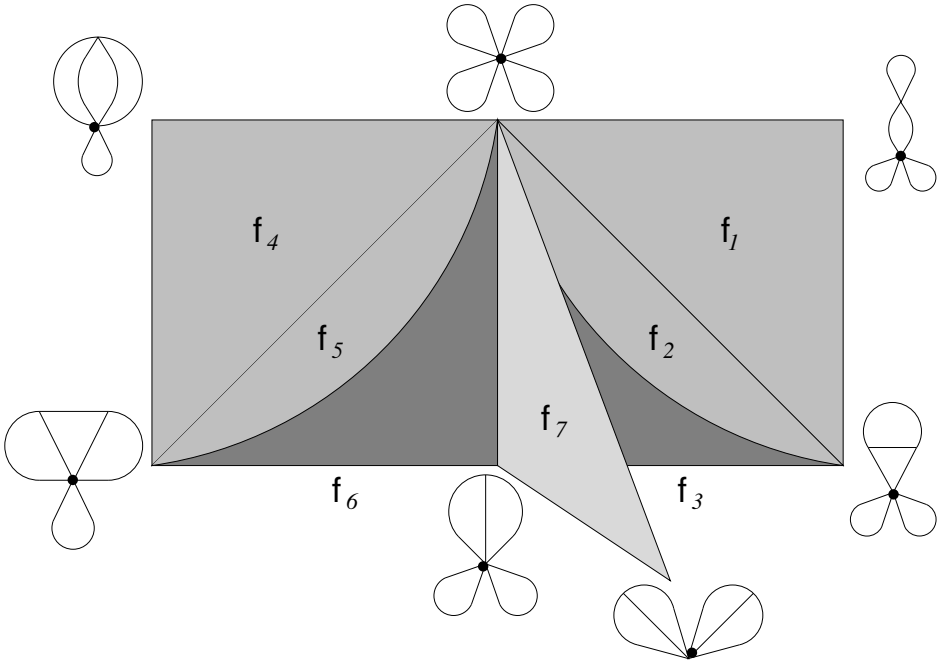

Figure 2.5: 2-Simplices in $K_2/Aut(F_n)$

7. $\sigma_{12}\eta\sigma_{13}\tau_2\eta\sigma_{12}(\sigma_{23}\eta\sigma_{13}\tau_2\eta)^2 = 1$

8. *relations in* W_n.

For $n = 3$, we obtain a presentation that differs only in that every relation involving indices greater than 3 is missing:

Theorem 2.2.3. *The group* $Aut(F_3)$ *is generated by* W_3 *and* η*, subject to the following relations:*

1. $\eta^2 = 1$

2. $(\sigma_{12}\eta)^3 = 1$

3. $(\eta\tau_3)^2 = 1$

4. $(\eta\sigma_{13}\tau_2\eta\sigma_{12})^4 = 1$

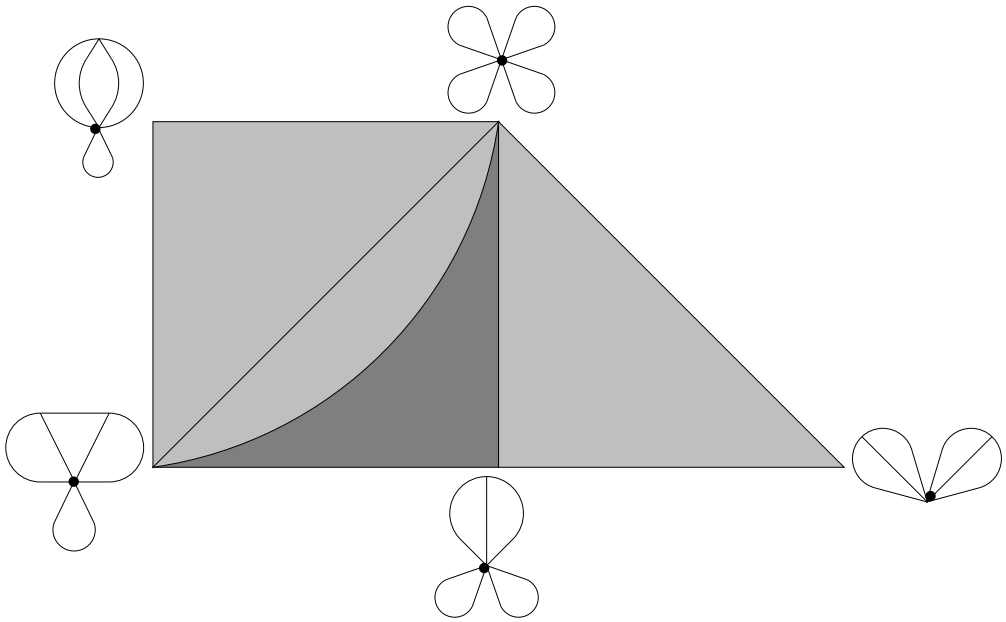

Figure 2.6: The quotient of κ by $Aut(F_n)$.

5. $\sigma_{12}\eta\sigma_{13}\tau_2\eta\sigma_{12}(\sigma_{23}\eta\sigma_{13}\tau_2\eta)^2 = 1$

6. *relations in* W_3.

These presentations have two defining properties. The first is that all of the generators have order 2. The second is that as n increases for $n \geq 4$, the only additional relations come from the increased rank of W_n.

While the proof of Theorem 2.2.1 is enough to establish these presentations by the methods used in [2], chapter 4 gives an explicit algebraic method to show that the relation $((\eta\tau_1)^2\tau_2)^2 = 1$ is implied by the relations in Theorem 2.2.2.

CHAPTER 3

TOPOLOGICAL CONSTRUCTIONS IN THE DEGREE SUBCOMPLEXES

In this chapter, definitions and properties of the degree subcomplexes are examined that will serve as the foundation for the results to follow. More specifically, section 1 develops notation and basic properties of the degree 1 subcomplex. Sections 2 and 3 explore different sets of subcomplexes which cover the degree 2 subcomplex. The subcomplexes defined in section 2 correspond to the Steinberg relations, and are called the *shingles* of K_2. In section 3 a set of subcomplexes is defined which cover K_2 and have disjoint interiors; elements of this cover are called the *tiles* of K_2. Section 4 uses these covers to prove that κ is simply-connected.

3.1 The Degree 1 Subcomplex

Here is a brief recounting of the basic properties of K_1.

1. K_1 is connected.
2. The vertices of K_1 are partitioned into two sets, vertices represented by points of the form (g, R_n) and vertices represented by points of the form (g, θ_n). The first of these is called the set of *rose vertices*, and the later is called the set of *Nielsen vertices*. Note that the set of rose vertices makes up the degree 0 subcomplex, K_0.
3. No two rose vertices are adjacent, and no two Nielsen vertices are adjacent. In particular, K_1 is bipartite. Edge paths in K_1 that begin and end at rose vertices are called *rose paths*. The *rose list* of an edge path is the list of rose vertices that the edge path passes through written in the order in which it

passes through them. If there is a length 2 rose path between two distinct roses, then this path is unique. So a rose list in which each subsequent pair of roses are connected by a non-backtracking length 2 rose path determines a rose path. These definitions can be generalized to loops by letting the initial and terminal roses be the same rose.

4. Each Nielsen vertex has valence 3 and each rose vertex has valence $4\binom{n}{2}$.

5. The action of $Aut(F_n)$ on K_1 preserves the partition on the vertices and acts transitively within the partitioned sets. Further, $Aut(F_n)$ acts transitively on the set of edges of K_1.

6. The smallest loops in K_1 have length 8. To see this check that the neighborhood of radius 3 about I is simply connected, where $I = (g_o, R_n)$ and $g_o : F_n \to \pi_1(R_n)$ takes a_i to a generator of the fundamental group of the i-th petal of R_n. Note that there are many possible choices for g_o, but all of them yield the same point in K_1. Since $Aut(F_n)$ acts transitively on rose vertices, this neighborhood establishes that there are no loops of length less than 8 in the entire space. An example of a length 8 loop is given in Figure 3.1.

3.2 Loops in the Degree 1 Subcomplex - Shingles

The degree 1 subcomplex has four classes of edges loops of length 8 and one class of loops of length 10 that will be studied in this section and throughout this thesis. These loops correspond to the Steinberg relations and in the next section we prove that these loops generate the fundamental group of K_1. In this section notation is fixed to aid in future discussion of these loops. Additionally, elementary fillings in K_2 of the loops are constructed. These fillings are combinatorial in that they are

given by combinatorial maps of D^2 equipped with a triangulation into K_2, where a map between simplicial complexes is *combinatorial* if it is simplicial and preserves the dimension of simplices. These fillings are not disjoint and do not give a tiling of K_2. The fillings will be referred to as shingles in K_2.

Before describing the shingles, some notation must be established. Let $S = \{a_1, \bar{a}_1, a_2, \bar{a}_2, \ldots, a_n, \bar{a}_n\}$. For $a, b \in S$ with $a \neq b, \bar{b}$, let E_{ab} be the Nielsen automorphism sending $a \mapsto ab$ and $c \mapsto c$ if $c \in S$, $c \neq a, \bar{a}$.

1. Let r_1 be the rose loop defined by the rose list I, $E_{a_1a_2} \cdot I$, $E_{a_1a_2}E_{a_3a_4} \cdot I$, $E_{a_1a_2}E_{a_3a_4}E_{a_1\bar{a}_2} \cdot I$, I. Additionally, let S_1 be the subcomplex of K_2 shown in Figure 3.1, and note that $r_1 : S^1 \to \partial S_1$. Figure 3.1 gives an explicit way to extend r_1 to a combinatorial bijection from D^2 to S_1. Let $Shin'_1 : D^2 \to S_1$ be this extension. S_1 will be referred to as shingle 1, and corresponds to the Steinberg relation $[E_{ab}, E_{cd}] = 1$.

2. Let r_2 be the rose loop defined by the rose list I, $E_{a_1a_2} \cdot I$, $E_{a_1a_2}E_{\bar{a}_1a_2} \cdot I$, $E_{a_1a_2}E_{\bar{a}_1a_2}E_{a_1\bar{a}_2} \cdot I$, I. Additionally, let S_2 be the subcomplex of K_2 shown in Figure 3.2, and note that $r_2 : S^1 \to \partial S_2$. Figure 3.2 gives an explicit way to extend r_2 to a combinatorial bijection from D^2 to S_2. Let $Shin'_2 : D^2 \to S_2$ be this extension. S_2 will be referred to as shingle 2, and corresponds to the Steinberg relation $[E_{ab}, E_{\bar{a}b}] = 1$.

3. Let r_3 be the rose loop defined by the rose list I, $E_{a_1a_2} \cdot I$, $E_{a_1a_2}E_{\bar{a}_1a_3} \cdot I$, $E_{a_1a_2}E_{\bar{a}_1a_3}E_{a_1\bar{a}_2} \cdot I$, I. Let S_3 be the subcomplex of K_2 shown in Figure 3.3, and note that $r_3 : S^1 \to \partial S_3$. Figure 3.3 gives an explicit way to extend r_3 to a combinatorial bijection from D^2 to S_3. Let $Shin'_3 : D^2 \to S_3$ be this extension. S_3 will be referred to as shingle 3, and corresponds to the Steinberg relation $[E_{ab}, E_{\bar{a}c}] = 1$.

4. Let r_4 be the rose loop defined by the rose list I, $E_{a_1a_2} \cdot I$, $E_{a_1a_2}E_{a_2a_3} \cdot I$, $E_{a_1a_2}E_{a_2a_3}E_{a_1\bar{a}_3} \cdot I$, $E_{a_1a_2}E_{a_2a_3}E_{a_1\bar{a}_3}E_{a_2\bar{a}_3} \cdot I$, I. Let S_4 be the subcomplex of K_2 shown in Figure 3.4, and note that $r_4 : S^1 \rightarrow \partial S_4$. Figure 3.4 gives an explicit way to extend r_4 to a combinatorial bijection from D^2 to S_4. Let $Shin'_4 : D^2 \rightarrow S_4$ be this extension. S_4 will be referred to as shingle 4, and corresponds to the Steinberg relation $[E_{ab}, E_{bc}] = E_{ac}$.

5. Let r_5 be the rose loop defined by the rose list I, $E_{a_1a_3} \cdot I$, $E_{a_1a_3}E_{a_2a_3} \cdot I$, $E_{a_1a_3}E_{a_2a_3}E_{a_1\bar{a}_3} \cdot I$, I. Let S_5 be the subcomplex of K_2 shown in Figure 3.5, and note that $r_5 : S^1 \rightarrow \partial S_5$. Figure 3.5 gives an explicit way to extend r_5 to a combinatorial bijection from D^2 to S_5. Let $Shin'_5 : D^2 \rightarrow S_5$ be this extension. S_5 will be referred to as shingle 5, and corresponds to the Steinberg relation $[E_{ac}, E_{bc}] = 1$.

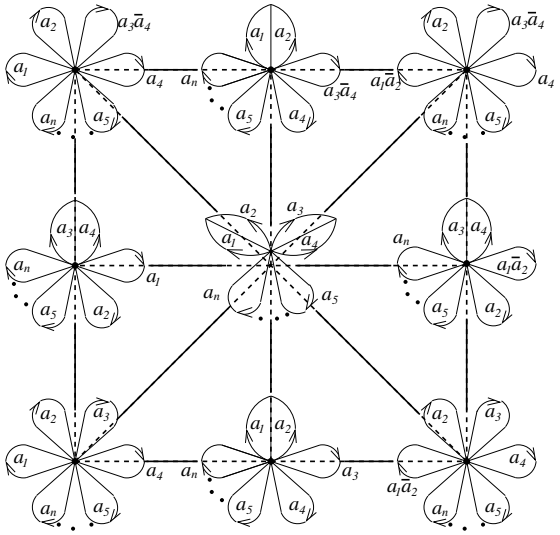

Figure 3.1: Shingle 1, the subcomplex S_1 of K_2

Even more generally, consider the map $Shin_i : Aut(F_n) \times D^2 \rightarrow K_2$ defined by the rule $Shin_i(\alpha, x) = \alpha \cdot Shin'_i(x)$. $Shin_i$ takes the α cross-section of $Aut(F_n) \times D^2$ to $\alpha \cdot S_i$.

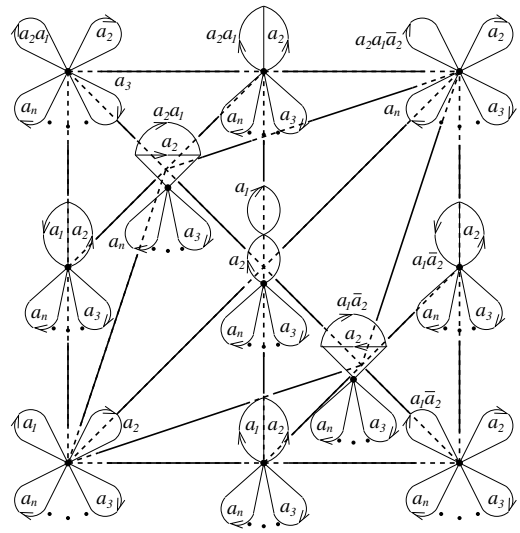

Figure 3.2: Shingle 2, the subcomplex S_2 of K_2

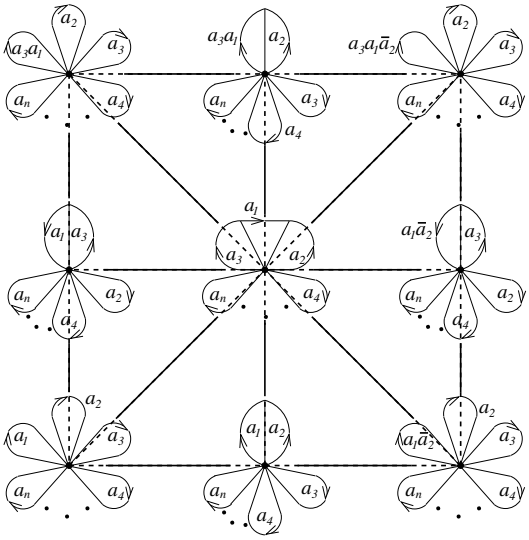

Figure 3.3: Shingle 3, the subcomplex S_3 of K_2

For fixed m and α a rose basepoint and orientation on $Shin_m(\alpha)|_{\partial D^2}$ yields a rose path. Specifically, selecting $Shin_m(\alpha)^{-1}(\alpha \cdot I) = v$ as the rose basepoint and the counter-clockwise orientation relative to Figures 3.1, 3.2, 3.3, 3.4, and 3.5 yields the rose paths listed earlier in this section.

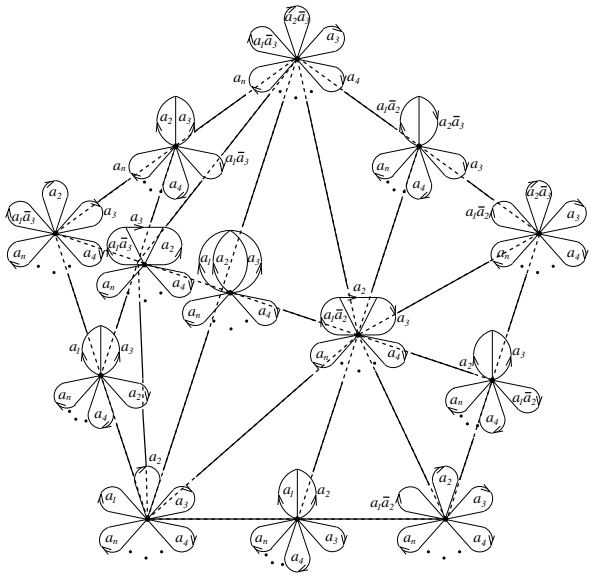

Figure 3.4: Shingle 4, the subcomplex S_4 of K_2

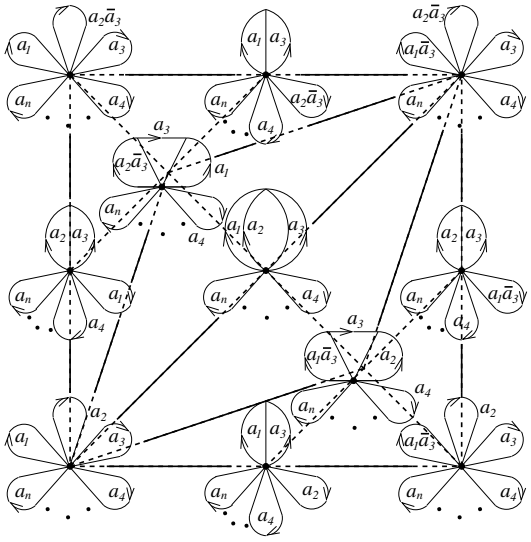

Figure 3.5: Shingle 5, the subcomplex S_5 of K_2

3.3 The Degree 2 Subcomplex - Tiles

While the shingles do not provide a tiling of K_2, the components of $K_2 \setminus K_1$ do. The connected components of $K_2 \setminus K_1$ have one of three forms that will be referred

to as tiles.

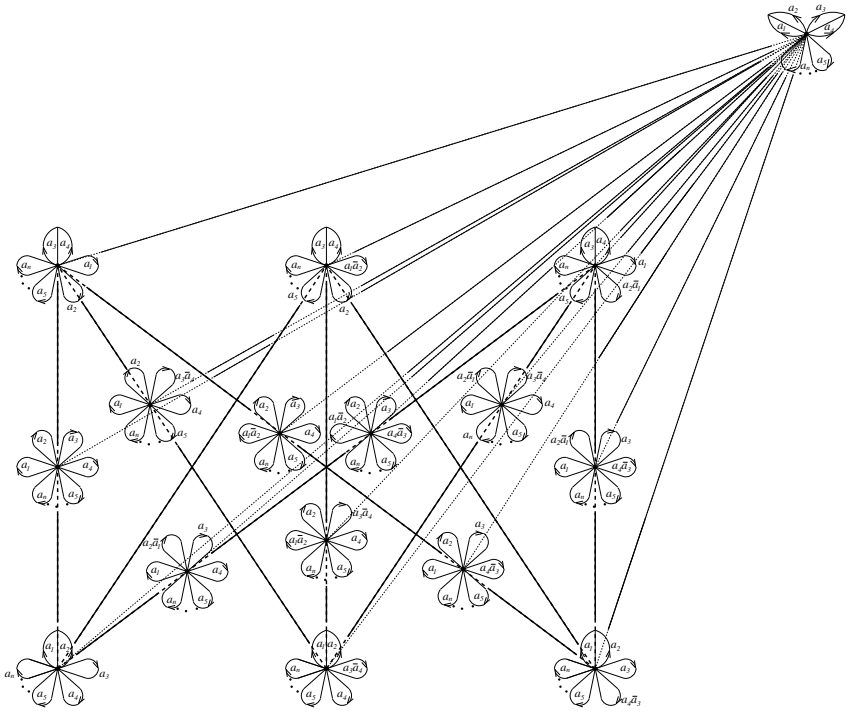

Figure 3.6: Tile 1, the subcomplex T_1 of K_2

1. Let T_1 be the subcomplex of K_2 shown in Figure 3.6, and call this subcomplex tile 1. S_1 is a subcomplex of T_1, and ∂T_1 is isometric to the bipartite graph on two sets of three vertices making T_1 is isometric to the cone on this graph. More specifically, $\pi_1(\partial T_1)$ is isomorphic F_4, and the generators of $\pi_1(\partial T_1)$ are the boundaries of translates of shingle 1 contained in T_1. The darkened edges in Figure 3.6 are ∂T_1. Note that the only shingles contained in T_1 are translates of shingle 1.

2. Let T_2 be the subcomplex of K_2 shown in Figure 3.7, and call this subcomplex tile 2. $\tau_2 \cdot S_2$ is a subcomplex of T_2, and ∂T_2 is isometric an infinite ladder. More specifically, $\pi_1(\partial T_2)$ is isomorphic F_∞. The generators $\pi_1(\partial T_2)$ are boundaries of translates of shingle 2 that are contained in T_2. The darkened

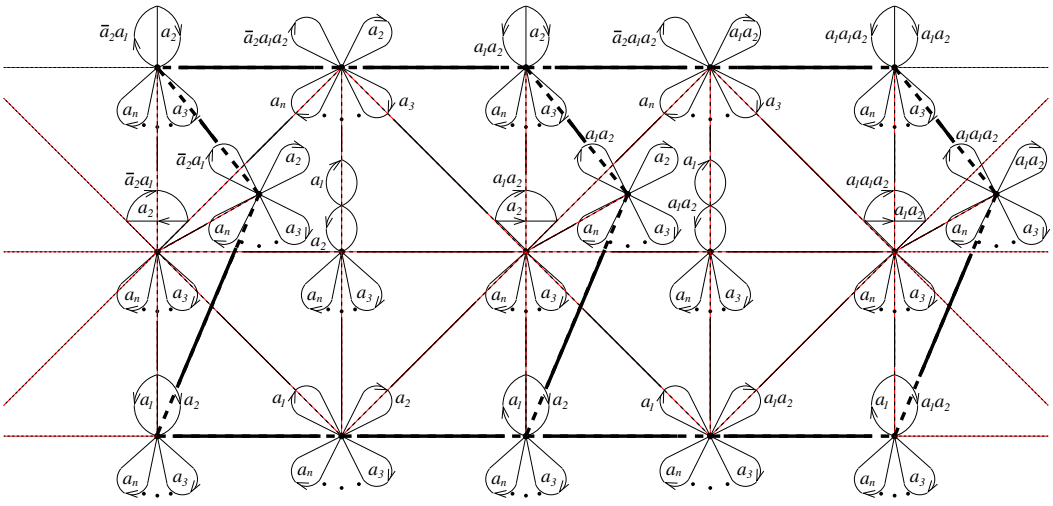

Figure 3.7: Tile 2, the subcomplex T_2 of K_2

edges in Figure 3.7 are ∂T_2. Note that the only shingles contained in T_2 are translates of S_2.

3. Let T_3 be the subcomplex of K_2 shown in Figure 3.8 and call this subcomplex tile 3. In the figure, all edges labeled i are identified for $1 \leq i \leq 4$. $\tau_3 \cdot S_3$, $\tau_3 E_{a_2 a_1} \cdot S_4$, and $\sigma_{12}\sigma_{23}\tau_2 E_{a_2 \bar{a}_3} \cdot S_5$ are subcomplexes of T_3. Note that $\pi_1(\partial T_3)$ is isomorphic F_9, where three of the generators are boundaries of translates of shingle 3 that are contained in T_3 and the other six generators are the boundaries of translates of shingle 4 contained in T_3. This implies that the boundary of S_5 can be filled by only considering translates of S_3 and S_4, a fact that will be discussed further in chapter 5. The darkened edges in Figure 3.8 are ∂T_3. Note that the only shingles that are contained in T_3 are translates of S_3, S_4, and S_5.

Let T and T' be $Aut(F_n)$ translates of these tiles. Then if $T \neq T'$, $T \cap T' \subset K_1$. In this sense, $Aut(F_n)$ translates of T_1, T_2, and T_3 tile K_2.

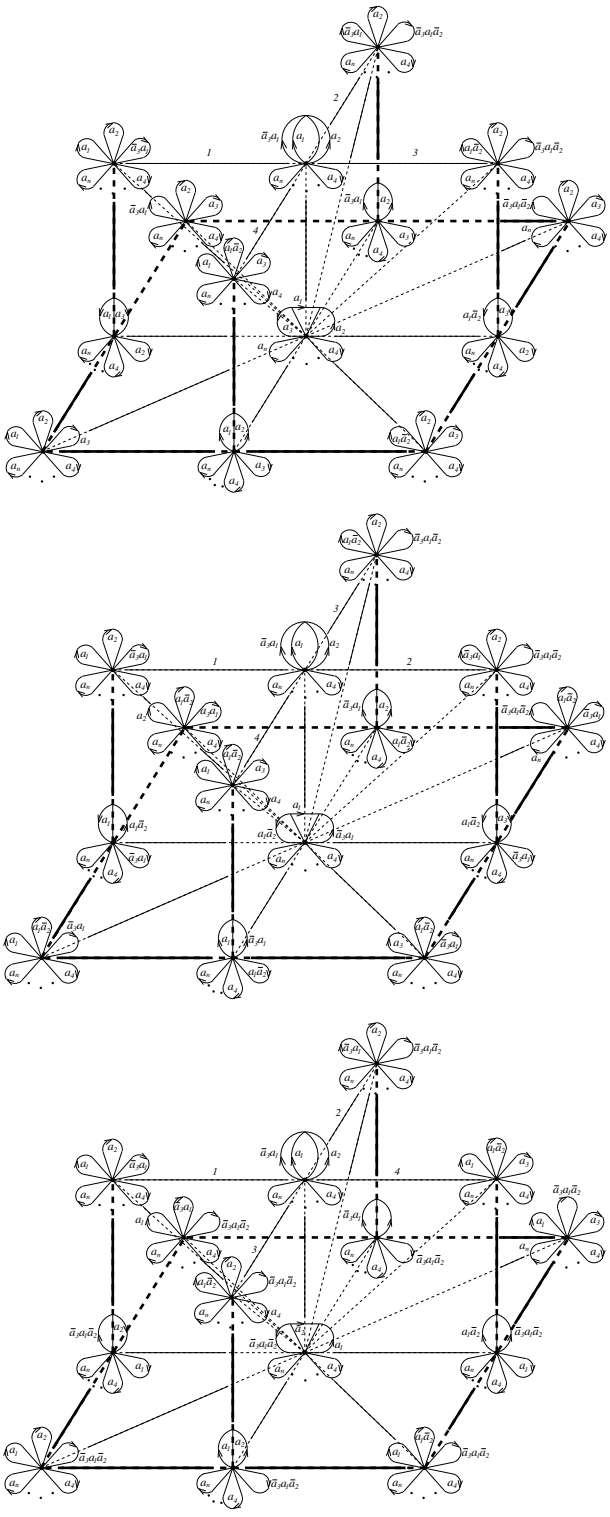

Figure 3.8: Tile 3, the subcomplex T_3 of K_2

The discussion above has provided all of the pieces to prove the following proposition:

Proposition 3.3.1. *Consider an $Aut(F_n)$ translate of a tile, $\alpha \cdot T_m$, for some α and some m. $\pi_1(\partial(\alpha \cdot T_m))$ is generated by the boundaries of the $Aut(F_n)$ translates of the shingles contained in $\alpha \cdot T_m$.*

Proof. Taking the tiles one-by-one:

$m = 1$ Since $\pi_1(\partial T_1)$ is generated by the boundaries of the translates of S_1 contained in T_1, acting α on these shingles gives a generating set for $\pi_1(\partial(\alpha \cdot T_1))$.

$m = 2$ Since $\pi_1(\partial T_2)$ is generated by the boundaries of the translates of S_2 contained in T_2, acting α on these shingles gives a generating set for $\pi_1(\partial(\alpha \cdot T_2))$.

$m = 3$ Since $\pi_1(\partial T_3)$ is generated by the boundaries of the translates of S_3 and S_4 contained in T_3, acting α on these shingles gives a generating set for $\pi_1(\partial(\alpha \cdot T_3))$.

□

3.4 κ is Simply-Connected

The main result of this section is that κ is simply-connected. This is accomplished by defining a retraction $R : K_2 \to \kappa$, and noting that this implies that map $i_* : \pi_1(\kappa) \to \pi_1(K_2)$ induced on the fundamental groups by inclusion is injective. Since K_2 is simply-connected, this implies that κ is also simply-connected.

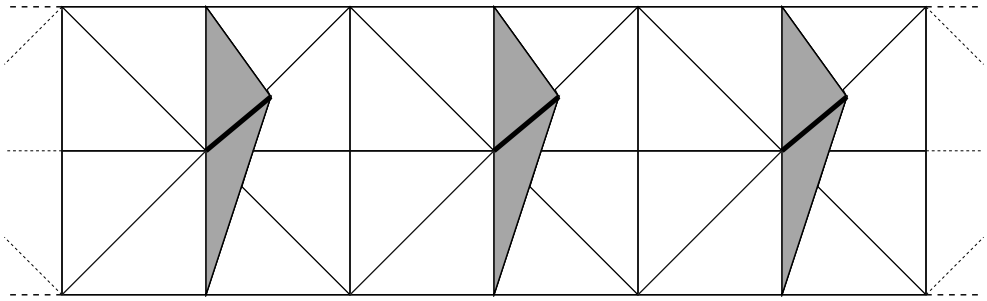

Figure 3.9: Simplices in $orbit(T_2^o)$ collapsed by R

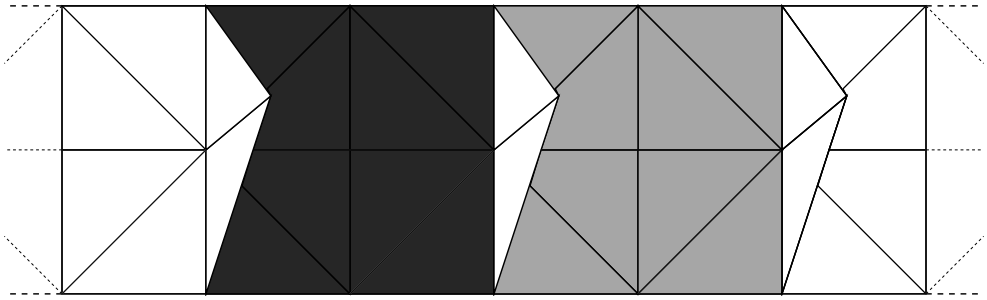

Figure 3.10: Simplices in $orbit(T_2^o)$ mapped to translates of S_0 by R

Proof of Theorem 2.2.1. The retraction $R : K_2 \to \kappa$ is defined as follows, let R be the identity on κ. Note that $K_2 \setminus \kappa = orbit(T_2^o)$ where T_2^o denotes the interior of T_2^o, and hence we have left to define R on these points. Figure 3.9 depicts an arbitrary translate of T_2. Consider the darkened simplices in Figure 3.9, and note that these simplices are translates of F_3. Each of these simplices contains a unique edge in K_1, and the retraction collapses each of these simplices linearly onto this edge in the unique way that takes the darkened edge to the vertex in K_0 to which it is incident.

The remaining simplices in $orbit(T_2^o)$ are partitioned into squares whose boundary maps to the boundary of a translate of S_2 under R. The shaded simplices in Figure 3.10 are two such squares. R takes the square whose boundary maps to

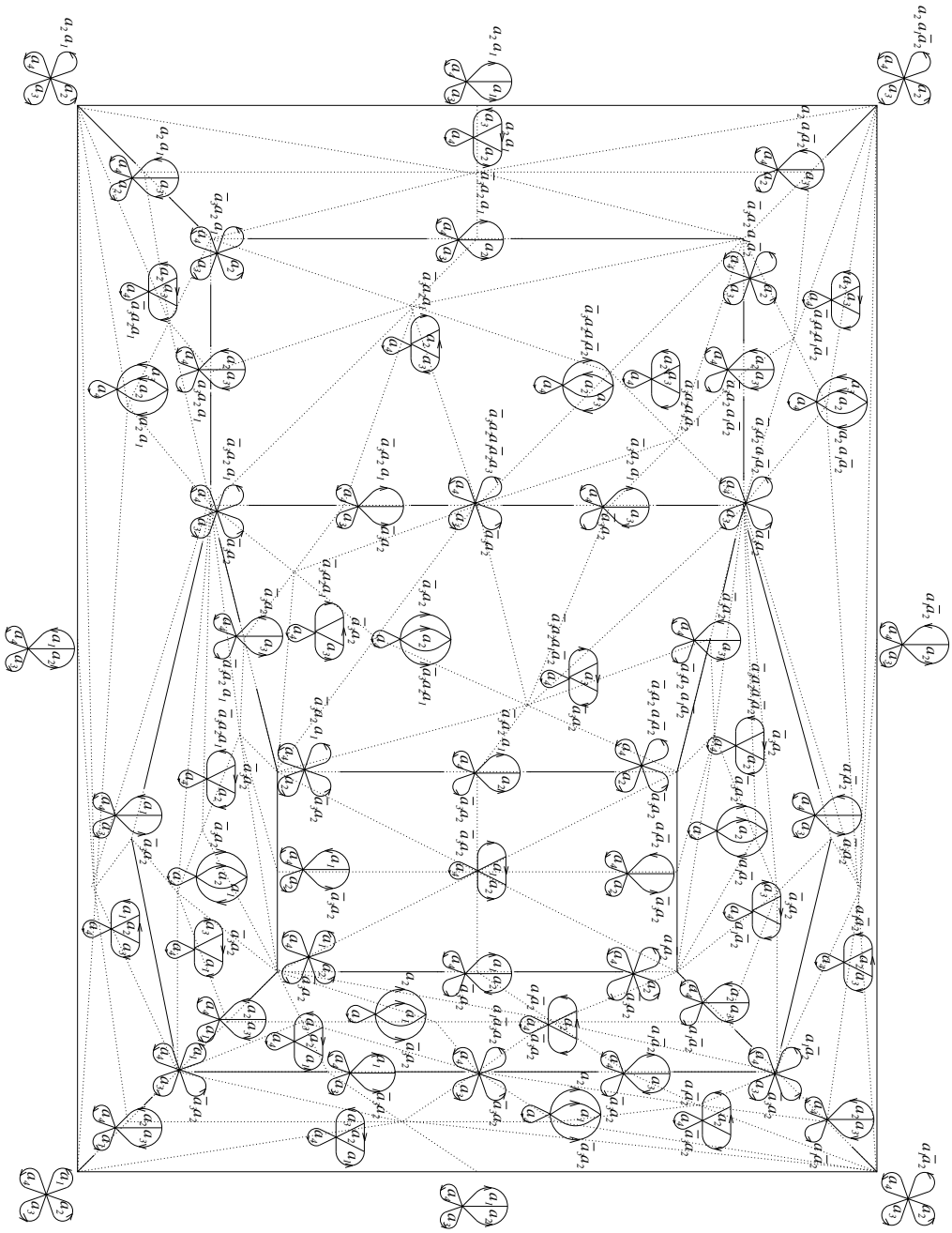

Figure 3.11: Subcomplex S_0 of κ

$\partial(\alpha \cdot S_2)$ to $\alpha \cdot S_0$, where S_0 is the subcomplex of κ shown in Figure 3.11. Figure 3.11 shows S_0 in the case of $n = 4$, though this complex can be defined for each $n \geq 3$. For $n \geq 4$, add $n - 4$ loops at the basepoint, and for $n = 3$ remove each

loop at the boasepoint that maps to a_4. With this definition, R is a retraction of K_2 to κ and κ is simply-connected. $\square$

CHAPTER 4

PRESENTATION

By Theorem 2.2.1, the methods of [2] can be applied to κ to produce the presentations in Theorems 2.2.2 and 2.2.3. These presentations differ from the presentations given in [2] only in that the relation $((\eta\tau_1)^2\tau_2)^2 = 1$ is removed. In this section Figure 3.11 is used to show that the relation $((\eta\tau_1)^2\tau_2)^2 = 1$ is redundant. The figure gives an explicit algebraic method to write $((\eta\tau_1)^2\tau_2)^2 = 1$ in terms of the other relations and verifies Theorems 2.2.2 and 2.2.3.

4.1 Gersten's Presentation

The main idea in using the subcomplex S_0 Figure 3.11 to show that the relation $((\eta\tau_1)^2\tau_2)^2 = 1$ is redundant is to lift $S_0 \cap K_1$ to the Cayley 2-complex of $Aut(F_n)$ given by the presentations in Theorems 2.2.2 and 2.2.3. As a convenient stepping stone, we first lift $S_0 \cap K_1$ to the Cayley 2-complex of $SAut(F_n)$, the subgroup of automorphisms of a free group with determinant one, associated to a presentation of Gersten shown below[6]. This presentation is used because it is generated by Nielsen automorphisms which correspond to length 2 rose paths.

Fix $n \geq 3$ and recall that $S = \{a_1, \bar{a}_1, a_2, \bar{a}_2 \ldots, a_n, \bar{a}_n\}$ and for $a, b \in S$ with $a \neq b, \bar{b}$, E_{ab} is the automorphism taking $a \mapsto ab$ and $c \mapsto c$ for all $c \in S$ where $c \neq a, \bar{a}$.

Theorem 4.1.1. (Gersten [6]) *For $n \geq 3$, $SAut(F_n)$ is generated by the Nielsen automorphisms, subject to the following types of relations:*

1. $E_{ab}^{-1} = E_{a\bar{b}}$ *for all* $a, b \in S$,

2. $[E_{ab}, E_{cd}] = 1$ *for all* $a, b, c, d \in S$ *with* $a \neq c, d, \bar{d}$ *and* $b \neq c, \bar{c}$,

3. $[E_{ab}, E_{bc}] = E_{ac}$ *for all* $a, b, c \in S$ *with* $a \neq c, \bar{c}$,

4. $w_{ab} = w_{\bar{a}\bar{b}}$ *where* $w_{ab} = E_{ba}E_{\bar{a}b}E_{\bar{b}\bar{a}}$ *for all* $a, b \in S$, *and*

5. $w_{ab}^4 = 1$ *for all* $a, b \in S$.

Let Y be the Cayley 2-complex of $SAut(F_n)$ associated to this presentation. The goal of the remainder of this section is to define an explicit map from the 1-skeleton Y^1 of Y to K_1. This map is not a covering map, but does enjoy some lifting properties. $SAut(F_n)$ is a subgroup of $Aut(F_n)$, $SAut(F_n)$ also acts on K_2. Since $Aut(F_n)$ is quasi-isometric to Y and $SAut(F_n)$ has index 2 in $Aut(F_n)$, K_2 is quasi-isometric to Y. Choosing a point $x \in K_2$ and mapping $\alpha \in SAut(F_n)$ to $\alpha \cdot x$ is the restriction to the 0-cells of Y of a quasi-isometry. Choosing $I = x$ is the first step in building the map $\Phi : Y^1 \to K_1$ that will discussed in this section. This map is defined as follows.

For $\alpha \in Y^0$, $\Phi(\alpha) = \alpha \cdot I$. Note that by this definition, Φ is equivariant with respect to the action of $SAut(F_n)$.

Let $\epsilon_{ab} \in Y^1$ be the edge from id to E_{ab} where id is the identity automorphism, and e_{ab} be the unique length 2 rose path from I to $E_{ab} \cdot I$. Let Φ map the barycentric subdivision of ϵ_{ab} combinatorially to e_{ab} in the unique way that agrees with the image of the endpoints of ϵ_{ab}. For $\epsilon \in Y^1$ incident to $\alpha, \beta \in Y^0$, note that $\epsilon = \alpha \cdot \epsilon_{ab}$ for some a and b. Let $\Phi(\epsilon) = \alpha \cdot e_{ab}$, and note that this is well defined. If $\beta = \alpha E_{ab}$ is chosen instead of α, $\epsilon = \beta \cdot \epsilon_{a\bar{b}}$, so $\Phi(\epsilon) = \beta \cdot e_{a\bar{b}} = \alpha E_{ab} \cdot e_{a\bar{b}} = \alpha \cdot e_{ab}$. Φ is equivariant with respect to the action of $SAut(F_n)$ by definition.

This completes the definition of $\Phi : Y \to K_1$. This map has some useful properties. Note that $\Phi(Y^1) = K_1$, as $\Phi(Y^1) \subseteq K_1$ by the definition. To see

that $K_1 \subseteq \Phi(Y^1)$ note that each $e \in K_1$ is part of at least two different length 2 rose paths, and that every length 2 rose path can be written as $\alpha \cdot e_{ab}$ for some $\alpha \in SAut(F_n)$ and some a and b, so $e \subset \Phi(\alpha \cdot \epsilon_{ab})$. We can assume that $\alpha \in SAut(F_n)$ because if it is not α can be precomposed with an element with determinant -1 from W_n, the stabilizer of I.

Φ is not a covering map, though rose paths lift to paths.

Proposition 4.1.1. *Let p be a non-backtracking length 2 rose path in K_1 starting at (g_1, R_n) traveling through (g_2, θ_n) and ending at (g_3, R_n). Given $\alpha \in SAut(F_n)$ with $\Phi(\alpha) = (g, R_n)$, there exists a unique edge ϵ incident to α so that $\Phi(\epsilon) = p$.*

Proof. Let $st(I)$ denote the star of I and note that $(\alpha^{-1} \cdot p) \cap st(I)$ is a length 1 path that has the form shown in Figure 4.1 for some $a, b, c_1, c_2, \ldots c_{n-2} \in S$. Hence, $\alpha^{-1} \cdot (g_3, R_n) = E_{ab} \cdot I$ or $E_{ba} \cdot I$, without loss of generality assume the former. Since Φ restricted to the Nielsen generators is injective, this description of $\alpha^{-1} \cdot (g_3, R_n)$ is unique, and $\epsilon = \alpha \cdot \epsilon_{ab}$ is the unique edge emanating from α that maps to p. □

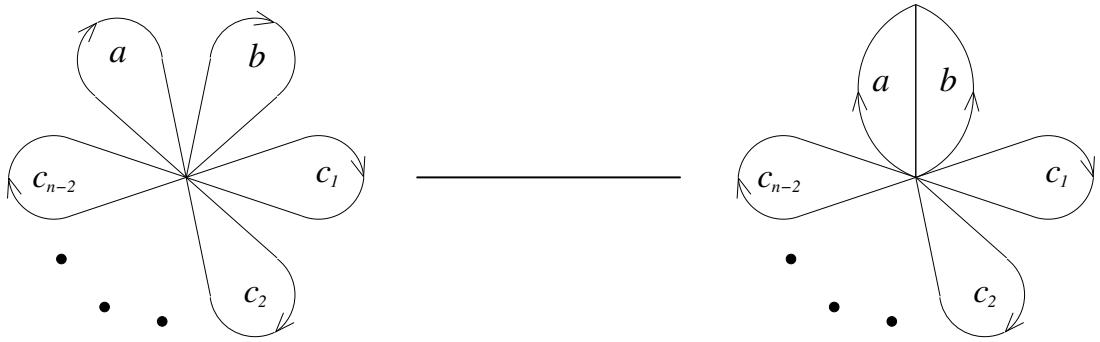

Figure 4.1: Length 1 path in $st(I)$

Note that by definition, the boundary of each shingle lifts to a loop traversing the boundary of a 2-cell in Y.

4.2 Loops in Figure 4.2

Since $SAut(F_n)$ is a subgroup of $Aut(F_n)$, Y maps quasi-isometrically into the Cayley 2-complex of $Aut(F_n)$ associated to the presentation in [2], where this map is inclusion on the 0-cells of Y. Note that writing each generator of $SAut(F_n)$ in terms of the generators in $Aut(F_n)$ defines a map of Y^1 into the 1-skeleton of the Cayley 2-complex of $Aut(F_n)$.

In this section, we show that $S_0 \cap K_1$ can be lifted to Y^1, and that the image of the 1-skeleton of this lift can be filled in the subcomplex of the Cayley 2-complex of $Aut(F_n)$ given by [2] that corresponds to the presentations in Theorems 2.2.2 and 2.2.3. The boundary of the image of S_0 in the Cayley 2-complex of $Aut(F_n)$ bounds a 2-cell corresponding to $((\eta\tau_1)^2\tau_2)^2 = 1$, proving Theorems 2.2.2 and 2.2.3.

Figure 4.2 enumerates loops traversing the boundaries of the shingles in S_0. For each of these loops, we lift the loop to Y as follows:

1. l_1 lifts to the path $E_{\bar{a}_2\bar{a}_3}E_{a_1a_2}([E_{a_1\bar{a}_2}, E_{\bar{a}_2a_3}]E_{a_1,\bar{a}_3})E_{a_1\bar{a}_2}E_{\bar{a}_2a_3}$.
2. l_2 lifts to the path $E_{a_1a_2}(E_{a_1a_3}[E_{a_3\bar{a}_2}, E_{a_1\bar{a}_3}])E_{a_1\bar{a}_2}$.
3. l_3 lifts to the path $E_{\bar{a}_1a_2}([E_{\bar{a}_1\bar{a}_2}, E_{\bar{a}_2a_3}]E_{\bar{a}_1\bar{a}_3}[E_{\bar{a}_1a_3}, E_{\bar{a}_2a_3}])E_{\bar{a}_1\bar{a}_2}$.
4. l_4 lifts to the path $E_{\bar{a}_1a_2}[E_{a_3\bar{a}_2}, E_{\bar{a}_1\bar{a}_2}]E_{\bar{a}_1\bar{a}_2}$.
5. l_5 lifts to the path $[E_{\bar{a}_1a_2}, E_{a_1\bar{a}_3}]$.
6. l_6 lifts to the path $[E_{\bar{a}_1a_2}, E_{a_3a_2}]$.
7. l_7 lifts to the path $E_{a_3\bar{a}_2}([E_{a_1a_3}, E_{a_3a_2}]E_{a_1\bar{a}_2}[E_{a_1a_2}, E_{a_3a_2}])E_{a_3a_2}$.
8. l_8 lifts to the path $E_{a_1a_2}E_{a_1a_3}E_{\bar{a}_2a_3}([E_{a_1\bar{a}_2}, E_{\bar{a}_2\bar{a}_3}]E_{a_1a_3}[E_{a_1\bar{a}_3}, E_{\bar{a}_2\bar{a}_3}])E_{\bar{a}_2\bar{a}_3}E_{a_1\bar{a}_3}$ $E_{a_1\bar{a}_2}$.

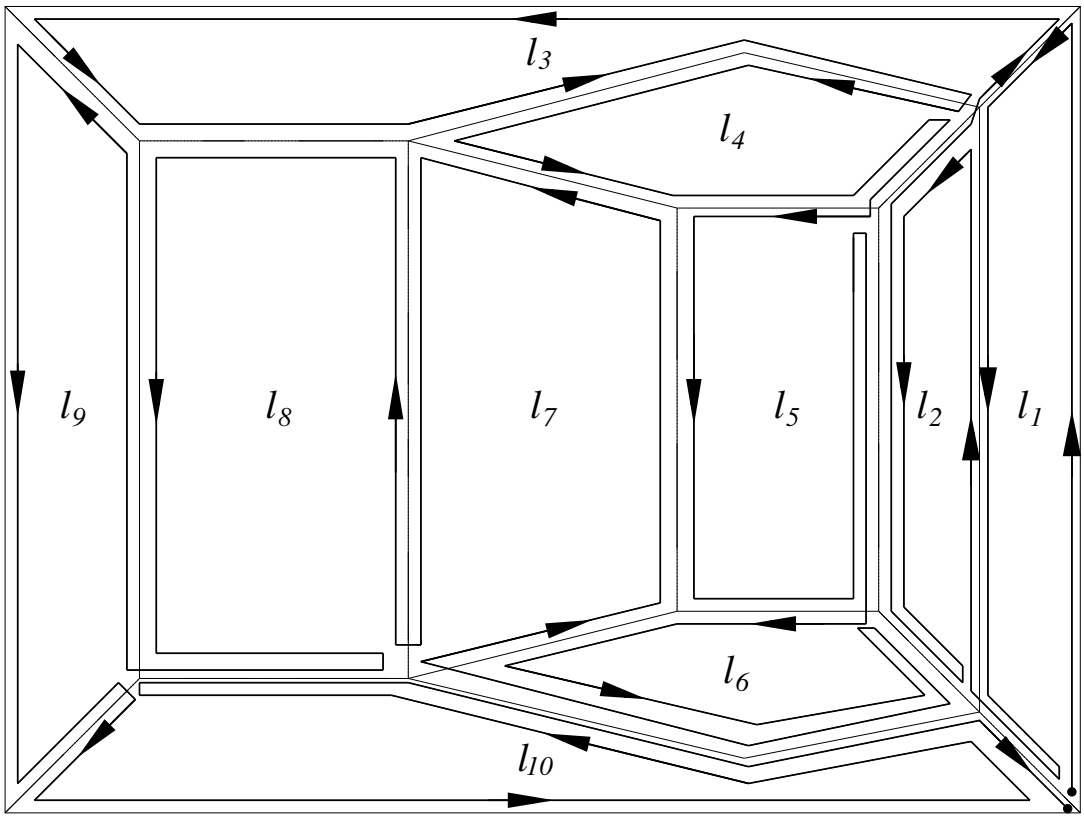

Figure 4.2: Enumeration of loops from Figure 3.11

9. l_9 lifts to the path $[E_{a_1a_2}, E_{\bar{a}_1a_3}]$.

10. l_{10} lifts to the path $E_{\bar{a}_1a_3}([E_{\bar{a}_1\bar{a}_2}, E_{\bar{a}_2\bar{a}_3}]E_{\bar{a}_1a_3})E_{a_1a_3}$.

Loops l_3, l_7, and l_8 correspond to the relation $[E_{ab}, E_{ca}] = E_{c\bar{b}}$ which is not a relation that yields a shingle. This relation can be made from the defining relations of shingles 3 and 4 by $[E_{ab}, E_{ca}]E_{cb} = E_{ab}([E_{ca}, E_{a\bar{b}}]E_{cb}[E_{c\bar{b}}, E_{a\bar{b}}])E_{a\bar{b}}$.

For brevity of notation denote the lift of the loop l_i as l_i. Now to see that S_0 lifts to Y note that the outside loop l lifts to $[E_{a_1a_2}, E_{\bar{a_1}a_2}]$ and by the same abuse of notation:

$$
\begin{aligned}
l &= [E_{a_1a_2}, E_{\bar{a}_1,a_2}] \\
&= E_{a_1a_2}E_{\bar{a_1}a_2}E_{a_1\bar{a_2}}E_{\bar{a_1}\bar{a_2}} \\
&= (E_{a_1a_2}E_{\bar{a}_2\bar{a}_3}E_{a_1\bar{a}_3}E_{a_1\bar{a}_2}E_{\bar{a}_2a_3})E_{\bar{a}_2\bar{a}_3}(E_{a_1a_2}E_{a_1a_3}E_{a_3\bar{a}_2}E_{a_1\bar{a}_3}E_{a_3a_2}) \\
&\quad E_{a_3\bar{a_2}}E_{a_1a_3}E_{a_3a_2}(E_{\bar{a_2}a_3}E_{\bar{a_1}a_2}E_{\bar{a_1}\bar{a_3}}E_{\bar{a_2}\bar{a_3}}E_{\bar{a_1}\bar{a_2}})(E_{\bar{a_1}a_2}E_{a_3\bar{a_2}}E_{\bar{a_1}\bar{a_2}}E_{a_3a_2}) \\
&\quad E_{a_3\bar{a_2}}(E_{\bar{a_1}a_2}E_{a_1\bar{a_3}}E_{\bar{a_1}\bar{a_2}}E_{a_1a_3})E_{a_1\bar{a_3}}(E_{\bar{a_1}a_2}E_{a_3a_2}E_{\bar{a_1}\bar{a_2}}E_{a_3\bar{a_2}}) \\
&\quad E_{a_3a_2}E_{\bar{a_1}a_2}(E_{a_3\bar{a_2}}E_{a_1a_3}E_{a_3a_2}E_{a_1\bar{a_3}}E_{a_1\bar{a_2}})(E_{a_1a_2}E_{a_1a_3}E_{\bar{a_2}a_3}E_{a_1\bar{a_2}}E_{\bar{a_2}\bar{a_3}}) \\
&\quad E_{\bar{a_2}a_3}(E_{a_1a_2}E_{\bar{a_1}a_3}E_{a_1\bar{a_2}}E_{\bar{a_1}\bar{a_3}})(E_{\bar{a_1}a_3}E_{\bar{a_1}\bar{a_2}}E_{\bar{a_2}\bar{a_3}}E_{\bar{a_1}a_2}E_{\bar{a_2}a_3})E_{\bar{a_2}\bar{a_3}}E_{\bar{a_1}\bar{a_2}}E_{\bar{a_2}a_3} \\
&= l_1E_{\bar{a_2}\bar{a_3}}l_2E_{a_3\bar{a_2}}E_{a_1a_3}E_{a_3a_2}l_3l_4E_{a_3\bar{a_2}}l_5E_{a_1\bar{a_3}}l_6E_{a_3a_2}E_{\bar{a_1}a_2}l_7l_8E_{\bar{a_2}a_3}l_9l_{10}E_{\bar{a_2}\bar{a_3}}E_{\bar{a_1}\bar{a_2}} \\
&\quad E_{\bar{a_2}a_3}.
\end{aligned}
$$

This shows that the lift of l is filled in Y. Now consider this lift of $S_0 \cap K_1$ in the Cayley 2-complex associated to the presentation of $Aut(F_n)$ given in [2]. This lift is accomplished by writing the generators from Gersten's presentation in terms of the generators from this presentation. Choosing τ_i for all $1 \leq i \leq n$ and σ_{ij} for all $1 \leq i \neq j \leq n$ as generators for W_n:

$$
\begin{aligned}
E_{a_ia_j} &= \sigma_{1i}\sigma_{2j}(\tau_1\tau_2\eta\tau_1)\sigma_{2j}\sigma_{1i}, \\
E_{\bar{a}_ia_j} &= \sigma_{1i}\sigma_{2j}(\tau_2\eta)\sigma_{2j}\sigma_{1i},
\end{aligned}
$$

where σ_{11} and σ_{22} are the identity automorphism. Recall that $E_{a\bar{b}} = E_{ab}^{-1}$, and each generator from the presentation in [2] has order 2. So the two equations above suffice to write E_{ab} in terms of the generators from the presentation in [2].

For l and the other ten loops, the loops are written in terms of the generators given in [2] below.

$$l = E_{a_1a_2}E_{\bar{a_1}a_2}E_{a_1\bar{a_2}}E_{\bar{a_1}\bar{a_2}} = (\tau_1\tau_2\eta\tau_1)(\tau_2\eta)(\tau_1\eta\tau_2\tau_1)(\eta\tau_2) = \tau_2\eta((\eta\tau_1)^2\tau_2)^2\eta\tau_2.$$

In the Cayley 2-complex of $Aut(F_n)$, l is conjugate to the relator $((\eta\tau_1)^2\tau_2)^2 = 1$. Confirming the presentation in Theorem 2.2.2 requires checking that each of the l_i in the Cayley 2-complex of $Aut(F_n)$ can be reduced to 1 only by using relations in Theorem 2.2.2. Below, this is shown for each of the l_i.

$$\begin{aligned}
l_1 &= E_{\bar{a}_2\bar{a}_3}E_{a_1a_2}([E_{a_1\bar{a}_2}, E_{\bar{a}_2a_3}]E_{a_1,\bar{a}_3})E_{a_1\bar{a}_2}E_{\bar{a}_2a_3} \\
&= E_{a_1a_2}E_{\bar{a}_2\bar{a}_3}E_{a_1\bar{a}_3}E_{a_1\bar{a}_2}E_{\bar{a}_2a_3} \\
&= (\tau_1\tau_2\eta\tau_1)(\sigma_{12}\sigma_{23}\eta\tau_2\sigma_{23}\sigma_{12})(\sigma_{23}\tau_1\eta\tau_2\tau_1\sigma_{23})(\tau_1\eta\tau_2\tau_1)(\sigma_{12}\sigma_{23}\tau_2\eta\sigma_{23}\sigma_{12}) \\
&= \tau_1\tau_2\eta\sigma_{12}\sigma_{23}\eta\tau_2\sigma_{13}\eta\sigma_{23}\eta\tau_2\sigma_{13}\sigma_{12}\eta\sigma_{12}\sigma_{13}\tau_1 \\
&= 1,
\end{aligned}$$

where applying relations in W_n and the relation $(\eta\tau_3)^2 = 1$ reduces from the third line to the fourth and applying relations in W_n, the relations $(\eta\sigma_{12})^3 = 1$, $\sigma_{12}\eta\sigma_{13}\tau_2\eta\sigma_{12}(\sigma_{23}\eta\sigma_{13}\tau_2\eta)^2 = 1$ and $\eta^2 = 1$ complete the reduction.

$$\begin{aligned}
l_2 &= E_{a_1a_2}(E_{a_1a_3}[E_{a_3\bar{a}_2}, E_{a_1\bar{a}_3}])E_{a_1\bar{a}_2} \\
&= E_{a_1a_2}E_{a_1a_3}E_{a_3\bar{a}_2}E_{a_1\bar{a}_3}E_{a_3a_2} \\
&= (\tau_1\tau_2\eta\tau_1)(\sigma_{23}\tau_1\tau_2\eta\tau_1\sigma_{23})(\sigma_{13}\tau_1\eta\tau_2\tau_1\sigma_{13})(\sigma_{23}\tau_1\eta\tau_2\tau_1\sigma_{23})(\sigma_{13}\tau_1\tau_2\eta\tau_1\sigma_{13}) \\
&= \tau_3\tau_1\tau_2\eta\sigma_{23}\eta\tau_2\sigma_{13}\sigma_{12}\eta\sigma_{12}\sigma_{13}\tau_2\eta\sigma_{12}\sigma_{23}\eta\sigma_{13}\tau_1\tau_3 \\
&= 1,
\end{aligned}$$

where applying relations in W_n and the relation $(\eta\tau_3)^2 = 1$ simplifies from the third to the fourth line and relations in W_n, relations $(\eta\sigma_{12})^3 = 1$,

$\sigma_{12}\eta\sigma_{13}\tau_2\eta\sigma_{12}(\sigma_{23}\eta\sigma_{13}\tau_2\eta)^2 = 1$ and $\eta^2 = 1$ complete the reduction.

$$\begin{aligned} l_3 &= E_{\bar{a}_1 a_2}([E_{\bar{a}_1\bar{a}_2}, E_{\bar{a}_2 a_3}]E_{\bar{a}_1\bar{a}_3}[E_{\bar{a}_1 a_3}, E_{\bar{a}_2 a_3}])E_{\bar{a}_1\bar{a}_2} \\ &= E_{\bar{a}_2 a_3}E_{\bar{a}_1 a_2}E_{\bar{a}_1\bar{a}_3}E_{\bar{a}_2\bar{a}_3}E_{\bar{a}_1\bar{a}_2} \\ &= (\sigma_{12}\sigma_{23}\tau_2\eta\sigma_{23}\sigma_{12})(\tau_2\eta)(\sigma_{23}\eta\tau_2\sigma_{23})(\sigma_{12}\sigma_{23}\eta\tau_2\sigma_{23}\sigma_{12})(\eta\tau_2) \\ &= \tau_3\sigma_{13}\eta\sigma_{12}\eta\sigma_{13}\tau_2\eta\sigma_{23}\eta\sigma_{13}\tau_2\eta\sigma_{23}\sigma_{12}\eta\tau_2\tau_3 \\ &= 1, \end{aligned}$$

where applying relations in W_n and the relations $[\eta, \tau_3] = 1$ and $(\eta\sigma_{12})^3 = 1$ simplifies from line three to line four and relations $\eta^2 = 1$, $\sigma_{12}\eta\sigma_{13}\tau_2\eta\sigma_{12}(\sigma_{23}\eta\sigma_{13}\tau_2\eta)^2 = 1$, along with relations in W_n complete the reduction.

$$\begin{aligned} l_4 &= E_{\bar{a}_1 a_2}[E_{a_3\bar{a}_2}, E_{\bar{a}_1\bar{a}_2}]E_{\bar{a}_1\bar{a}_2} \\ &= E_{\bar{a}_1 a_2}E_{a_3\bar{a}_2}E_{\bar{a}_1\bar{a}_2}E_{a_3 a_2} \\ &= (\tau_2\eta)(\sigma_{13}\tau_1\eta\tau_2\tau_1\sigma_{13})(\eta\tau_2)(\sigma_{13}\tau_1\tau_2\eta\tau_1\sigma_{13}) \\ &= \tau_3(\tau_2\eta\sigma_{13}\eta\sigma_{13})^2\tau_3 \\ &= 1, \end{aligned}$$

where applying relations in W_n and the relation $[\eta, \tau_3] = 1$ reduces from the third line to the fourth and relations $\sigma_{13} = \sigma_{23}\sigma_{12}\sigma_{23}$ and $\sigma_{12}\eta\sigma_{13}\tau_2\eta\sigma_{12}(\sigma_{23}\eta\sigma_{13}\tau_2\eta)^2 = 1$ combine to complete the reduction, shown below:

$$
\begin{aligned}
l_4 &= \tau_3(\tau_2\eta\sigma_{13}\eta\sigma_{13})^2\tau_3 \\
&= \tau_3\tau_2\eta\sigma_{23}\sigma_{12}\sigma_{23}\eta\sigma_{13}\tau_2\eta\sigma_{23}\sigma_{12}\sigma_{23}\eta\sigma_{13}\tau_3 \\
&= \tau_3\tau_2\eta\sigma_{23}\sigma_{12}\sigma_{12}\eta\sigma_{13}\tau_2\eta\sigma_{12}\eta\sigma_{13}\tau_2\eta\sigma_{12}\sigma_{23}\eta\sigma_{13}\tau_3 \\
&= \tau_3\tau_2\eta\sigma_{23}\eta\sigma_{13}\tau_2\eta(\sigma_{12}\eta\sigma_{13}\tau_2\eta\sigma_{12}(\sigma_{23}\eta\sigma_{13}\tau_2\eta)^2)\eta\tau_2\sigma_{13}\eta\sigma_{23}\eta\tau_2\tau_3 \\
&= 1.
\end{aligned}
$$

$$
\begin{aligned}
l_5 &= [E_{\bar{a}_1 a_2}, E_{a_1\bar{a}_3}] \\
&= E_{\bar{a}_1 a_2}E_{a_1\bar{a}_3}E_{\bar{a}_1\bar{a}_2}E_{a_1 a_3} \\
&= (\tau_2\eta)(\sigma_{23}\tau_1\eta\tau_2\tau_1\sigma_{23})(\eta\tau_2)(\sigma_{23}\tau_1\tau_2\eta\tau_1\sigma_{23}) \\
&= \tau_2(\eta\tau_1\sigma_{23})^4\tau_2 \\
&= \tau_2\sigma_{12}\eta\sigma_{12}(\eta\sigma_{13}\tau_2\eta\sigma_{12})^4\sigma_{12}\eta\sigma_{12}\tau_2 \\
&= 1,
\end{aligned}
$$

where applying relations in W_n and the relation $[\eta, \tau_3] = 1$ simplifies from the third line to the fourth and the relations $\sigma_{23} = \sigma_{12}\sigma_{13}\sigma_{12}$, $(\sigma_{12}\eta)^3 = 1$, $(\eta\sigma_{13}\tau_2\eta\sigma_{12})^4 = 1$, and $\eta^2 = 1$ along with relations in W_n complete the reduction.

$$
\begin{aligned}
l_6 &= [E_{\bar{a}_1 a_2}, E_{a_3 a_2}] \\
&= E_{\bar{a}_1 a_2}E_{a_3 a_2}E_{\bar{a}_1\bar{a}_2}E_{a_3\bar{a}_2} \\
&= (\tau_2\eta)(\sigma_{13}\tau_1\tau_2\eta\tau_1\sigma_{13})(\eta\tau_2)(\sigma_{13}\tau_1\eta\tau_2\tau_1\sigma_{13}) \\
&= \tau_3\tau_2(\eta\sigma_{13}\tau_2\eta\sigma_{13})^2\tau_2\tau_3 \\
&= 1,
\end{aligned}
$$

where applying relations in W_n and the relation $[\eta, \tau_3] = 1$ reduces from the third line to the fourth and the same procedure that was applied in reducing l_4 can also be used here. Specifically, relations $\sigma_{13} = \sigma_{23}\sigma_{12}\sigma_{23}$ and $\sigma_{12}\eta\sigma_{13}\tau_2\eta\sigma_{12}(\sigma_{23}\eta\sigma_{13}\tau_2\eta)^2 = 1$ combine to complete the reduction shown below:

$$\begin{aligned}
l_6 &= \tau_3\tau_2(\eta\sigma_{13}\tau_2\eta\sigma_{13})^2\tau_2\tau_3 \\
&= \tau_3\tau_2\eta\sigma_{13}\tau_2\eta\sigma_{23}\sigma_{12}\sigma_{23}\eta\sigma_{13}\tau_2\eta\sigma_{23}\sigma_{12}\sigma_{23}\tau_2\tau_3 \\
&= \tau_3\tau_2\eta\sigma_{13}\tau_2\eta\sigma_{23}\sigma_{12}\sigma_{12}\eta\sigma_{13}\tau_2\eta\sigma_{12}\eta\sigma_{13}\tau_2\eta\sigma_{12}\sigma_{23}\tau_2\tau_3 \\
&= \tau_3\tau_2\eta\sigma_{13}\tau_2\eta\sigma_{23}\eta\sigma_{13}\tau_2\eta(\sigma_{12}\eta\sigma_{13}\tau_2\eta\sigma_{12}(\sigma_{23}\eta\sigma_{13}\tau_2\eta)^2)\eta\tau_2\sigma_{13}\eta\sigma_{23}\eta\tau_2\sigma_{13}\eta\tau_2\tau_3 \\
&= 1.
\end{aligned}$$

$$\begin{aligned}
l_7 &= E_{a_3\bar{a}_2}([E_{a_1a_3}, E_{a_3a_2}]E_{a_1\bar{a}_2}[E_{a_1a_2}, E_{a_3a_2}])E_{a_3a_2} \\
&= E_{a_3\bar{a}_2}E_{a_1a_3}E_{a_3a_2}E_{a_1\bar{a}_3}E_{a_1\bar{a}_2} \\
&= (\sigma_{13}\tau_1\eta\tau_2\tau_1\sigma_{13})(\sigma_{23}\tau_1\tau_2\eta\tau_1\sigma_{23})(\sigma_{13}\tau_1\tau_2\eta\tau_1\sigma_{13})(\sigma_{23}\tau_1\eta\tau_2\tau_1\sigma_{23})(\tau_1\eta\tau_2\tau_1) \\
&= \tau_3\tau_1\sigma_{13}\eta\sigma_{13}\sigma_{23}\eta\sigma_{23}\sigma_{13}\tau_1\eta\tau_1\sigma_{13}\sigma_{23}\eta\sigma_{23}\eta\tau_2\tau_1\tau_3 \\
&= \tau_3\tau_2\tau_1\eta\sigma_{23}\eta\tau_2\sigma_{13}\eta((\eta\tau_2\sigma_{13}\eta\sigma_{23})^2\sigma_{12}\eta\tau_2\sigma_{13}\eta\sigma_{12})\eta\sigma_{13}\tau_2\eta\sigma_{23}\eta\tau_2\tau_1\tau_3 \\
&= 1,
\end{aligned}$$

where relations in W_n and the relations $[\eta, \tau_3] = 1$ and $(\eta\sigma_{12})^3 = 1$ reduces from the third line to the fourth and using relations in W_n, $(\eta\sigma_{12})^3 = 1$, $\eta^2 = 1$, and $\sigma_{12}\eta\sigma_{13}\tau_2\eta\sigma_{12}(\sigma_{23}\eta\sigma_{13}\tau_2\eta)^2 = 1$ completes the reduction.

$$
\begin{aligned}
l_8 &= E_{a_1a_2}E_{a_1a_3}E_{\bar{a}_2a_3}([E_{a_1\bar{a}_2},E_{\bar{a}_2\bar{a}_3}]E_{a_1a_3}[E_{a_1\bar{a}_3},E_{\bar{a}_2\bar{a}_3}])E_{\bar{a}_2\bar{a}_3}E_{a_1\bar{a}_3}E_{a_1\bar{a}_2}\\
&= E_{a_1a_2}E_{a_1a_3}E_{\bar{a}_2a_3}E_{a_1\bar{a}_2}E_{\bar{a}_2\bar{a}_3}\\
&= (\tau_1\eta\tau_2\tau_1)(\sigma_{12}\sigma_{23}\eta\tau_2\sigma_{23}\sigma_{12})(\tau_1\tau_2\eta\tau_1)(\sigma_{23}\tau_1\tau_2\eta\tau_1\sigma_{23})(\sigma_{12}\sigma_{23}\tau_2\eta\sigma_{23}\sigma_{12})\\
&= \tau_3\tau_2\eta\sigma_{23}\eta\sigma_{13}\tau_2\eta\sigma_{23}\sigma_{12}\eta\tau_2\sigma_{12}\sigma_{23}\eta\sigma_{23}\sigma_{12}\tau_3\\
&= \tau_3\sigma_{13}\eta((\eta\tau_2\sigma_{13}\eta\sigma_{23})^2\sigma_{12}\eta\tau_2\sigma_{13}\eta\sigma_{12})\eta\sigma_{13}\tau_3\\
&= 1,
\end{aligned}
$$

where relations in W_n and $[\eta,\tau_3]=1$ take us from the third line to the fourth and relations $(\eta\sigma_{12})^3=1$, $\eta^2=1$, $\sigma_{12}\eta\sigma_{13}\tau_2\eta\sigma_{12}(\sigma_{23}\eta\sigma_{13}\tau_2\eta)^2=1$, and relations in W_n combine to complete the reduction.

$$
\begin{aligned}
l_9 &= [E_{a_1a_2},E_{\bar{a}_1a_3}]\\
&= E_{a_1a_2}E_{\bar{a}_1a_3}E_{a_1\bar{a}_2}E_{\bar{a}_1\bar{a}_3}\\
&= (\tau_1\tau_2\eta\tau_1)(\sigma_{23}\tau_2\eta\sigma_{23})(\tau_1\eta\tau_2\tau_1)(\sigma_{23}\eta\tau_2\sigma_{23})\\
&= \tau_3\tau_2\tau_1(\eta\tau_1\sigma_{23})^4\tau_1\tau_2\tau_3\\
&= \tau_3\tau_2\tau_1(\eta\tau_1\sigma_{12}\sigma_{13}\sigma_{12})^4\tau_1\tau_2\tau_3\\
&= \tau_3\tau_2\tau_1\sigma_{12}\eta\sigma_{12}(\eta\tau_2\sigma_{13}\eta\sigma_{12})^4\sigma_{12}\eta\sigma_{12}\tau_1\tau_2\tau_1\\
&= 1,
\end{aligned}
$$

where relations in W_n and $[\eta,\tau_3]=1$ simplify from the third line to the fourth and the relations in W_n, $\sigma_{23}=\sigma_{12}\sigma_{13}\sigma_{12}$, $\eta^2=1$ and $(\eta\tau_2\sigma_{13}\eta\sigma_{12})^4=1$ complete the reduction.

$$
\begin{aligned}
l_{10} &= E_{\bar{a}_1 a_3}([E_{\bar{a}_1\bar{a}_2}, E_{\bar{a}_2\bar{a}_3}]E_{\bar{a}_1 a_3})E_{a_1 a_3} \\
&= E_{\bar{a}_1 a_3}E_{\bar{a}_1\bar{a}_2}E_{\bar{a}_2\bar{a}_3}E_{\bar{a}_1 a_2}E_{\bar{a}_2 a_3} \\
&= (\sigma_{23}\tau_2\eta\sigma_{23})(\eta\tau_2)(\sigma_{12}\sigma_{23}\eta\tau_2\sigma_{23}\sigma_{12})(\tau_2\eta)(\sigma_{12}\sigma_{23}\tau_2\eta\sigma_{23}\sigma_{12}) \\
&= \sigma_{23}\tau_2\eta\sigma_{23}\eta\tau_2\sigma_{13}\sigma_{12}\eta\sigma_{12}\sigma_{13}\tau_2\eta\sigma_{12}\sigma_{23}\eta\sigma_{23}\sigma_{12} \\
&= \sigma_{23}\tau_2\eta\sigma_{23}\eta\tau_2\sigma_{13}\eta(\sigma_{12}\eta\sigma_{13}\tau_2\eta\sigma_{12}(\sigma_{23}\eta\sigma_{13}\tau_2\eta)^2)\eta\sigma_{13}\tau_2\eta\sigma_{23}\eta\tau_2\sigma_{23} \\
&= 1,
\end{aligned}
$$

where applying relations in W_n and the relation $[\eta, \tau_3] = 1$ take us from the third line to the fourth and relations in W_n, together with relations $(\eta\sigma_{12})^3 = 1$, $\eta^2 = 1$, and $\sigma_{12}\eta\sigma_{13}\tau_2\eta\sigma_{12}(\sigma_{23}\eta\sigma_{13}\tau_2\eta)^2 = 1$ complete the reduction.

Now $l_i = 1$ for each i. Hence,

$$
\begin{aligned}
((\eta\tau_1)^2\tau_2)^2 &= \eta\tau_2 l_1 E_{\bar{a_2}\bar{a_3}} l_2 E_{a_3\bar{a_2}} E_{a_1 a_3} E_{a_3 a_2} l_3 l_4 E_{a_3\bar{a_2}} l_5 E_{a_1\bar{a_3}} l_6 E_{a_3 a_2} E_{\bar{a_1} a_2} l_7 l_8 E_{\bar{a_2} a_3} \\
&\quad l_9 l_{10} E_{\bar{a_2}\bar{a_3}} E_{\bar{a_1}\bar{a_2}} E_{\bar{a_2} a_3} \tau_2\eta \\
&= \eta\tau_2 E_{\bar{a_2}\bar{a_3}} E_{a_3\bar{a_2}} E_{a_1 a_3} E_{a_3 a_2} E_{a_3\bar{a_2}} E_{a_1\bar{a_3}} E_{a_3 a_2} E_{\bar{a_1} a_2} E_{\bar{a_2} a_3} E_{\bar{a_2}\bar{a_3}} E_{\bar{a_1}\bar{a_2}} E_{\bar{a_2} a_3} \\
&\quad \tau_2\eta \\
&= 1.
\end{aligned}
$$

Note that $E_{ij}E_{i\bar{j}} = 1$ is a consequence of the fact that each of the generators in Theorem 2.2.3 are involutions. Thus, only relations in Theorem 2.2.3 were used in reducing $((\eta\tau_1)^2\tau_2)^2 = 1$, confirming Theorems 2.2.2 and 2.2.3.

CHAPTER 5

PATCHED FILLINGS

In this chapter, we take an arbitrary filling of an edge loop in K_1 and produce a combinatorial filling that has the structure of shingles, where a map between two simplicial complexes is combinatorial if it is simplicial and preserves the dimension of the simplices. Such fillings are called *patched fillings*. A patched filling D^2 is tiled by *patches*, connected subcomplexes of D^2 that map combinatorially to a shingle. In section 1, we develop notation necessary to define patched fillings. In sections 2 and 3 we prove Theorem 5.2.1 which states that all embedded edge paths in K_1 have a patched filling. This is proved by transforming an arbitrary filling into patched filling. In section 4, the methods sections 2 and 3 are used to study the relationship between which tiles the arbitrary filling passes through and which shingles are used in the resulting patched filling. In section 5, we show that the structure of patched fillings can be simplified so that *Nielsen points* in D^2, 0-simplices that map to vertices of the form (g, θ_n), are contained in no more than three patches. Patched fillings with this property are called *simple patched fillings*. Simple patched fillings are the context for chapters 6, 7, and 8. In these chapters we will prove that several subcomplexes of K_2 are not simply-connected by showing that for each of these subcomplexes there exists a loop for which no simple patched filling exists.

5.1 Notation - Patches and Disk Trees

Before defining patched fillings, we need to develop notation regarding sets of loops in a triangulated disk. These sets of loops will be used extensively in the proofs in sections 2 and 3.

5.1.1 Patches and Loop Systems

Suppose that D^2 is equipped with a triangulation. Let $\lambda : S^1 \to D^2$ be an edge loop. The interior of λ, λ^o, is the union of the connected components of $D^2 \setminus im(\lambda)$ that do not contain ∂D^2. The closure of λ, $\bar{\lambda} = im(\lambda) \cup \lambda^o$.

Definition 5. *A set of embedded edge loops λ_1, λ_2, $\ldots \lambda_k$ in D^2 is a* loop cover *if* $\bigcup_{i=1}^{k} \bar{\lambda}_i = D^2$.

Definition 6. *For a subset X of D^2, X is* enclosed *by a finite set of loops λ_1, λ_2, $\ldots$, λ_k in D^2 if $X \subseteq \bar{\lambda}_j$ for some j. A loop $\lambda : S^1 \to D^2$ is enclosed by this finite set of loops if $\bar{\lambda}$ is enclosed.*

Definition 7. *A loop cover λ_1, λ_2, $\ldots$, λ_k of D^2 is a* loop system *for D^2 if λ_i is not enclosed by $\lambda_1, \lambda_2, \ldots, \lambda_{i-1}, \lambda_{i+1}, \ldots, \lambda_k$ for all i.*

Remark: This definition of loop system is equivalent to the following definition: a loop cover λ_1, λ_2, $\ldots \lambda_k$ is a loop system if for all $i \neq j$, $\lambda_i^o \cup \lambda_j^o = \emptyset$. Further given a loop cover, a loop system can be produced by discarding enclosed loops.

Thus far, we have described loop covers and systems in triangulated disks only. This is slightly more structure than is necessary, all that is actually needed for the arguments in this chapter is that the images of the loops in D^2 must have a 1-dimensional simplicial structure. We will use this weakened definition at some points, as sometimes we will ignore or alter the simplicial structure of the disk the is not contained in the image of a loop cover or system.

Definition 8. *For a loop system λ_1, λ_2, $\ldots \lambda_k$ of D^2, the set of subcomplexes $\bar{\lambda}_1$, $\bar{\lambda}_2$, $\ldots \bar{\lambda}_k$ is called a* patch system *of D^2, and each $\bar{\lambda}_i$ is called a* patch.

Definition 9. *A combinatorial map $\Delta : D^2 \to K_2$ is a patched filling if D^2 has a patch system where Δ maps each patch bijectively onto a translate of a shingle.*

Given an arbitrary filling $\Delta' : D^2 \to K_2$ of an embedded edge loop in K_1, a patched filling $\Delta : D^2 \to K_2$ will be constructed. This construction is a proof that the $Aut(F_n)$ translates of the boundaries of the shingles generate $\pi_1(K_1)$, as a loop in K_1 is homotopic to a concatenation of embedded edge loops.

The maps $Shin_j(\alpha)$ are trivial patched fillings for all α and j. A more complicated patched filling is shown in Figure 8.1. Figure 3.11 is not a patched filling because loops l_3, l_7, and l_8 from Figure 4.2 do not map to the boundary of a shingle. These loops can be replaced by boundaries of translates of shingles 3 and 4 to make Figure 3.11 a patched filling.

Let $\rho : S^1 \to K_1$ be an embedded edge loop, and note that since K_2 is simply-connected there is a filling $\Delta' : D^2 \to K_2$ of ρ. By passing to a homotopic map, and taking barycentric subdivisions of the simplicial structure pulled back onto D^2, assume that Δ' is simplicial and that $\Delta'|_{\partial D^2}$ is unchanged. In the next two sections Δ' is used to construct a patched filling Δ of ρ. The main idea of the construction of Δ is to produce a loop system of D^2 where Δ maps each loop to the boundary of a tile. By Proposition 3.3.1, the images of these loops can be filled by shingles. Though the images of these loops need not be embedded and so we must generalize patched fillings. The next subsection provides a context for patched structures for non-embedded loops.

5.1.2 Disk Trees

For an edge loop $\rho : S^1 \to K_1$, if ρ is not embedded it is more natural to fill ρ as a disk tree $\mathcal{D}$ than as D^2.

Definition 10. *A* disk tree $\mathcal{D}$ *is a 2-dimensional simply connected CW-complex where each map of the boundary of a 2-cell into the 1-skeleton* $\mathcal{D}^1$ *of* $\mathcal{D}$ *is an embedding and the intersection of the closures of any pair of 2-cells is either empty or a point.*

Note that a disk tree is determined by its 1-skeleton, as there is a 2-cell for each generator of π_1 of the 1-skeleton. The boundary loops of 2-cells in a disk tree will be called the *loops* of the disk tree. Let $\mathcal{D}$ be a disk tree, and consider the following operations on $\mathcal{D}$:

1. Loop Collapse: Suppose a loop is made up of two 1-cells. Deleting the 2-cell and identifying the two 1-cells will be called performing a loop collapse and creates a new CW-complex. Figure 5.1 is an example of a loop collapse in a disk tree.
2. 0-Cell Identification: Suppose there is more than one 0-cell in a loop and choose two of these 0-cells. Deleting the 2-cell, identifying these two 0-cells, and filling in the two resulting loops with 2-cells will be called 0-cell identification and creates a new CW-complex. Figure 5.2 is an example of a 0-cell identification in a disk tree.

Note that for each operation there is a natural quotient map taking the original disk tree to the new disk tree. The restriction of the quotient to the one skeleton of the original disk tree is a combinatorial map.

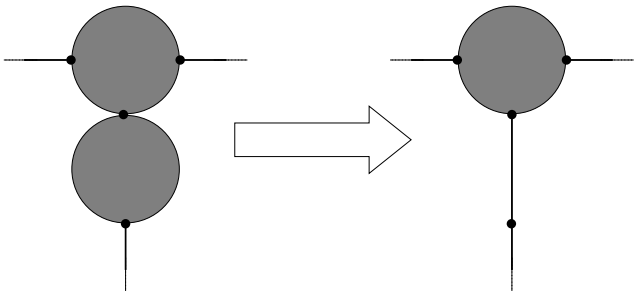

Figure 5.1: Example of loop collapse in a disk tree

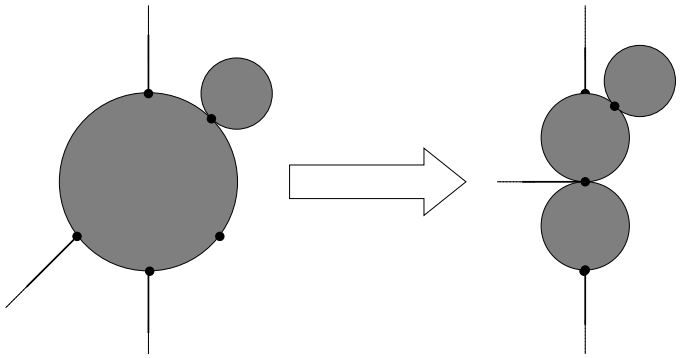

Figure 5.2: Example of 0-cell identification in a disk tree

Proposition 5.1.1. *Let $\mathcal{D}$ be a disk tree. The CW-complex obtained by performing a loop collapse or a 0-cell identification on $\mathcal{D}$ is a disk tree.*

Proof. Let $\mathcal{D}'$ result from applying a loop collapse to $\mathcal{D}$. Note that $\pi_1(\mathcal{D}) \simeq \pi_1(\mathcal{D}')$, and since no 2-cells were added $\mathcal{D}'$ is a disk tree.

Let $\mathcal{D}'$ result from applying 0-cell identification to $\mathcal{D}$. Then $\pi_1(\mathcal{D}) \simeq \pi_1(\mathcal{D}')$. Suppose that there are two 2-cells in $\mathcal{D}'$ whose intersection is more than a point. Then there must be two 2-cells in $\mathcal{D}$ that also intersect on more than a point, and $\mathcal{D}$ is not a disk tree. Hence, $\mathcal{D}'$ is a disk tree. □

Both loop collapses and 0-cell identification can be applied to the 1-skeleton of

a disk tree to produce the 1-skeleton of another disk tree.

Consider a combinatorial map $\phi : \mathcal{D}^1 \to X$ where X is a simplicial complex. Through the application of loop collapsing and 0-cell identification, we can construct a 1-dimensional simplicial complex $\mathcal{D}^1_s$, a combinatorial map $\phi_s : \mathcal{D}^1_s \to X$ and a combinatorial quotient map $q : \mathcal{D}^1 \to \mathcal{D}^1_s$ so that $\phi = \phi_s \circ q$ and ϕ_s is an embedding when restricted to each loop of $\mathcal{D}^1_s$. This is accomplished by considering a loop on $\mathcal{D}^1$, and supposing that ϕ is not an embedding when restricted to this loop. Then if two 0-cells in the loop map to the same point under ϕ, perform 0-cell identification on these 0-cells. If there is no such pair of 0-cells, then the loop has only two 1-cells each of which map to the same edge in X, so perform a loop collapse on these 1-cells. ϕ factors through this new disk loop via the quotient map. Applying this procedure to each loop on each resulting disk tree produces a chain of 1-skeletons of disk trees and quotient maps $\mathcal{D}^1 \xrightarrow{q_1} \mathcal{D}^1_1 \xrightarrow{q_2} \mathcal{D}^1_2 \ldots \xrightarrow{q_k} \mathcal{D}^1_k$ and where ϕ factors through $\mathcal{D}^1_k$ as a map ϕ_k such that ϕ_k is an embedding on each loop in $\mathcal{D}^1_k$. This procedure must terminate since at each step the total number of 1-cells and 0-cells has been reduced. Then $\mathcal{D}^1_s = \mathcal{D}^1_k$, $\phi_s = \phi_k$, and $q = q_k \circ \ldots \circ q_2 \circ q_1$. Note that this construction depends upon the choices of 0-cells that are identified as it is possible that more than two 0-cells in a given loop map to the same point in X.

Definition 11. *A* patched disk tree *is a disk tree $\mathcal{D}$ together with a combinatorial map $\Delta_{\mathcal{D}} : \mathcal{D} \to K^2$ so that $\Delta_{\mathcal{D}}$ is a patched filling when restricted to each closed 2-cell in $\mathcal{D}$.*

Proposition 5.1.2. *Let $\rho : S^1 \to \partial(\alpha \cdot T_m)$ be an embedded edge loop for some $\alpha \in Aut(F_n)$ and some m. Then there exists a patched filling Δ of ρ that only uses patches mapping to shingles contained in $\alpha \cdot T_m$.*

Proof. By Proposition 3.3.1 ρ can be written as a concatenation of loops in K_1, $\rho = \rho_1\rho_2 \dots \rho_{k-1}\rho_k$, and $\rho_i = \lambda_i Shin_{j_i}(\alpha_i)|_{\partial D^2}\lambda_i^{-1}$ where $im(Shin_{j_i}(\alpha_i)) \subset \alpha \cdot T_m$ and λ_i is a path from a basepoint in $\partial(\alpha \cdot T_m)$ to a point on $\partial(\alpha_i \cdot \mathsf{f}_{j_i})$.

ρ_i factors through a disk tree $\mathcal{D}_i$, the "lollipop" disk tree, as ρ_i'. $\mathcal{D}_i$ consists of two 0-cells, two 1-cells one that passes between the two 0-cells and the other gluing both of its boundary points to a single 0-cell, and one 2-cell whose boundary glues to the 1-cell that is a loop. $\mathcal{D}_i$, together with the map constructed by pasting $Shin_{j_i}(\alpha_i)$ on the 2-cell in $\mathcal{D}_i$ and ρ_i', is a patched disk tree. This is a continuous map, moreover is combinatorial for a triangulation of $\mathcal{D}_i$. The homotopy in $\partial(\alpha \cdot T_m)$ taking ρ to the concatenation above gives identifications between the boundaries of these patched disk trees that yield a patched filling for ρ. □

Note that patches mapping to translates of shingle 5 are not needed to make patched fillings for any embedded edge loops $\rho : S^1 \to \partial(\alpha \cdot T_m)$ for any $\alpha \in Aut(F_n)$ and any m. This is because there is a patched filling for $Shin_5(\alpha, x)$ that only uses patches mapping to translates of shingles 3 and 4.

5.2 Constructing Patched Fillings - Stage 1: Combinatorial Loop System

Let $\rho : S^1 \to K_1$ be an embedded edge loop and since K_2 is simply-connected there exists a filling $\Delta' : D^2 \to K_2$. By passing to a homotopic map, assume that Δ' is simplicial and $\Delta'|_{\partial D^2} = \rho$. The goal of this section and the next is to prove the following.

Theorem 5.2.1. *There exists a patched filling $\Delta : D^2 \to K_2$ of ρ.*

To produce Δ, we will create a loop cover and subsequent loop system by considering loops in the boundary of the connected components of $D^2 \setminus \Delta'^{-1}(K_1)$.

Definition 12. *For X a connected subcomplex of the 1-skeleton of D^2, an embedded edge loop λ of X is called an* outer loop *of X if $\phi^o \subseteq \bar{\lambda}$ for all edge loops $\phi : S^1 \to X$.*

Note that each connected component of the boundary of a component of $D^2 \setminus \Delta'^{-1}(K_1)$ has a unique outer loop up to orientation. These outer loops form a loop cover for D^2, and removing the enclosed loops from this cover produces a loop system. Δ is produced in two stages. In the first, we make Δ combinatorial on the image of the loops by collapsing all edges in this image that map to vertices. After stage 1, each loop in the system maps combinatorially into the boundary of a tile. In stage 2, each of the loops in the system is replaced by the 1-skeleton of a disk tree, where each loop of the disk tree embeds in the boundary of a tile. Now each of these loops can be filled by shingles, creating the patched filling Δ. In this section, we perform stage 1 of this procedure.

Definition 13. *The connected components of $D^2 \setminus \Delta'^{-1}(K_1)$ are called* non-trivial pieces of D^2. *The 2-simplices that map to K_1 under Δ' are called* trivial pieces of D^2. *Together the trivial and non-trivial pieces of D^2 are called the* pieces *of D^2.*

For each piece of D^2 consider the components of the boundary of that piece, and choose an outer loop for each component.

Definition 14. *Let NE be the subset of these chosen outer loops that are not enclosed by any other chosen outer loop.*

NE has the following properties:

1. NE is a loop system for D^2,

2. for $\lambda \in NE$, $im(\Delta' \circ \lambda) \subseteq \partial(\alpha \cdot T_m)$ for some m and some $\alpha \in Aut(F_n)$, and

3. for $\lambda \in NE$, $\Delta' \circ \lambda$ is simplicial.

We would like $\Delta' \circ \lambda$ to be combinatorial for each of these loops.

Definition 15. *Let λ_1, λ_2, ..., λ_k be a loop system. A* loop system map *is a simplicial map of $\bigcup_{i=1}^{k} im(\lambda_i)$ into a simplicial complex.*

Let Γ' be the subcomplex of D^2 given by the image of the elements in NE. Γ' is a graph containing the boundary D^2. Currently $\Delta' : \Gamma' \to K_1$ is a loop system map, though we would like to make this map combinatorial. Let ∂ be the subgraph of Γ' in ∂D^2 and $Triv$ be the set of all edges in Γ' that map to a vertex under Δ'. Note that $Triv$ and ∂ are disjoint since ρ is an edge loop. Let $h : [0,1] \times \Gamma' \to D^2$ be a homotopy with the following properties:

1. $h(0)$ is the inclusion map of Γ' into D^2,

2. $h(\partial)$ is fixed pointwise for all t,

3. $h(1, e)$ is a point for all e in $Triv$, and

4. $h(t)$ is an embedding on $\Gamma' \setminus Triv$ for all t.

Such a homotopy exists and is obtained by collapsing all edges in $Triv$ while keeping the boundary fixed. Let Γ be the graph obtained from Γ' by collapsing all edges in $Triv$. Then we will think of Γ as being contained in D^2 as the image of $h(1)$. This graph Γ may have bi-gons, which are removed by extending the homotopy h so that the images of edges in Γ' that map to bi-gons are identified. By reparameterizing the homotopy, let $h(1)$ map Γ' to Γ in D^2 where Γ has no bi-gons and all edges of Γ' whose images mapped to points under Δ' are vertices

in Γ. Note that since ρ is an embedding, at least one of the edges in each of the bi-gons was not in ∂, and the outer boundary of Γ is still an embedded edge loop. Note that $h(1, x)$ is a quotient map from Γ' to Γ.

Define Δ on Γ by $\Delta(e) = \Delta'(h^{-1}(1, e))$ for each edge e, and note that $\Delta|_{\partial D^2} = \rho$. Note that Δ is combinatorial by construction, and Δ is well-defined since the preimages of e under $h^{-1}(1)$ all map to the same edge in K_2 by Δ'.

A loop system for Γ is given by a slight alteration to the loops in NE, specifically given $\lambda' \in NE$, consider $\lambda : S^1 \to \Gamma$ defined by $\lambda(x) = h(1, \lambda'(x))$. Let $\lambda'_1, \lambda'_2, \ldots \lambda'_k$ be the elements of NE, and $\lambda_1, \lambda_2, \ldots \lambda_k$ be the loops in Γ determined in this way after any edges in the domain S^1 that map to vertices are collapsed. Note that some λ_i may be constant loops and nullhomotopic loop, but after discarding these loops the remaining loops form a loop system for D^2 the maps to Γ. Δ is a combinatorial loop system map for this system.

To illustrate this method, consider Figures 5.3, 5.4, 5.5, and 5.6. In Figure 5.3 a triangulation on D^2 is shown where the darkened edges are $\Gamma' \setminus Triv$ and the dashed darkened edges are $Triv$. Figure 5.4 ignores the simplicial structure of D^2 and only shows Γ', while Figure 5.5 shows the graph Γ. There is one bi-gon in Figure 5.5, it is removed in Figure 5.6. The loops in Figure 5.6 are a loop system.

5.3 Constructing Patched Fillings - Stage 2: Embedding Loop Systems

At this point in the proof, we have D^2 equipped with a loop system and a combinatorial loop system map so that the image of each loop is contained in the

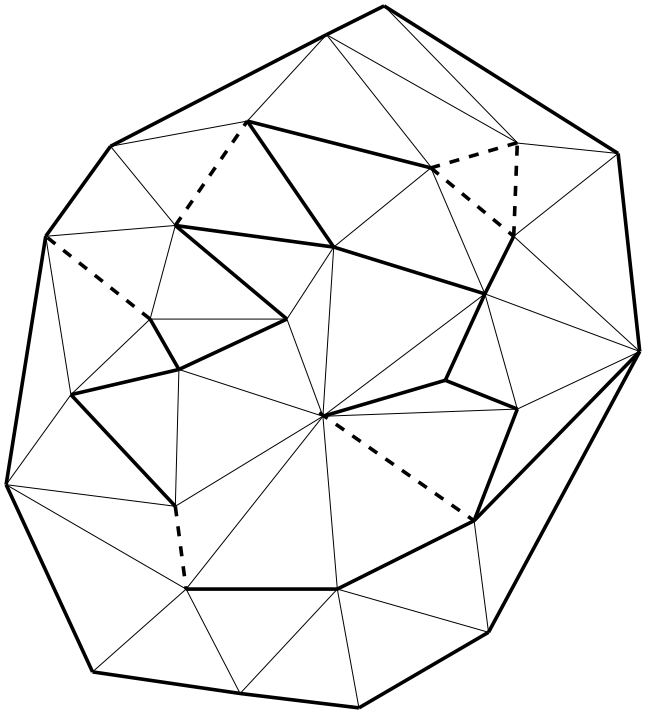

Figure 5.3: Triangulation of D^2

boundary of a tile. We would like for the image of each loop in the system to be an embedding into the boundary of a tile. If this was the case, Proposition 3.3.1 would complete the construction of Δ. In this section, we will provide a method to create these embeddings.

Proposition 5.3.1. *Let λ_1, λ_2, ..., λ_k be a combinatorial loop system and let $f : \bigcup_{i=1}^{k} im(\lambda_i) = X \to Y$ be a loop system map where $f|_{\partial D^2}$ is an embedding. Then there exists a loop system λ'_1, λ'_2, ..., $\lambda'_{k'}$ and a combinatorial loop system map $f' : \bigcup_{i=1}^{k'} im(\lambda'_i) = X' \to Y$ so that:*

1. *For each j' there exists j so that $im(f' \circ \lambda'_{j'}) \subseteq im(f \circ \lambda_j)$,*
2. *$f' \circ \lambda'_{j'}$ is an embedding for all j', and*
3. *$f = f'$ on ∂D^2.*

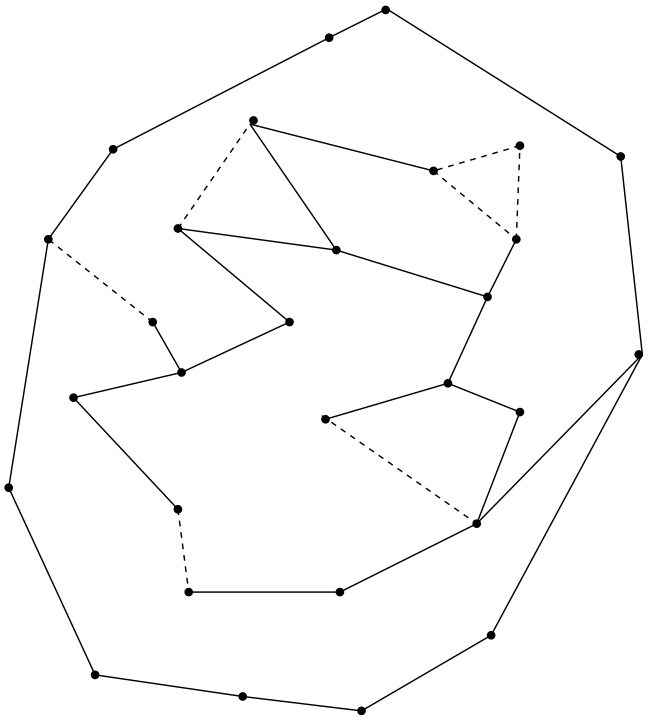

Figure 5.4: D^2 with Γ'

Proof. The idea of this proof is to apply 0-cell identification and loop collapse to each map $f \circ \lambda_i$. Applying these techniques produces a disk tree $\mathcal{D}_i$ that $f \circ \lambda_i$ factors through. We can use this disk tree to define a new loop system, where $im(\lambda_i)$ is replaced by a copy of this disk tree. This replacement causes some technical issues, which are detailed below.

We will proceed by induction. Let $\lambda_1, \lambda_2, \ldots, \lambda_k$ be a loop system and f be a combinatorial loop system map where $f \circ \lambda_j$ is an embedding for $j > i$. From this data we construct a loop system $\lambda'_1, \lambda'_2, \ldots, \lambda'_{k'}$ and a combinatorial loop system map f' where $f' \circ \lambda'_j$ is an embedding for all $j > i - 1$, $f' = f$ on ∂D^2, and for every j' there exist j so that $im(f' \circ \lambda'_{j'}) \subseteq im(f \circ \lambda_j)$. 0-cell identification and loop collapse are applied to $f \circ \lambda_i$ to produce a disk tree $\mathcal{D}$ that $f \circ \lambda_i$ factors through as $f_i \circ q = f \circ \lambda_i$, where $q : S^1 \to \mathcal{D}$ is the natural quotient map.

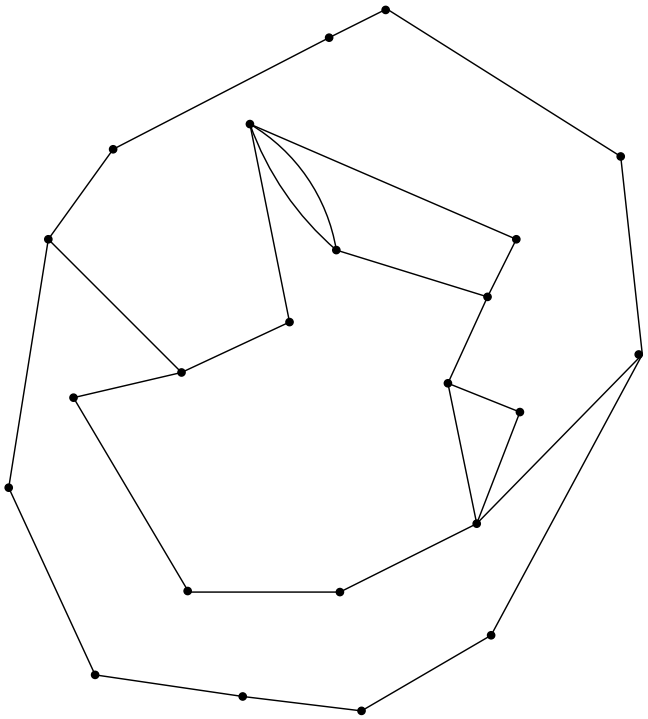

Figure 5.5: D^2 with Γ

Note that there exists a homotopy on $g : [0,1] \times D^2 \to D^2$ with the following properties:

1. $g(0,x)$ is the identity map,
2. $g(t, \partial D^2)$ is fixed pointwise for all t,
3. $g(1, im(\lambda_i))$ is homeomorphic to $\mathcal{D}$, and so $g(1, \lambda_i(x))$ factors through $\mathcal{D}$ as $g(1,\lambda_i) = \lambda_i' \circ q$,
4. the sets $g(t, \bar{\lambda}_1)$, $\ldots g(t, \bar{\lambda}_k)$ cover D^2 for all t, and
5. $g(t, \lambda_l^o) \cap g(t, \lambda_m^o) = \emptyset$ if $l \neq m$ for all t.

This homotopy is given by considering X as a graph in D^2 and performing 0-cell identification and loop collapsing on $im(\lambda_i)$, and altering the remainder of

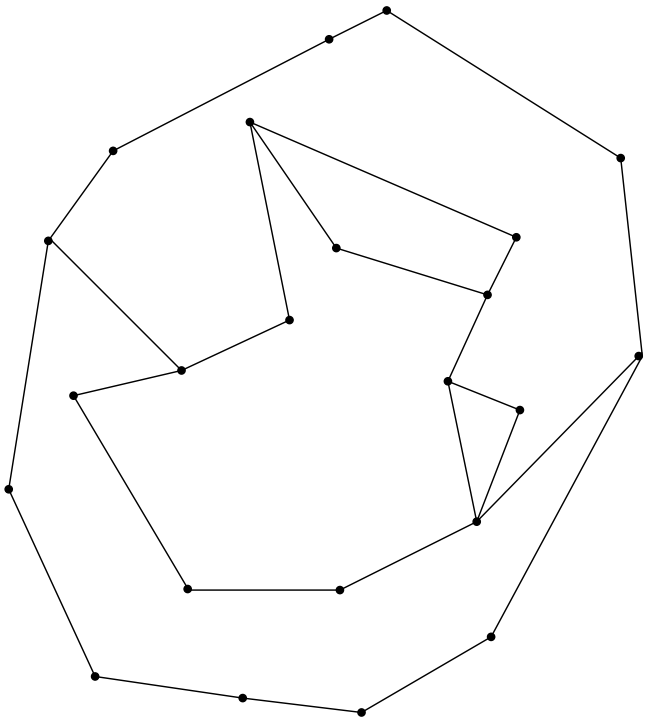

Figure 5.6: D^2 with Γ after bigons are removed

X so that ∂D^2 remains fixed. Note that since $f(\partial D^2)$ is injective, no two points in ∂D^2 were identified. The natural construction at this point would be to take $\lambda'_j = g(1, \lambda_j)$ for all $j \neq i$ and to take these maps together with the loops of the disk tree $g(1, im(\lambda_i))$ as a loop system for D^2. This is not quite correct as $g(1, \lambda_j)$ may not be an embedding for $j < i$. $g(1, \lambda_j)$ is an embedding for $j > i$ since $f \circ \lambda_j$ is an embedding. For $j < i$, $g(1, \lambda_j)$ may not be an embedding as points in $im(\lambda_j) \cap im(\lambda_i)$ may be identified by g. In this case, $g(1, \lambda_j)$ is replaced by its outer loop $\widetilde{g(1, \lambda_j)}$. For each j so that $g(1, \lambda_j)$ is not an embedding, let $\lambda'_j = \widetilde{g(1, \lambda_j)}$, and for all other j let $\lambda'_j = g(1, \lambda_j)$. Further let $\lambda'_{k+1}, \lambda'_{k+2}, \ldots \lambda'_l$ be λ'_i restricted to the loops of $\mathcal{D}$. Consider the list of loops $\lambda'_1, \lambda'_2, \ldots \lambda'_{i-1}, \lambda'_{i+1}, \ldots \lambda'_l$. Note that this is a loop cover, so taking the sublist consisting of all loops that are not enclosed by any other loop in this list and altering the indices to preserve order yields a

loop system $\lambda'_1, \ldots, \lambda'_{k'}$. Further $\bigcup_{j=1}^{k'} im(\lambda'_j)$ is a simplicial complex, as it inherited the simplicial structure of X from $g(1)$. This structure is well-defined, as the only identifications that occur identify pairs of 0-simplices and pairs of 1-simplices.

Given x in the image of one of these loops, define $f'(x) = f(g^{-1}(1, x))$. Observe that f' is well-defined since all inverse images of $x \in \bigcup_{j=1}^{k'} im(\lambda'_j)$ map to the same point under f, $f = f'$ on ∂D^2, and f' is a combinatorial loop system map. Also by definition for every j' there exists j so that $im(f' \circ \lambda'_{j'}) \subseteq im(f \circ \lambda_j)$. So if $im(f' \circ \lambda'_{j'}) \subseteq im(f \circ \lambda_j)$ and $f \circ \lambda_j$ is an embedding, $f' \circ \lambda'_{j'}$ must also be an embedding. Further if $\lambda'_{j'}$ is a restriction of $g(1, \lambda_i)$ to a loop of $\mathcal{D}$, then $f' \circ \lambda'_j$ is an embedding. Hence, for all $j > i - 1$, $f' \circ \lambda'_j$ is an embedding. $\lambda'_1, \ldots, \lambda'_{k'}$ is a loop system with combinatorial loop system map f', $f' \circ \lambda'_j$ is an embedding for $j > i - 1$, and $f = f'$ on the ∂D^2. This completes the induction step.

Applying this procedure to each loop in the original loop system produces a new loop system and combinatorial loop system map with the required properties. □

Figures 5.7, 5.8, 5.9, 5.10, and 5.11 are an example of applying this procedure. Figure 5.7 depicts the image of the loop system in D^2 from Figure 5.6, where the dotted lines denote the first loop to which 0-cell identification and loop collapsing will be applied. Figure 5.8 shows the result of replacing the dotted loop with the disk tree obtained by this procedure. Figure 5.9 shows the new loop system obtained by considering outer loops and removing enclosed loops, where the shaded region indicates which loops are embeddings under the image of the system map. Figure 5.11 shows a possible result of the entire procedure where the shading in Figures 5.10 and 5.11 denote the correspondence between the loops in these figures.

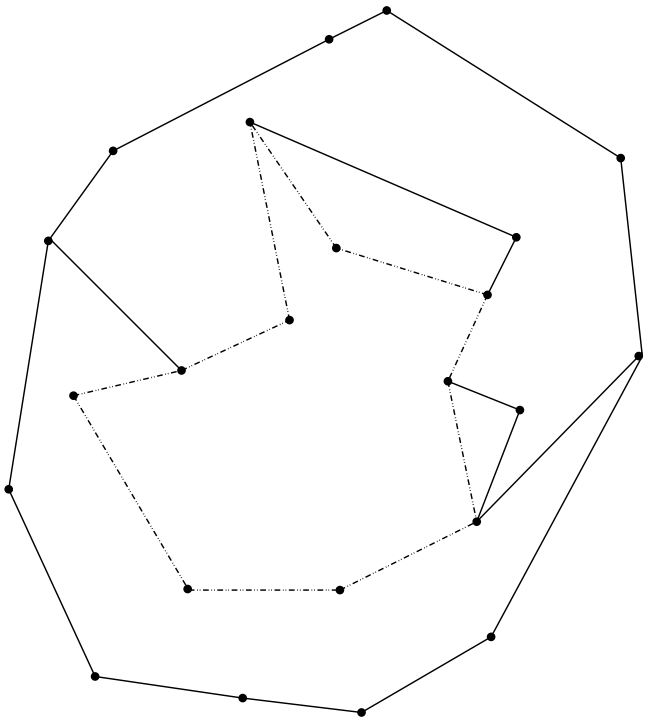

Figure 5.7: Loop system in D^2

Proof of Theorem 5.2.1. Applying the methods of section 5.2 to Δ' produces a loop system for D^2 so that each loop maps into the boundary of a tile. By Proposition 5.3.1, we can replace this loop system and map Δ' with a new loop system and map Δ so that Δ embeds the image of each loop in the boundary of a tile. Let λ_1, λ_2, ..., λ_k be this loop system. Since $\Delta \circ \lambda_i$ is an embedding into the boundary of a tile, by Proposition 5.1.2 there exists a patched filling δ_i of $\Delta \circ \lambda_i$. Since λ_i is an embedded edge path in D^2, λ_i can be extended to a map Λ_i of D^2 into $\bar{\lambda}_i$ and δ_i trivially factors through this map. Define Δ_i by $\Delta_i \circ \Lambda_i = \delta_i$, and note that on the boundary of the image of λ_i, Δ and Δ_i agree. By the pasting lemma, the maps Δ_i can be pasted together to make a single map from D^2 to K_2, rename this map Δ. Since λ_1, λ_2, ..., λ_k is a loop system their closures cover D^2, Δ is a patched filling of ρ, completing the theorem. $\square$

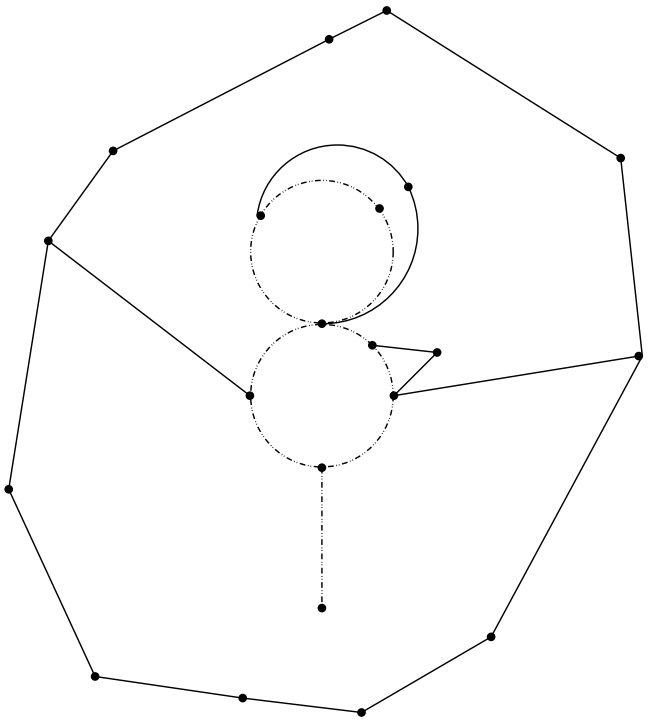

Figure 5.8: Loop system in D^2 after a loop is replaced by a disk tree

Note that since the fillings given for embedded edge loops in Proposition 5.1.2 do not use shingle 5, these patched fillings do not need to use patches mapping to translates of shingle 5.

5.4 Relationship Between Tiles in $im(\Delta')$ and Shingles in $im(\Delta)$

The arguments of sections 5.2 and 5.3 not only show that for each embedded edge path in K_1 a patched filling exists, but show that the types of patches used in the patched filling depend directly upon the simplicial filling Δ'. For a subcomplex $f \in K_2$ let f^o denote its interior. If $\Delta' : D^2 \to K_2 \setminus orbit(T_1^o)$ then there are no

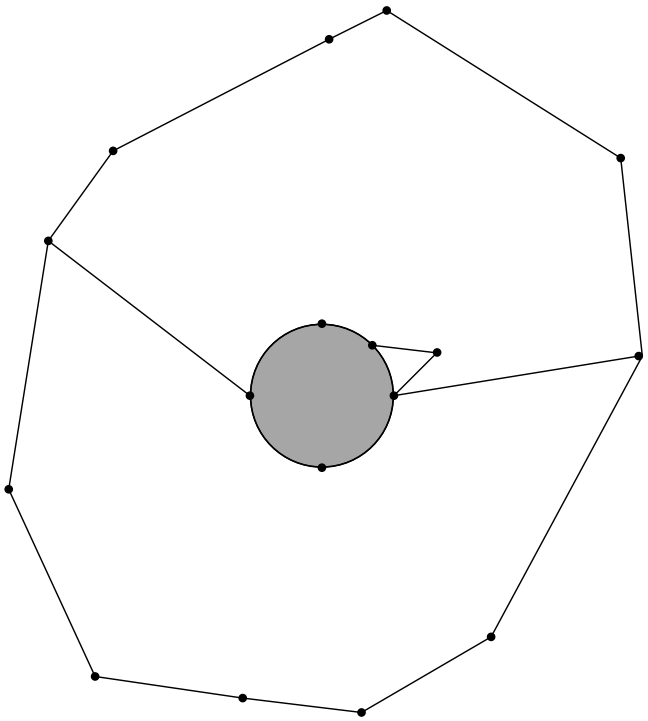

Figure 5.9: Loop system in D^2 after enclosed loops are removed

patches that map to translates of shingle 1. If $\Delta' : D^2 \to \kappa = K_2 \setminus orbit(T_2^o)$, then there are no patches that map to translates of shingle 2. Further, if $\Delta' : D^2 \to K_2 \setminus orbit(T_3^o)$ then there are no patches that map to translates of shingles 3, or 4. This observation also holds if Δ' is the original arbitrary filling of ρ, because if Δ' avoids $orbit(T_i^o)$ then the homotopy making Δ' simplicial does as well.

Much of this work will investigate the question, "what is the minimal simply-connected subcomplex of K_2 that is preserved under the action of $Aut(F_n)$?" To this end, we will be considering subcomplexes of K_2 obtained by removing the interiors of all representatives of given 2-simplices in $K^2/Aut(F_n)$, and determining if these subcomplexes have trivial fundamental group. The following corollary is a step in understanding the topology of these subcomplexes.

Corollary 5.4.1. *Let $\rho : S^1 \to K_1$ be an embedded edge loop and $\Delta' : D^2 \to K_2$ be a*

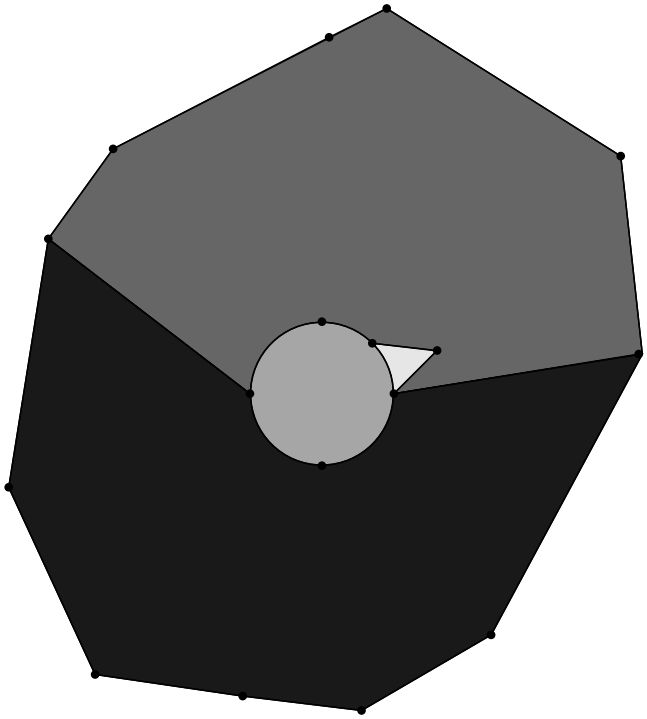

Figure 5.10: Loop system in D^2 with shading corresponding to Figure 5.11

filling of ρ.

1. *If the image of* Δ' *is contained in* $K_2 \setminus orbit(\mathsf{F}_7^o)$*, then there exists a patched filling of* ρ *where there are no patches that map to translates of shingle* 1.
2. *If the image of* Δ' *is contained in* $K_2 \setminus orbit(\mathsf{F}_1^o)$*,* $K_2 \setminus orbit(\mathsf{F}_2^o)$*, or* $K_2 \setminus orbit(\mathsf{F}_3^o)$ *then there exists a patched filling of* ρ *where there are no patches that map to translates of shingle* 2.
3. *If the image of* Δ' *is contained in* $K_2 \setminus orbit(\mathsf{F}_6^o)$*, then there exists a patched filling of* ρ *where there are no patches that map to translates of shingle* 3.
4. *If the image of* Δ' *is contained in* $K_2 \setminus orbit(\mathsf{F}_4^o)$*,* $K_2 \setminus orbit(\mathsf{F}_5^o)$*, or* $K_2 \setminus orbit(\mathsf{F}_6^o)$ *then there exists a patched filling of* ρ *where there are no patches that map to translates of shingle* 4.

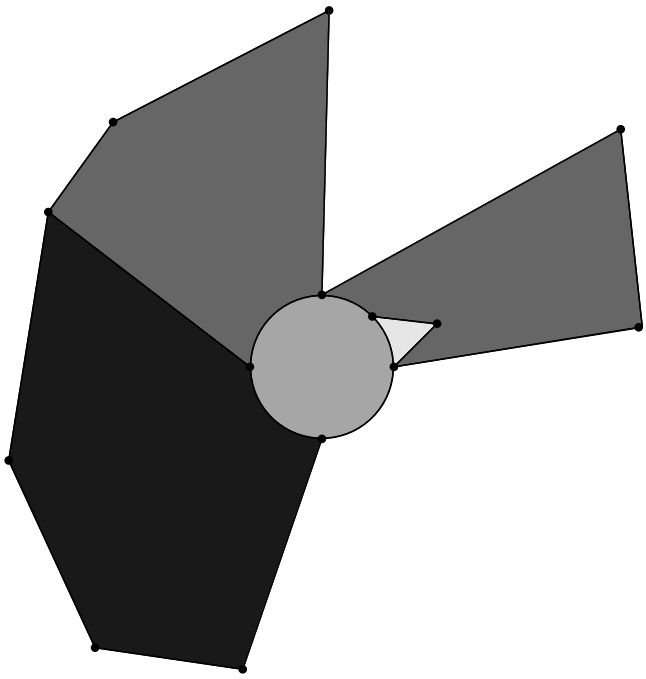

Figure 5.11: Loop system in D^2 with shading corresponding to Figure 5.10

Proof. 1. This is clear since $orbit(T_1^o) = orbit(\mathsf{F}_7^o)$.

2. Figure 5.12 shows the translates of F_1, F_2, and F_3 in T_2. The dark shaded simplices are translates of F_1, the unshaded simplices are translates of F_2, and the lightly shaded simplices are translates of F_3.

   Note that removing the translates of F_1 from tile 2 disconnects the interior of the tile. The intersection of the boundary of each of these pieces with K_1 has trivial fundamental group. The arguments of sections 5.2 and 5.3 apply. The only difference is that any edge loop ρ in the boundary of one of these pieces has a patched disk tree with no 2-cells since the image of ρ is nullhomotopic. Patches corresponding to shingle 2 are not needed to make a patched filling.

   Removing the translates of F_2 from tile 2 leaves tile 2 as a sequence of 2-dimensional simplicial complexes connected to each other by 0-simplices not in K_1. In particular, the intersection of the boundary of the remainder of

tile 2 and K_1 is a disjoint union of trees, and any loop in this boundary is nullhomotopic. This implies that any edge loop in this boundary has a patched disk tree with no 2-cells and patches that map to translates of shingle 2 are not needed to make a patched filling.

Removing the translates of F_3 from tile 2 leaves an infinite ribbon where the intersection of the boundary of the ribbon and K_1 is two disjoint copies of the line which have trivial fundamental group. As stated above, this implies that patches that map to translates of shingle 2 are not needed to make a patched filling.

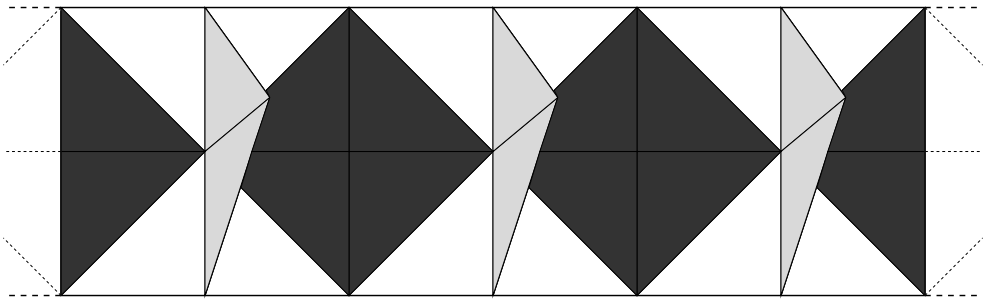

Figure 5.12: Translates of F_1, F_2, and F_3 in T_2.

3. Figure 5.13 shows the translates of F_4, F_5, and F_6 in T_3. The unshaded/transparent simplices are translates of F_4, the lightly shaded simplices are translates of F_5, and the dark shaded simplices are translates of F_6.

   Removing the translates of F_6 from tile 3 leaves the intersection K_1 and the boundary of the remainder of tile 3 as a disjoint union of trees. This implies that any edge loop in this boundary has a patched disk tree with no 2-cells since the image of ρ is nullhomotopic in K_1. No patches that map to shingles 3 or 4 are needed to make a patched filling.

4. Note that removing the translates of F_4 from tile 3 disconnects the interior of the tile into three pieces. The boundary of each of these pieces has fundamental group F_1 which is generated by the boundary of an $Aut(F_n)$ translate of shingle 3. The arguments of sections 5.2 and 5.3 apply. The only difference is that any edge loop ρ in the boundary of one of these pieces has a patched disk tree where each 2-cell maps to a translate of shingle 3. Patches that map to translates of shingle 4 are not needed to make a patched filling.

   Removing the translates of F_5 from tile 3 leaves tile 3 as a union of four 2-complexes connected at 0-simplices that are not in K_0. For three of these four pieces, the intersection of their boundary and K_1 is the boundary circle of an $Aut(F_n)$ translate of shingle 3. The other 2-complex has only zero dimensional intersection with K_1. This implies that patches that map to translates of shingle 4 are not needed to make a patched filling.

   To see that shingle 4 is unnecessary if translates of F_6 are removed, see part 3 of this corollary.

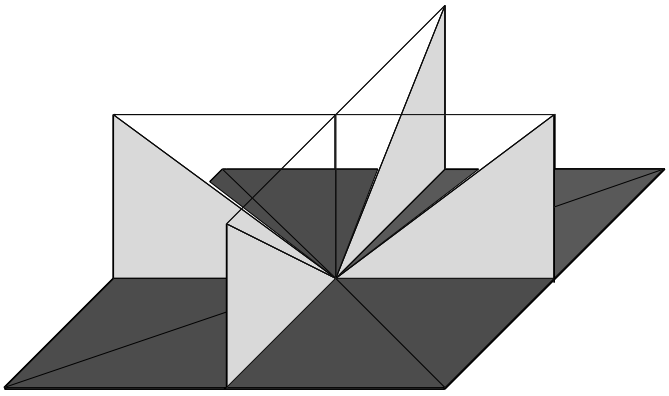

Figure 5.13: Translates of F_4, F_5, and F_6 in T_3.

□

5.5 Simplifying Patched Fillings - M-pod Simplification

In the chapters to follow it will not only be necessary to consider patched fillings of edge loops in K_1, but we will need these patched fillings to be in the simplest form possible. Specifically, this section simplifies neighborhoods in D^2 of Nielsen points, vertices that map to vertices in K_1 represented by (g, θ_n) for some marking g. The main result of this section is that each embedded edge loop has a patched filling where each of these neighborhoods intersect at most 3 patches, a property that will be useful in proving that certain loops cannot be nullhomotoped in subcomplexes of K_2. Such patched fillings will be called *simple patched fillings.*

Definition 16. *A patched filling $\Delta : D^2 \to K_2$ of an embedded edge loop $\rho : S^1 \to K_1$ is* simple *if every Nielsen point of D^2 is contained in no more than 3 patches, and if each Nielsen point of D^2 in ∂D^2 in contained in no more than 2 patches.*

The main result of this section is the following proposition:

Proposition 5.5.1. *For each embedded edge loop $\rho : S^1 \to K_1$, with a patched filling $\Delta : D^2 \to K_2$ there exists a simple patched filling $\Delta_S : D^2 \to K_2$ of ρ so that Δ_S uses patches of the same types as Δ.*

Proof. Let $\rho : S^1 \to K_1$ be an embedded edge loop with patched filling $\Delta : D^2 \to K_2$ and let x be a Nielsen point in D^2. Note that $st(\Delta(x)) \cap K_1$ is a tripod, where $st(x)$ denotes the star of x. Enumerate the non-backtracking paths between boundary points of $st(\Delta(x)) \cap K_1$ as γ_0, γ_1, and γ_2. Each translated shingle that contains $\Delta(x)$ only contains one of these three paths. A translated shingle is of type i if it contains γ_i. Further, a patch containing x is of type i if its image under Δ is a shingle of type i.

To make this more precise, consider the topological space constructed by taking 3 copies of $[0,1] \times [0,1] = X$, and ordering these copies X_0, X_1, and X_2. Identify $\{0\} \times x$ in X_i with $\{0\} \times 1 - x$ in X_{i+1}, for $0 \leq x \leq \frac{1}{2}$ so that $(0, \frac{1}{2})$ is identified in all three squares and where $0 \leq i \leq 2$ and $i + 1$ is taken mod 3. Call this space Y. The subcomplex of K_2 consisting of all shingles that contain $\Delta(x)$ maps onto Y by taking x to the unique point that is in the intersection of the three X_i, and shingles of type i to X_i. Denote this map q.

Traversing the boundary of a small neighborhood of x, starting at a point on that boundary whose image under Δ is in K_1, produces a word in the numbers 0, 1, and 2 given by the type of patch passed through, or alternately the X_i passed through by the image of this boundary loop under q. Passing to a cyclic word makes this independent of the chosen starting point. If the same number appears consecutively in this word, apply the alteration to Δ depicted in Figure 5.14. In Figure 5.14, the black dots are rose points, vertices that map to K_0, and the white dots are Nielsen points. The new point x now has the same cyclic word as x did previously with those consecutive numbers removed.

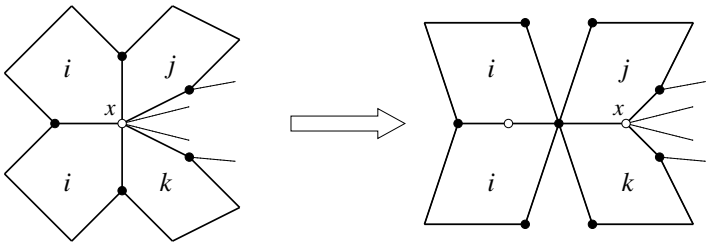

Figure 5.14: Double letter M-pod simplification.

More descriptively, suppose that $\ldots jiik \ldots$ appears in the word associated to x, and consider the subcomplex of D^2 made up of the patches corresponding to this subword. The intersection of $st(x) \cap \Delta^{-1}(K_1)$ and the interior of this subcomplex is either a tripod or a 4-pod the branches of which separate patches in

the subcomplex. This simplification can be viewed as cutting a slit along the branch separating the patch of type j and a patch of type i and the branch separating the patch of type k and a patch of type i. Following this cutting, fold this slit closed by identifying the branches along the patches of type i with one another and identifying the branch along the patch of type j with the branch along the patch of type k in the unique way that respects the simplicial structure of D^2. Δ is well-defining after this refolding is because the images of the folded edges under Δ agree. This simplification can be applied successively until there are no further double letters appearing in the cyclic word associated to x.

Since the word associated to x contains no double letters, $q \circ \Delta$ restricted to the boundary of a small neighborhood of x locally injects into Y. Hence, the word associated to x can have one of two forms: $\ldots 012012 \ldots$ or $\ldots 210210 \ldots$, where the difference is only due to the orientation chosen to pass around the neighborhood of x. Without loss of generality choose the direction that puts the word in the former form. For each instance of $\ldots 20120 \ldots$ in the word apply the simplification depicted in Figure 5.15. In Figure 5.15, the black dots are rose points and the white dots are Nielsen points.

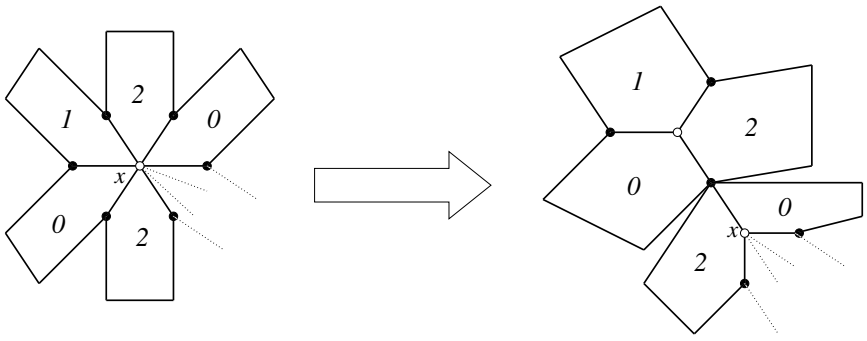

Figure 5.15: 012 M-pod simplification.

Consider the subcomplex of D^2 made up of the patches corresponding to this

subword. The intersection of $st(x) \cap \Delta^{-1}(K_1)$ and the interior of this subcomplex is a 4-pod, the branches of which separate patches in the subcomplex. Similarly to the removal of double numbers in the string associated to x, this simplification can be viewed as a cut and fold operation. In particular, the branches on the 4-pod separating patches of types 0 and 2 are cut, and then these edges are refolded so that the edges on patches of type 0 are identified with the unique edge in the slit that is on a patch of type 2 that the edge was not originally identified with. The folding is done in the unique way that respects the simplicial structure of D^2, and Δ is well-defined after the folding because the images of the folded edges under Δ agree. Repeated application of this simplification removes 012 from the word associated to x until there is only one instance of 012 remaining. For this new filling, there is a neighborhood of x that only intersects 3 patches.

For the case where $x \in S^1$, we perform the same process with one small alteration. There is a number associated to x given by the image of the star of x in S^1. This image is a path γ_i for some i, since ρ is a simple loop. To define the cyclic word associated to x, note that in traveling along the boundary of a neighborhood of x this loop must pass through x, and upon passing through x add the number i on to the end of the word. This is done because there is an implicit patch outside of D^2 of type i that may thought of as connecting to D^2 along the star of x in S^1. Given this alteration, the previously described steps of the simplification proceed without difficulty. Note that these alterations do not change the edges in S^1, and that after this simplification x is contained in no more than 2 patches.

A new patched filling of ρ has been produced so that each Nielsen point on the boundary of D^2 is contained in no more than 2 patches, while all other Nielsen points are contained in no more than 3 patches. $\square$

Proposition 5.5.1 together with Theorem 5.2.1 and the Degree Theorem gives the following corollary:

Corollary 5.5.1. *For each embedded edge loop $\rho : S^1 \to K_1$, there exists a simple patched filling of ρ.*

CHAPTER 6

COMPLEXITY MEASURE ON PATHS IN K_1

Over the next three chapters, the question "Can we do better?" is investigated. More specifically, is there a simply-connected subcomplex of K_2 that is preserved under the action of $Aut(F_n)$ that does not contain κ? The motivation for asking this question comes from Theorems 2.2.2 and 2.2.3, in that we would like to know if it is possible to simplify this presentation further by considering a different subcomplex of K_2. In the next three chapters we will prove Theorem 8.5.2 which answers this question in the negative direction. Specifically, Theorem 8.5.2 states that every simply-connected subcomplex of K_2 that is preserved under the action of $Aut(F_n)$ contains κ. In this way κ is minimal and the presentations in Theorems 2.2.2 and 2.2.3 cannot be simplified by this method.

The idea of the proof is to take the orbits of 2-simplices in K_2 one at a time and prove that K_2 without that orbit is not simply-connected. In this chapter, we show that $K_2 \setminus orbit(\mathsf{F}_7^o)$ is not simply-connected by proving Theorem 6.5.1 which states that the loop $Shin_1(id)|_{\partial D^2}$ is not nullhomotopic in $K_2 \setminus orbit(\mathsf{F}_7^o)$, where F_7^o is the of interior of a representative of the 2-simplex f_7 in $K_2/Aut(F_n)$ shown in Figure 2.5. Suppose that there is nullhomotopy of $Shin_1(id)|_{\partial D^2}$ in $K_2 \setminus orbit(\mathsf{F}_7^o)$, by Corollary 5.4.1(a) assume that the nullhomotopy is a simple patched filling with no patches corresponding to shingle 1. To show that no such filling exists, we will construct a complexity measure on loops in K_1 that returns a vector. The construction of this complexity measure and its application to $Shin_1(id)|_{\partial D^2}$ are the focus of this chapter. Unfortunately, this complexity measure is not useful for the other parts of the proof of minimality of κ, and this is the only chapter that will use this method.

We will study the change in the complexity that occurs when loops pass over shingles. For the constant loop, this measure will return the zero vector, and we will show that the vector given by the boundary of $Shin_1(id)|_{\partial D^2}$ cannot be reduced to the zero vector by shifting the loop over shingles of types 2, 3, or 4. This will complete the proof that $K_2 \setminus orbit(\mathsf{F}_7^o)$ is not simply-connected.

6.1 Tensor Products on Automorphism Lists

By Proposition 4.1.1 edge paths in K_1 can be lifted by the map $\Phi : Y^1 \to K_1$ where Y^1 is the Cayley graph associated to Gersten's presentation of $SAut(F_n)$. Before defining the complexity of an edge path in K_1, we will instead define the complexity of an automorphism list, and then use this lift to define complexity for edge paths in K_1. This section takes the first step to defining complexity on automorphism lists, and gives a matrix construction on these lists.

Definition 17. *For $\alpha, \beta \in Aut(F_n)$ the homomorphism $\delta : F_n \to F_n$ mapping a_i to $\beta(a_i)\alpha(a_i)^{-1}$ is the* difference of α and β.

For example, let $n = 2$ and note that the difference δ of $E_{a_2\bar{a}_1}$ and γ is

$$\delta\colon \begin{cases} a_1 \mapsto \bar{a}_1\bar{a}_1a_2 \\ a_2 \mapsto \bar{a}_1\bar{a}_1a_2a_1\bar{a}_2, \end{cases}$$

where γ is given by

$$\gamma\colon \begin{cases} a_1 \mapsto \bar{a}_1\bar{a}_1a_2a_1 \\ a_2 \mapsto \bar{a}_1\bar{a}_1a_2. \end{cases}$$

Definition 18. *Let $\mathcal{P}$ be the map from self-homomorphisms of F_n to $n \times n$ matrices with coefficients in $\mathbb{Z}/2$ induced by abelianizing the generators of F_n, and then taking coefficients in $\mathbb{Z}/2$.*

For example, note that

$$\mathcal{P}(\gamma) = \begin{bmatrix} 1 & 1 \\ 0 & 1 \end{bmatrix},$$

and that

$$\mathcal{P}(\delta) = \begin{bmatrix} 0 & 1 \\ 1 & 0 \end{bmatrix}.$$

Definition 19. *For $\alpha, \beta \in Aut(F_n)$ let $\alpha \times \beta$ denote the tensor product $\mathcal{P}(\beta) \otimes \mathcal{P}(\delta)$.*

For a quick example

$$E_{a_2\bar{a}_1} \times \gamma = \begin{bmatrix} 0 & 1 & 0 & 1 \\ 1 & 0 & 1 & 0 \\ 0 & 0 & 0 & 1 \\ 0 & 0 & 1 & 0 \end{bmatrix}.$$

For this chapter, all arithmetic on matrices and vectors with coefficients in $\mathbb{Z}/2$ will be taken mod 2.

Definition 20. *Let $A = \alpha_1, \alpha_2, \ldots, \alpha_k$ be a list of automorphisms. Then the matrix ξ of this automorphism list is given by $\xi(A) = \sum_{i=1}^{k-1} \alpha_i \times \alpha_{i+1}$.*

Example: Let the homomorphism that takes a_i to b_i be denoted by the n-tuple $(b_1, b_2, \ldots, b_n)$, and the empty word be denoted by 1. Let $n = 3$ and consider the automorphism list $C = id$, $E_{a_1\bar{a}_2}$, $E_{a_2\bar{a}_3}E_{a_1\bar{a}_2}$, $E_{a_1a_2}E_{a_2\bar{a}_3}E_{a_1\bar{a}_2}$, $E_{a_2a_3}E_{a_1a_2}E_{a_2\bar{a}_3}E_{a_1\bar{a}_2}$,

id. Then

$$\begin{aligned}\xi(A) &= E_{a_1\bar{a}_2} \times (a_1\bar{a}_2\bar{a}_1, 1, 1) + E_{a_2\bar{a}_3}E_{a_1\bar{a}_2} \times (1, a_2\bar{a}_3\bar{a}_2, 1) \\ &+ E_{a_1a_2}E_{a_2\bar{a}_3}E_{a_1\bar{a}_2} \times (a_1\bar{a}_3a_2\bar{a}_1, 1, 1) + E_{a_2a_3}E_{a_1a_2}E_{a_2\bar{a}_3}E_{a_1\bar{a}_2} \\ &\times (1, a_2a_3\bar{a}_2, 1) + id \times (a_1a_3\bar{a}_1, 1, 1).\end{aligned}$$

Calculating these tensor products yields:

$$\left[\begin{array}{ccc|ccc|ccc} 0&1&0&0&1&0&0&0&0\\ 0&0&0&0&0&0&0&0&0\\ 0&0&0&0&0&0&0&0&0\\ \hline 0&0&0&0&1&0&0&0&0\\ 0&0&0&0&0&0&0&0&0\\ 0&0&0&0&0&0&0&0&0\\ \hline 0&0&0&0&0&0&0&1&0\\ 0&0&0&0&0&0&0&0&0\\ 0&0&0&0&0&0&0&0&0 \end{array}\right] + \left[\begin{array}{ccc|ccc|ccc} 0&0&0&0&0&0&0&0&0\\ 0&0&1&0&0&1&0&0&0\\ 0&0&0&0&0&0&0&0&0\\ \hline 0&0&0&0&0&0&0&0&0\\ 0&0&0&0&0&1&0&0&1\\ 0&0&0&0&0&0&0&0&0\\ \hline 0&0&0&0&0&0&0&0&0\\ 0&0&0&0&0&0&0&0&1\\ 0&0&0&0&0&0&0&0&0 \end{array}\right] +$$

$$\left[\begin{array}{ccc|ccc|ccc} 0&1&1&0&0&0&0&1&1\\ 0&0&0&0&0&0&0&0&0\\ 0&0&0&0&0&0&0&0&0\\ \hline 0&0&0&0&1&1&0&1&1\\ 0&0&0&0&0&0&0&0&0\\ 0&0&0&0&0&0&0&0&0\\ \hline 0&0&0&0&0&0&0&1&1\\ 0&0&0&0&0&0&0&0&0\\ 0&0&0&0&0&0&0&0&0 \end{array}\right] + \left[\begin{array}{ccc|ccc|ccc} 0&0&0&0&0&0&0&0&0\\ 0&0&1&0&0&0&0&0&1\\ 0&0&0&0&0&0&0&0&0\\ \hline 0&0&0&0&0&0&0&0&0\\ 0&0&0&0&0&1&0&0&0\\ 0&0&0&0&0&0&0&0&0\\ \hline 0&0&0&0&0&0&0&0&0\\ 0&0&0&0&0&0&0&0&1\\ 0&0&0&0&0&0&0&0&0 \end{array}\right] +$$

$$\left[\begin{array}{ccc|ccc|ccc}
0&0&1&0&0&0&0&0&0\\
0&0&0&0&0&0&0&0&0\\
0&0&0&0&0&0&0&0&0\\
\hline
0&0&0&0&0&1&0&0&0\\
0&0&0&0&0&0&0&0&0\\
0&0&0&0&0&0&0&0&0\\
\hline
0&0&0&0&0&0&0&0&1\\
0&0&0&0&0&0&0&0&0\\
0&0&0&0&0&0&0&0&0
\end{array}\right] = \left[\begin{array}{ccc|ccc|ccc}
0&0&0&0&1&0&0&1&1\\
0&0&0&0&0&1&0&0&1\\
0&0&0&0&0&0&0&0&0\\
\hline
0&0&0&0&0&0&0&1&1\\
0&0&0&0&0&0&0&0&1\\
0&0&0&0&0&0&0&0&0\\
\hline
0&0&0&0&0&0&0&0&0\\
0&0&0&0&0&0&0&0&0\\
0&0&0&0&0&0&0&0&0
\end{array}\right] = \xi(C).$$

6.2 Action of the Symmetric Group

When generalizing ξ to paths in K_1, we will encounter the issue that there are multiple lifts under Φ of the same path. These lifts are related by the action of the signed symmetric group W_n of $Aut(F_n)$ that permutes and inverts the generators. Since inverting does not effect coefficients in $\mathbb{Z}/2$, in this section we will be studying the action of the symmetric group Σ_n on the complexity measure.

Throughout this chapter, x will be an integer with $1 \leq x \leq n^2$ and u and v be the unique integers with $x = n(u-1)+v$ and $1 \leq u, v \leq n$. Σ_n acts on $n^2 \times n^2$ matrices. For a matrix M and $s \in \Sigma_n$, this action is given by $s \cdot M_{x,y} = M_{n(s(u)-1)+s(v),y}$. The effect of s on $\alpha \times \beta$ is that s permutes the rows, though not all permutations are allowed. There are two orbits for rows of $\alpha \times \beta$ under this action, the $(1+(n+1)z)$-th rows for some integer z form an n row orbit and the remaining rows form an $n^2 - n$ row orbit. Choosing an orbit, and adding the entries down each column that is in the orbit gives a new complexity measure that is invariant under the action of Σ_n.

Definition 21. *Let M be an $n^2 \times n^2$ matrix. Let $\nu(M)$ be a $1 \times n^2$ vector where $\nu_i(M) = \sum_{j=1}^{n} M_{1+(n+1)(j-1),i}$. Let $\mu(M)$ be a $1 \times n^2$ vector, where $\mu_i(M) = (\sum_{j=1}^{n^2} M_{j,i}) - \nu_i(M)$.*

Definition 22. *For an automorphism list A, $\nu(\xi(A))$ and $\mu(\xi(A))$ will be called the* symmetric complexity *and* anti-symmetric complexity *of A respectively.*

Proposition 6.2.1. *$\nu(\xi(A)) = \nu(s\xi(A))$, and $\mu(\xi(A)) = \mu(s\xi(A))$ for all automorphism lists A and all $s \in \Sigma_n$.*

Proof. The proof is immediate from the definition of the action of Σ_n on $n^2 \times n^2$ matrices. □

Abusing notation, $\nu(\xi(A))$ and $\mu(\xi(A))$ will be written as $\nu(A)$ and $\mu(A)$.

Example: Let $n = 3$ and consider the automorphism list from the example in the previous section $C = id$, $E_{a_1\bar{a}_2}$, $E_{a_2\bar{a}_3}E_{a_1\bar{a}_2}$, $E_{a_1a_2}E_{a_2\bar{a}_3}E_{a_1\bar{a}_2}$, $E_{a_2a_3}E_{a_1a_2}E_{a_2\bar{a}_3}E_{a_1\bar{a}_2}$, id. Then:

$$\nu(C) = \begin{bmatrix} 0 & 0 & 0 & 0 & 1 & 0 & 0 & 1 & 0 \end{bmatrix}, \text{ and}$$

$$\mu(C) = \begin{bmatrix} 0 & 0 & 0 & 0 & 0 & 1 & 0 & 1 & 0 \end{bmatrix}.$$

The complexity of an automorphism list is a particular sum of the symmetric and antisymmetric complexity. To describe this sum, some notation must be mentioned first. Let f be the natural bijection from $1 \times n^2$ vectors to $n \times n$ matrices given by $f(V_x) = M_{u,v}$. Then for a $1 \times n^2$ vector let $V^T = f^{-1}(f(V)^T)$.

Definition 23. *The* complexity χ *of an automorphism list* A *is the sum* $\chi(A) = \mu(A) + \nu(A)^T + \nu(A)$

Building on the above example:

$$\begin{aligned}
\chi(C) &= \begin{bmatrix} 0 & 0 & 0 & 0 & 0 & 1 & 0 & 1 & 0 \end{bmatrix} + \begin{bmatrix} 0 & 0 & 0 & 0 & 1 & 1 & 0 & 0 & 0 \end{bmatrix} \\
&+ \begin{bmatrix} 0 & 0 & 0 & 0 & 1 & 0 & 0 & 1 & 0 \end{bmatrix} \\
&= \begin{bmatrix} 0 & 0 & 0 & 0 & 0 & 0 & 0 & 0 & 0 \end{bmatrix}
\end{aligned}$$

More generally, we will see in this chapter that if A is an automorphism list obtained by traversing the boundary of any shingle that is not a translate of shingle 1, then $\chi(A)$ is the zero vector. This in combination with the observation that χ is non-zero for the automorphism list given by traversing the boundary of shingle 1 will prove that there is no nullhomotopy of the boundary of shingle 1 that does not use translates of shingle 1.

6.3 Passing from Paths in K_1 to Automorphism Lists

Automorphism lists can be obtained from paths in K_1. Let ρ be an edge path in K_1 and let $r = r_1, r_2, \ldots, r_k$ be the rose list determined by ρ. Choose α_1 to be an automorphism so that $\alpha_1 \cdot I = r_1$. By Proposition 4.1.1, choosing α_1 fixes a unique list of automorphisms $\alpha_2, \alpha_3, \ldots \alpha_k$, so that for $2 \leq i \leq k$,

1. $\alpha_i = E_{ab}\alpha_{i-1}$ or $\alpha_i = \alpha_{i-1}$, and
2. $\alpha_i \cdot I = r_i$.

Note that for $s \in W_n$, $\alpha_1 s \cdot I = r_1$, so we are making a choice here. Suppose β_1 is another possible choice and let $\beta_1 = \alpha_1 s$. Then note that $\beta_i = \alpha_i s$ for all i with $1 \leq i \leq k$.

Accounting for the fact that automorphisms act by altering labels by their inverses, consider the inverse of the automorphism lists A and B. Let $A^{-1} = \alpha_1^{-1}, \alpha_2^{-1}, \ldots \alpha_k^{-1}$ and $B^{-1} = \beta_1^{-1}, \beta_2^{-1}, \ldots, \beta_k^{-1}$. Direct calculation yields $\xi(B^{-1}) = s'\xi(A^{-1})$, where $s' \in \Sigma_n$ is given by $s \in W_n$ by forgetting inverses. Hence, $\nu(A^{-1}) = \nu(B^{-1})$ and $\mu(A^{-1}) = \mu(B^{-1})$ leading to the following definition:

Definition 24. *Let ρ be an edge path in K_1 and A be an automorphism list given by ρ as described above. Then let $\nu(\rho) = \nu(A^{-1})$, $\mu(\rho) = \mu(A^{-1})$, and $\chi(\rho) = \chi(A^{-1})$ be the* symmetric complexity of ρ, *the* antisymmetric complexity of ρ, *and the* complexity of ρ *respectively.*

6.4 Loop Operations

A simple patched filling of an edge path in K_1 defines a sequence of edge paths so that two successive paths are related by passing over a shingle and the last path is the constant path. The goal of the remainder of this chapter is to show that $Shin_1(id)|_{\partial D^2}$ is not nullhomotopic in $K_2 \setminus orbit(\mathsf{F}_7^o)$ by showing that there is no simple patched filling of $Shin_1(id)|_{\partial D^2}$ that has no patches mapping to shingle 1. This will be accomplished by showing that no sequence of edges paths in K_1 beginning with $Shin_1(id)|_{\partial D^2}$, where successive paths are related by passing over a shingle other than shingle 1, can result in the constant path. The complexity will be the key ingredient in this proof, and studying how the complexity changes when a path moves over a shingle is important to the proof. This section defines

operations on edge paths in K_1 that correspond to passing over shingles. The next section will consider the effect of these operations on the complexity.

For an edge path ρ in K_1, let ρ_i be the initial subpath of ρ that ends once ρ has traversed i rose vertices counted with multiplicity. ρ'_i is the terminal subpath of ρ that begins once p has traversed i rose vertices counted with multiplicity. For the remainder of this chapter we will assume that edge paths do not backtrack at Nielsen vertices. In other words, whenever an edge path traverses a Nielsen vertex it must enter and leave through two distinct edges. This assumption causes no problems because all of the operations that will be described preserve this property, and $Shin_1(id)|_{\partial D^2}$ has this property to begin with it.

To start, an operation corresponding to each shingle is defined. Let $\mathcal{S}^j_{k,\alpha}$ the *shingle j operation* be defined so that $\mathcal{S}^j_{k,\alpha}(\rho)$ is the edge path given by first traversing ρ_k then $Shin_j(\alpha)|_{\partial D^2}$ and lastly ρ'_k. This operation can only be applied if the k-th rose traversed by ρ is $\alpha \cdot I$. This requirement is enforced on all of the operations defined below as well. We do not consider shingle 5 operations, as discussed in chapter 5, patches mapping to shingle 5 are not needed in simple patched fillings.

For each shingle operation there is a reverse shingle operation that corresponds to traversing the boundary of the shingle in the clockwise direction. The *reverse shingle j operation* is denoted $\mathcal{S}'^j_{k,\alpha}$. When $\mathcal{S}'^j_{k,\alpha}$ is applied to ρ, the resulting edge path is given by first traversing ρ_k then $Shin_j(\alpha)|_{\partial D^2}$ in the clockwise direction and lastly ρ'_k. Note that $\mathcal{S}'^1_{k,\alpha} = \mathcal{S}^1_{k,\alpha\sigma_{13}\sigma_{24}}$, so for each reverse shingle 1 operation there exists a shingle 1 operation that has the same effect. Reverse shingle 1 operations are not considered for this reason.

The shingle and reverse shingle operations cover all of the necessary cases

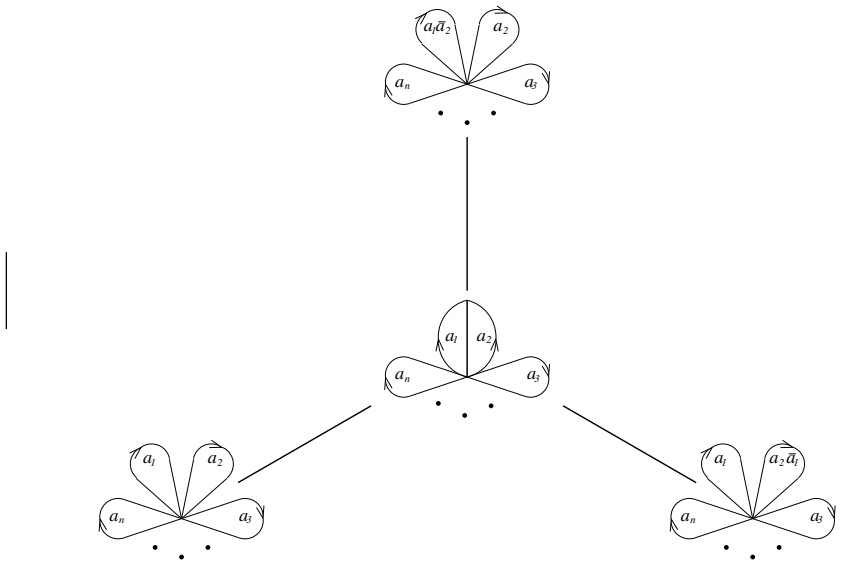

Figure 6.1: Defining tripod for Nielsen operations

of branching that can occur between two edge paths at rose vertices. However, branching can also occur at Nielsen vertices. To cover the cases of branching occurring at Nielsen vertices, one additional operation is included, the *Nielsen operation.* A Nielsen operation corresponds to traversing an $Aut(F_n)$ translate of the tripod shown in Figure 6.1 in the counter-clockwise direction. Specifically, $\mathcal{N}_{k,\alpha}(\rho)$ is the rose path that first traverses ρ_k then the α translate of the tripod shown in Figure 6.1 in the counterclockwise direction starting at $\alpha \cdot I$ and lastly ρ'_k. Observe that the action of σ_{12} on Figure 6.1 flips the tripod, so that traversing this tripod in the clockwise direction is the same as traversing its σ_{12} translate in the counter-clockwise direction. A reverse Nielsen move $\mathcal{N}'_{k,\alpha}$ would be given by $\mathcal{N}_{k,\sigma_{12}\alpha}$ and is unnecessary for this reason. Since we are assuming that we have a simple patched filling, no other operations are necessary to handle branching at Nielsen vertices.

To complete the set of operations that can be performed on edge paths to allow them to pass over a shingle, consider operations that correspond to inserting or

deleting backtracking edges. More specifically, $\mathcal{A}_{k,\alpha}(\rho)$ traverses ρ_k followed by the length two rose path from $\alpha \cdot I$ to $\alpha E_{a_1 a_2} \cdot I$, that same length 2 rose path backwards, and ending with ρ'_k. To apply $\mathcal{D}_{k,\alpha}$ it is required that the k-th and $k+2$-th roses traversed by ρ are the same. This means that the piece of ρ between the k-th and $k+2$-th roses is a length 4 edge path where in third and fourth edges backtrack the second and first respectively. $\mathcal{D}_{k,\alpha}(\rho)$ is ρ with this backtracking deleted, the edge path given by traversing ρ_k followed by ρ'_{k+2}. These operations are called *addition*, and *deletion* operations respectively.

Definition 25. *The combined set of shingle, reverse shingle, Nielsen, addition, and deletion operations are called* loop operations *and denoted $\mathcal{O}$. An edge path that can be reduced to the trivial path by a sequence of loop operations is called* collapsible.

Remark: Note that inserting a collapsible edge path into a collapsible edge path produces a collapsible edge path.

Note that $Shin_j(\alpha)|_{\partial D^2}$ is collapsible by applying one reverse shingle j operation and four deletion operations if $j = 1, 2$, or 3 and five deletion operations if $j = 4$. Further, the edge path given by traversing $Shin_j(\alpha)|_{\partial D^2}$ in the clockwise direction is also collapsible, the only alteration is that a shingle j operation is needed.

Proposition 6.4.1. *Let $\rho : S^1 \to K_1$ be an edge loop with simple patched filling Δ. Then ρ is collapsible.*

Proof. Recall that ρ can be written as a concatenation $\rho = \rho_1 \rho_2 \dots \rho_k$ where $\rho_j = \gamma_j \lambda_j \gamma_j^{-1}$, λ_j is an edge loop traversing the boundary of a shingle or the edge loop traversing Figure 6.1, γ_j is a path from the first rose point traversed by ρ to the starting point of λ_j. $\gamma_j \lambda_j \gamma_j^{-1}$ can be collapsed by first collapsing λ_j using either a

shingle, reverse shingle, or Nielsen operation and addition and deletion operations, and then by collapsing $\gamma_j\gamma_j^{-1}$ with deletion operations. Since ρ is a concatenation of collapsible edge paths, it is collapsible. □

Proposition 6.4.2. *Let $\rho : S^1 \to K_1$ be an edge loop and let $\Delta : D^2 \to K_2$ be a filling of ρ. If the image of Δ is contained in $K_2 \backslash orbit(\mathsf{F}_7^o)$, then ρ can be collapsed without using any shingle 1 operations.*

Proof. The types of shingle and reverse shingle operations that need to be used in collapsing an edge loop equipped with a simple patched filling are given by the shingles that the patches of the simple patched filling map to. If there are no patches mapping to shingle j, then no shingle j nor reverse shingle j operations are necessary to collapse the edge loop. This proposition is now immediate from Corollary 5.4.1. □

6.5 Effect of Loop Operations on Complexity

The central question of this section is, what effect do loop operations have on the complexity of an edge loop in K_1? How are $\chi(\rho)$ and $\chi(\mathcal{O}_o(\rho))$ related for an edge loop ρ and loop operation $\mathcal{O}_o$? We will begin by calculating $\nu(\mathcal{O}_o(\rho)) - \nu(\rho)$ and $\mu(\mathcal{O}_o(\rho)) - \mu(\rho)$ for each loop operation.

Before giving the results of these calculations, note the following notation. Recall that for an integer x with $1 \leq x \leq n^2$, let u and v be the unique integers with $x = (u-1)n + v$ with $1 \leq u, v \leq n$. Also, for $w \in F_n$, let $|w|_k$ be the number of occurrences of a_k or $\bar{a}_k$ that appear in w taken mod 2. Then:

1. $[\mu(\mathcal{S}^1_{k,\alpha^{-1}}(\rho)) - \mu(\rho)]_x = |\alpha(a_2)|_u|\alpha(a_4)|_v + |\alpha(a_4)|_u|\alpha(a_2)|_v$

2. $[\mu(\mathcal{S}^2_{k,\alpha^{-1}}(\rho)) - \mu(\rho)]_x = [\mu(\mathcal{S}'^2_{k,\alpha^{-1}}(\rho)) - \mu(\rho)]_x = 0$

3. $[\mu(\mathcal{S}^3_{k,\alpha^{-1}}(\rho)) - \mu(\rho)]_x = [\mu(\mathcal{S}'^3_{k,\alpha^{-1}}(\rho)) - \mu(\rho)]_x = 0$

4. $[\mu(\mathcal{S}^4_{k,\alpha^{-1}}(\rho)) - \mu(\rho)]_x = |\alpha(a_2)|_u|\alpha(a_3)|_v + |\alpha(a_3)|_u|\alpha(a_2)|_v$

5. $[\mu(\mathcal{S}'^4_{k,\alpha^{-1}}(\rho)) - \mu(\rho)]_x = |\alpha(a_2)|_u|\alpha(a_3)|_v + |\alpha(a_3)|_u|\alpha(a_2)|_v$

6. $[\mu(\mathcal{N}_{k,\alpha^{-1}}(\rho)) - \mu(\rho)]_x = |\alpha(a_2)|_u|\alpha(a_1)|_v + |\alpha(a_1)|_u|\alpha(a_2)|_v$

7. $[\mu(\mathcal{A}_{k,\alpha^{-1}}(\rho)) - \mu(\rho)]_x = [\mu(\mathcal{D}_{k,\alpha^{-1}}(\rho)) - \mu(\rho)]_x = 0$

8. $[\nu(\mathcal{S}^1_{k,\alpha^{-1}}(\rho)) - \nu(\rho)]_x = |\alpha(a_2)|_u|\alpha(a_2)|_v + |\alpha(a_4)|_u|\alpha(a_4)|_v$

9. $[\nu(\mathcal{S}^2_{k,\alpha^{-1}}(\rho)) - \nu(\rho)]_x = [\nu(\mathcal{S}'^2_{k,\alpha^{-1}}(\rho)) - \nu(\rho)]_x = 0$

10. $[\nu(\mathcal{S}^3_{k,\alpha^{-1}}(\rho)) - \nu(\rho)]_x = [\nu(\mathcal{S}'^3_{k,\alpha^{-1}}(\rho)) - \nu(\rho)]_x = |\alpha(a_2a_3)|_u|\alpha(a_2a_3)|_v$

11. $[\nu(\mathcal{S}^4_{k,\alpha^{-1}}(\rho)) - \nu(\rho)]_x = |\alpha(a_2a_3)|_u|\alpha(a_2)|_v$

12. $[\nu(\mathcal{S}'^4_{k,\alpha^{-1}}(\rho)) - \nu(\rho)]_x = |\alpha(a_2a_3)|_u|\alpha(a_3)|_v$

13. $[\nu(\mathcal{N}_{k,\alpha^{-1}}(\rho)) - \nu(\rho)]_x = |\alpha(a_2)|_u|\alpha(a_2)|_v + |\alpha(a_1)|_u|\alpha(a_1)|_v + |\alpha(a_1)|_u|\alpha(a_2)|_v$

14. $[\nu(\mathcal{A}_{k,\alpha^{-1}}(\rho)) - \nu(\rho)]_x = [\nu(\mathcal{D}_{k,\alpha^{-1}}(\rho)) - \nu(\rho)]_x = |\alpha(a_2)|_u|\alpha(a_2)|_v$

Since $\chi(\mathcal{O}_o(\rho)) - \chi(\rho) = \mu(\mathcal{O}_o(\rho)) - \mu(\rho) + \nu(\mathcal{O}_o(\rho))^T - \nu(\rho)^T + \nu(\mathcal{O}_o(\rho)) - \nu(\rho)$ we can now calculate, $\chi(\mathcal{O}_o(\rho)) - \chi(\rho)$ for each loop operation. In particular, for all operations other than $\mathcal{S}^1_{k,\alpha^{-1}}$, $\chi(\mathcal{O}_o(\rho)) - \chi(\rho) = 0$. This is not necessarily true for shingle 1 operations.

Example:

$$\begin{aligned}
\mu(Shin_1(id)|_{\partial D^2})_x &= |a_2|_u|a_4|_v + |a_4|_u|a_2|_v, \\
\nu(Shin_1(id)|_{\partial D^2})_x &= |a_2|_u|a_2|_v + |a_4|_u|a_4|_v \text{ and,} \\
\chi(Shin_1(id)|_{\partial D^2})_x &= |a_2|_u|a_4|_v + |a_4|_u|a_2|_v.
\end{aligned}$$

In particular, $\chi(Shin_1(id)|_{\partial D^2})_8 = |a_2|_2|a_4|_4 + |a_4|_2|a_2|_4 = 1$.

Lemma 6.5.1. *Let $\mathcal{O}_1$, $\mathcal{O}_2$, $\ldots\mathcal{O}_m$ be a list of loop operations that collapses $Shin_1(id)|_{\partial D^2}$. Then at least one of the operations must be a shingle 1 operation.*

Proof. From the above example, $\chi(Shin_1(id)|_{\partial D^2})_8 = 1$. Further, suppose that the sequence of loop operations $\mathcal{O}_1$, $\mathcal{O}_2$, $\ldots\mathcal{O}_m$ collapses $Shin_1(id)|_{\partial D^2}$ and that there is no i so that $\mathcal{O}_i$ is a shingle 1 operation. For $\mathcal{O}_o = \mathcal{O}_m \circ \ldots\mathcal{O}_2 \circ \mathcal{O}_1$, $\chi(\mathcal{O}_o(Shin_1(id)|_{\partial D^2}))_8 = 1 \neq 0$. But $\mathcal{O}_o(Shin_1(id)|_{\partial D^2}))$ is the constant path, and $\chi(\mathcal{O}_o(Shin_1(id)|_{\partial D^2})))$ is the zero vector giving a contradiction. No such collapsing sequence of $Shin_1(id)|_{\partial D^2}$ exists. □

Theorem 6.5.1. *$Shin_1(id)|_{\partial D^2}$ is not nullhomotopic in $K_2 \setminus orbit(\mathsf{F}_7^o)$.*

Proof. Consider the loop $Shin_1(id)|_{\partial D^2}$, and suppose there is a filling $\Delta : D^2 \to K_2 \setminus orbit(\mathsf{F}_7^o)$. By Proposition 6.4.2, $Shin_1(id)|_{\partial D^2}$ can be collapsed without using any shingle 1 operations contradicting Lemma 6.5.1. Hence, there exists no filling of $Shin_1(id)|_{\partial D^2}$ in $K_2 \setminus orbit(\mathsf{F}_7^o)$. □

CHAPTER 7

NIELSEN CONNECTION GRAPH

Over the next two chapters, we will complete the proof that κ is the minimal simply-connected subcomplex of K_2 that is preserved under the action of $Aut(F_n)$. The main piece of this proof that remains is Theorem 8.5.1 which states that every simple patched filling of $Shin_4(id, x)|_{\partial D^2}$ must use shingle 4, which shows that $Shin_4(id, x)|_{\partial D^2}$ is not nullhomotopic in $K_2 \setminus orbit(\mathsf{F}_4^o)$, $K_2 \setminus orbit(\mathsf{F}_5^o)$, or $K_2 \setminus orbit(\mathsf{F}_6^o)$. In this proof, the *Nielsen connection graph* $\mathcal{N}$ is defined and plays a key role. $\mathcal{N}$ can be defined by considering shingles in K_2 and we will be show in Proposition 7.4.2 that each connected component of $\mathcal{N}$ embeds in K_2.

7.1 Basic Definitions

In this section $\mathcal{N}$ and the map ϕ of $\mathcal{N}$ into K_2 are defined and many basic properties of these objects are discussed.

Recall from chapter 3, that a Nielsen vertex is a vertex represented by (g, θ_n) in K_2. For example, Figures 2.1 and 7.6 are a Nielsen vertices.

Definition 26. *Two Nielsen vertices are* opposed to each other in T*, an* $Aut(F_n)$ *translate of Shingle 1, 2, or 3, containing both points and the radius 1 neighborhoods of these points in* $T \cap K_1$ *are disjoint.*

Two sets of opposed vertices are shown in Figure 7.1. Recall from chapter 5 that shingle 5 is not necessary to construct a simple patched filling, and so will not be considered here.

Definition 27. *The* Nielsen connection graph $\mathcal{N}$ *of* K_2 *is a graph whose vertices*

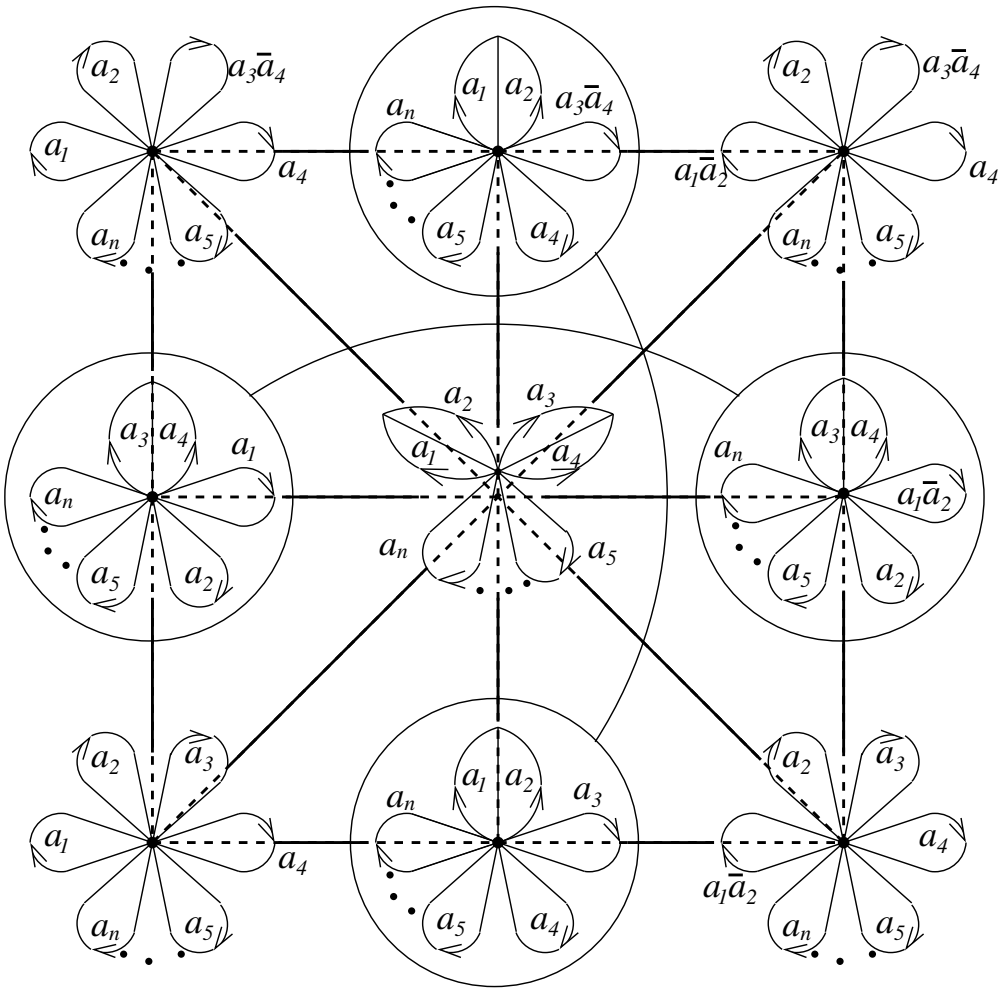

Figure 7.1: Opposed points in K_2

correspond to Nielsen vertices and in which two vertices are connected by an edge if the corresponding Nielsen vertices are opposed to each other.

Part of $\mathcal{N}$ for $n = 2$ is shown in Figure 7.2.

Note that $\mathcal{N}$ maps to K_2 in the natural way, taking vertices to the corresponding Nielsen vertices, and taking the edges of $\mathcal{N}$ to the straight path in the shingle containing the images of both vertices as shown in Figures 7.3, 7.4, and 7.5. This map is denoted ϕ. Note that if v_1, $v_2 \in V\mathcal{N}$ are opposed points whose ϕ-images

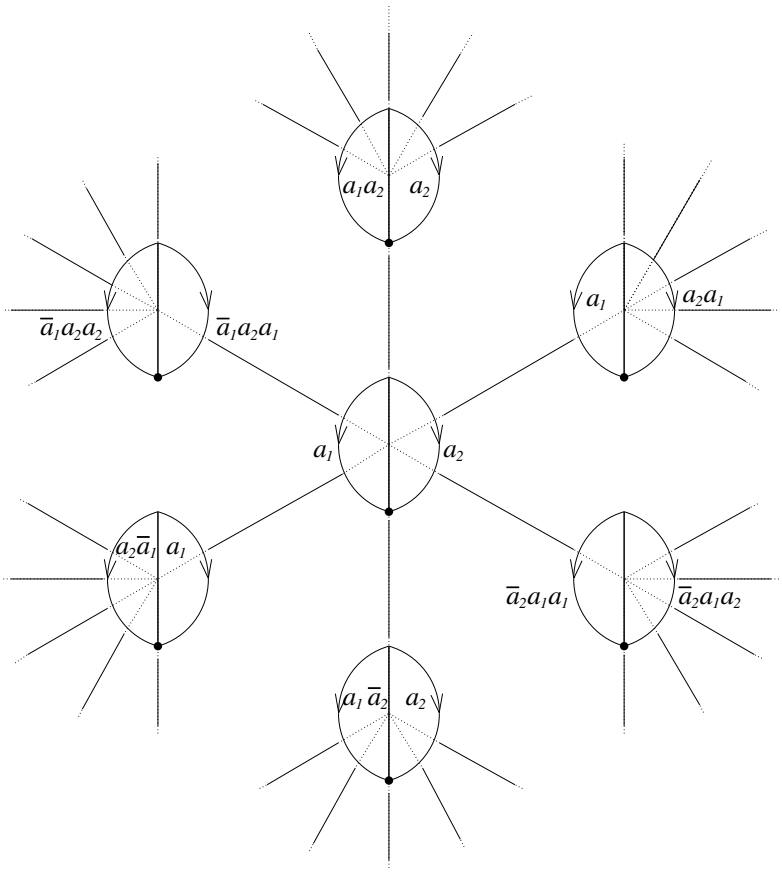

Figure 7.2: Part of the Nielsen connection graph in K_2

are contained in a translate of shingle 1, then they are both contained in 3 distinct translates of shingle 1. However, the edge between v_1 and v_2 maps into the intersection of these 3 shingles and ϕ is well-defined on this edge. In the case that $\phi(v_1)$ and $\phi(v_2)$ are instead opposed points in a translate of shingle 2 or 3, then the translated shingle containing both points is unique. Figures 3.6, 3.7, and 3.8 make these observations straightforward. Note that if two Nielsen vertices are opposed to each other then they are opposed to each other in each shingle containing both of them.

ϕ is not an embedding, as there is a point where the images of distinct edges intersect at the center of each translate of shingle 1, 2, or 3.

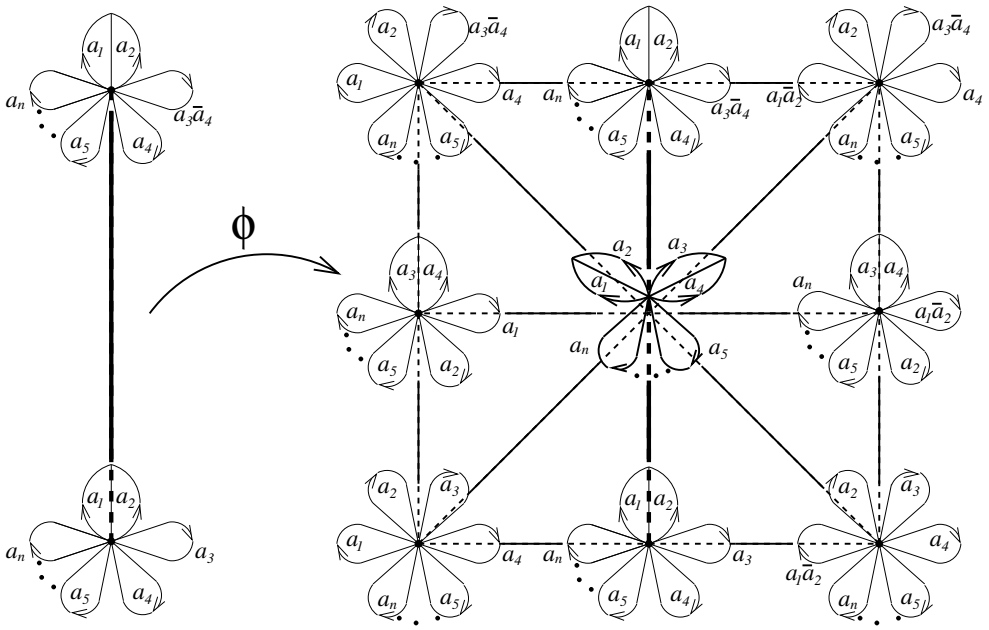

Figure 7.3: Path in shingle 1

Definition 28. *Two Nielsen vertices* cross each other in T*, a translate of shingle 1, 2, or 3, if they are contained in* T *and are not opposed to each other in* T*.*

We will say that two vertices in $\mathcal{N}$ are opposed in T if their images under ϕ are opposed in T, and that they cross each other in T if their images under ϕ cross each other in T. For two vertices in $\mathcal{N}$ that cross each other in T, the images under ϕ of the stars of these vertices intersect at the center of T.

The action of $Aut(F_n)$ on K_2 induces an action on $\mathcal{N}$. Let the Nielsen vertex shown in Figure 7.6 be denoted $\mathcal{I}$. This point will act as a basepoint for $\mathcal{N}$. Further, note that by definition the action of $Aut(F_n)$ is equivariant with respect to ϕ.

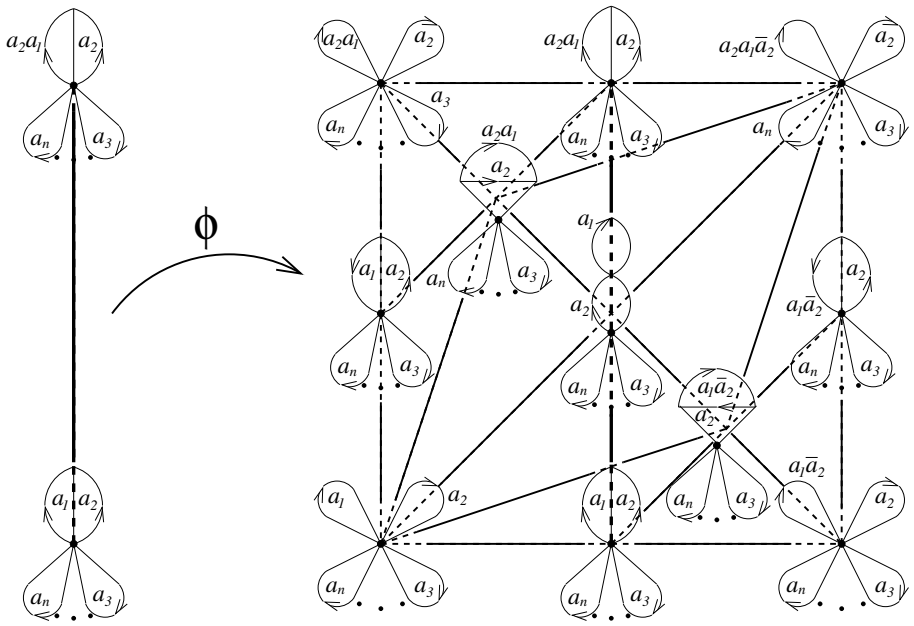

Figure 7.4: Path in shingle 2

7.2 The $n = 2$ Case

For this section, attention is restricted to the case of $n = 2$. Note that in this case the valence of each vertex in $\mathcal{N}$ is 6, and all shingles are translates of shingle 2. Figures 7.7, and 7.8 show the union of the 6 patches that contain $\mathcal{I}$. In future sections, both the $n = 2$ and the case of general n will be discussed, and when it is necessary to differentiate between these two settings, a subscript will be added to $\mathcal{N}$, $\mathcal{I}$, ϕ, and K_2 to denote the rank of the free group.

Consider the map from $SAut(F_2)$ to $\mathcal{N}$ defined by mapping the automorphism α to $\alpha^{-1} \cdot \mathcal{I}$, and denote this map p. As shown in Figures 7.7 and 7.8, observe that the 6 vertices in $st(\mathcal{I})$ are $p(E_{a_1 a_2})$, $p(E_{a_1 \bar{a}_2})$, $p(E_{a_2 a_1})$, $p(E_{a_2 \bar{a}_1})$, $p(E_{\bar{a}_2 \bar{a}_1} E_{\bar{a}_1 a_2} E_{\bar{a}_2 a_1})$, and $p(E_{\bar{a}_2 \bar{a}_1} E_{\bar{a}_1 \bar{a}_2} E_{\bar{a}_2 a_1})$.

Definition 29. *Let λ be an embedded loop in $\mathcal{N}$ that passes through vertices $\mathcal{I} = y_1$,*

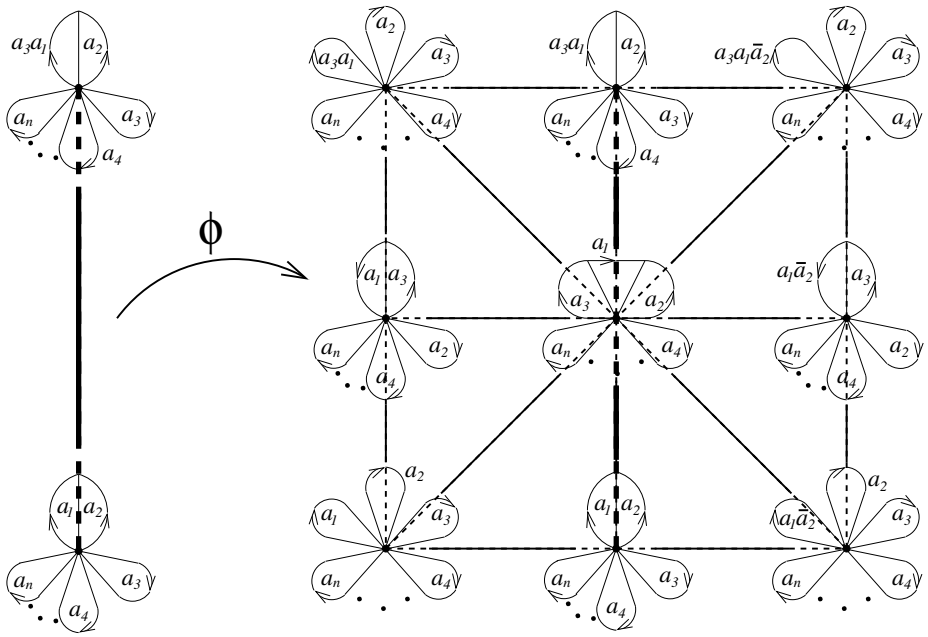

Figure 7.5: Path in shingle 3

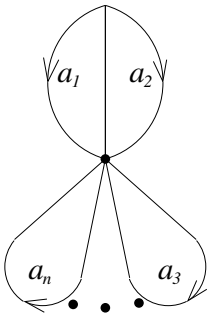

Figure 7.6: The marked graph $\mathcal{I}_n$

$y_2, \ldots y_m$ in order. By the observation regarding $st(\mathcal{I})$ above, there exists a unique list of special automorphisms α_1, α_2, $\ldots \alpha_m$ so that

1. $\alpha_1 = id$,
2. $p(\alpha_i) = y_i$, *and*
3. $\alpha_i \in \{ E_{a_1 a_2}\alpha_{i-1}, \ E_{a_1 \bar{a}_2}\alpha_{i-1}, \ E_{a_2 a_1}\alpha_{i-1}, \ E_{a_2 \bar{a}_1}\alpha_{i-1}, E_{\bar{a}_2 \bar{a}_1}E_{\bar{a}_1 a_2}E_{\bar{a}_2 a_1}\alpha_{i-1},$

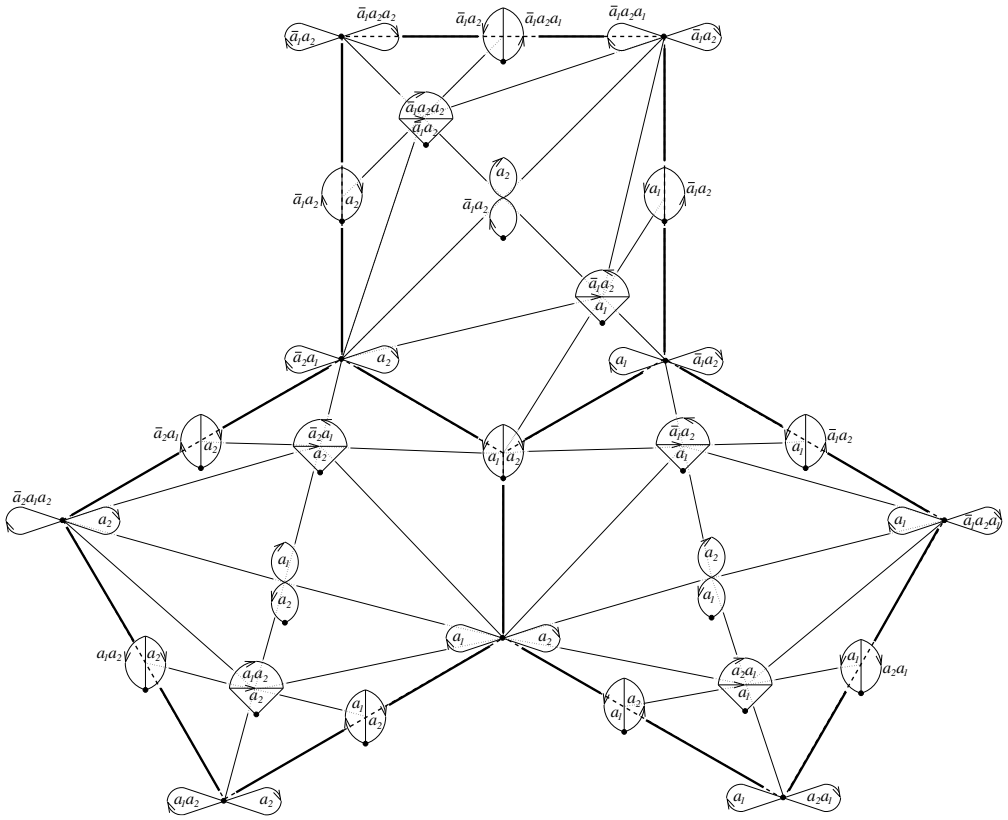

Figure 7.7: 3 of the shingles containing a Nielsen vertex for $n = 2$

$E_{\bar{a}_2\bar{a}_1}E_{\bar{a}_1\bar{a}_2}E_{\bar{a}_2a_1}\alpha_{i-1}\}$, *for all* i.

This list of special automorphisms is called the consistent lift *of* λ.

The consistent lift is used in the follow proposition:

Proposition 7.2.1. *When restricted to a connected component of* $\mathcal{N}$, ϕ *is an embedding.*

Proof. The elements of $SAut(F_2)$ that may be in the consistent lift of λ are contained in the subgroup H of $SAut(F_2)$ generated by $E_{a_1a_2}, E_{a_2a_1}$, and $E_{\bar{a}_2\bar{a}_1}E_{\bar{a}_1a_2}E_{\bar{a}_2a_1}$. Note that H is a subgroup of K where K is generated by $E_{a_1a_2}$, $E_{a_2a_1}$, and $E^2_{\bar{a}_2\bar{a}_1}$. To see this note that

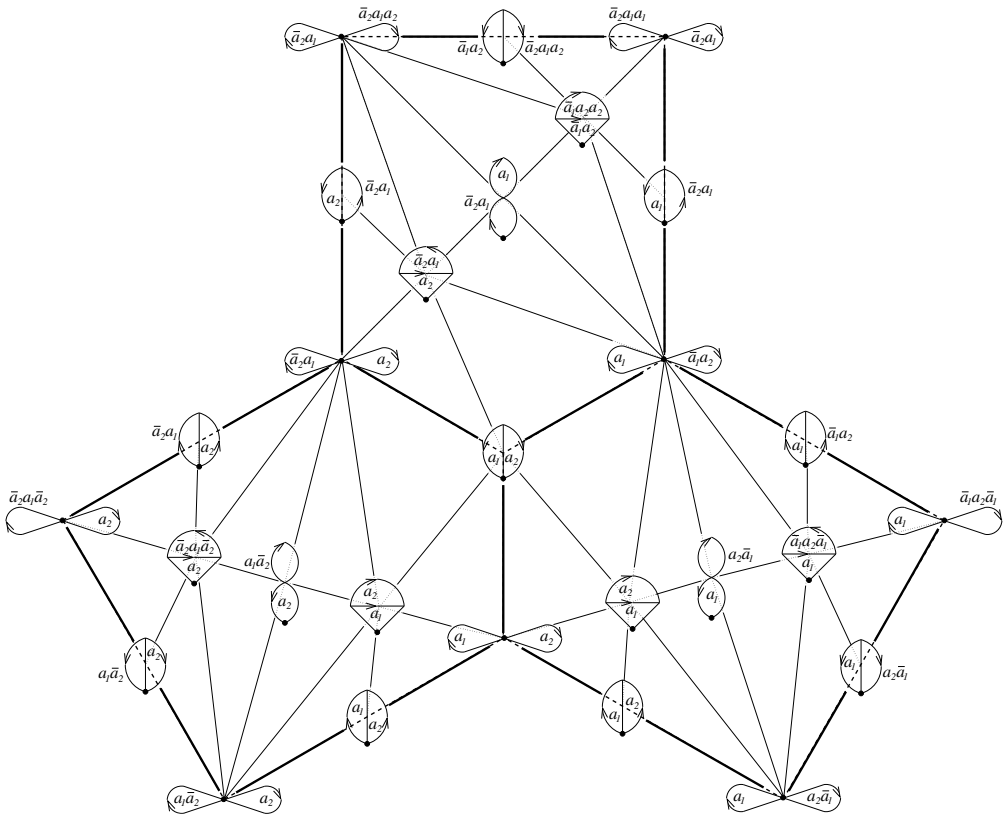

Figure 7.8: The other 3 shingles containing a Nielsen vertex for $n = 2$

$$E_{\bar{a}_2\bar{a}_1}E_{\bar{a}_1a_2}E_{\bar{a}_2a_1} = E^2_{\bar{a}_2\bar{a}_1}E_{a_1\bar{a}_2}E_{a_2a_1}E_{a_1a_2}E^{-2}_{\bar{a}_2\bar{a}_1}.$$

In Appendix 1, MAGMA is used to show that K does not contain any lifts of $p(E_{\bar{a}_1a_2})$, and this proves that the connected component of $\mathcal{N}$ that contains $\mathcal{I}$ does not contain $p(E_{\bar{a}_1a_2})$. $p(E_{\bar{a}_1a_2})$ and $\mathcal{I}$ are contained in one of the translates of shingle 2 shown in Figure 7.7, and further $p(E_{\bar{a}_1a_2})$ and $\mathcal{I}$ cross each other. The two edges in $\mathcal{N}$ that map to the shingle containing $p(E_{\bar{a}_1a_2})$ and $\mathcal{I}$ are in different connected components of $\mathcal{N}$. By the action of $Aut(F_n)$ the inverse image of each translate of shingle 2 in $\mathcal{N}$ must be two edges in different connected components on $\mathcal{N}$. Since shingle 2 is the only shingle in K_2 for $n = 2$, this shows that a

connected component of $\mathcal{N}$ does not contain any pair of vertices that cross each other, completing the proposition. □

Since ϕ is an embedding when restricted to a connected component N of $\mathcal{N}$, we can define $\phi|_N^{-1}$ on $\phi(N)$. ϕ^{-1} will always denote such a map, and usually the particular connected component of $\mathcal{N}$ will be clear from context, and when it is not it will be stated it explicitly.

7.3 Loops and Corners in the $n = 2$ Case

This section focuses on embedded loops in $\mathcal{N}$. More specifically, notions of straightness and corner turning are defined for paths in $\mathcal{N}$. With these ideas in place, the types of turns that loops are allowed to make are restricted and the consequences of these restrictions are investigated. Loops adhering to the restrictions examined here are important in the next chapter.

Definition 30. *Figure 7.9 illustrates a subgraph $\mathcal{A}$ of $\mathcal{N}$ and its image in K_2. This subgraph and all of its $Aut(F_n)$ translates in $\mathcal{N}$ are called the* axes *of $\mathcal{N}$.*

Note that for each vertex v in $\mathcal{A}$, $v = E^k_{a_2\bar{a}_1} \cdot \mathcal{I}$ for some k.

Proposition 7.3.1. *For axes $\mathcal{A}_1$ and $\mathcal{A}_2$ in $\mathcal{N}$ exactly one of the following holds:*

1. $\mathcal{A}_1 = \mathcal{A}_2$,
2. $\mathcal{A}_1 \cap \mathcal{A}_2 = \emptyset$, *or*
3. $\mathcal{A}_1 \cap \mathcal{A}_2$ *is a single vertex.*

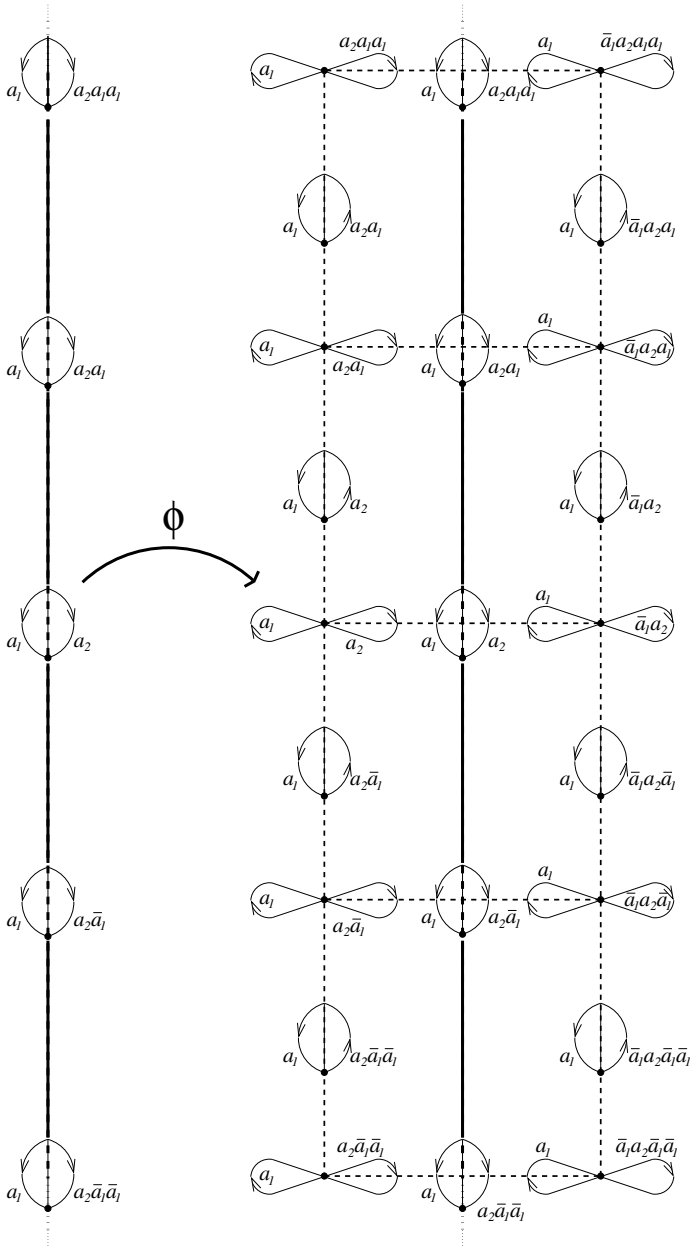

Figure 7.9: Axis $\mathcal{A}$ in $\mathcal{N}$

Proof. For any vertex v in $\mathcal{N}$, every axis passing through v must contain either $E_{a_1\bar{a}_2} \cdot v$, $E_{a_2\bar{a}_1} \cdot v$, or $E_{\bar{a}_2\bar{a}_1} E_{\bar{a}_1\bar{a}_2} E_{\bar{a}_2 a_1} \cdot v$. Further, depending upon which of these vertices $\mathcal{A}$ contains each vertex in $\mathcal{A}$ can be written as $E^k_{a_1\bar{a}_2} \cdot v$, $E^k_{a_2\bar{a}_1} \cdot v$, or $E_{\bar{a}_2\bar{a}_1} E_{\bar{a}_1\bar{a}_2} E^k_{\bar{a}_2 a_1} \cdot v$ respectively.

Suppose $\mathcal{A}_1 \cap \mathcal{A}_2$ is non-empty, hence this intersection must contain a vertex v. If both of these contain $E_{a_2\bar{a}_1} \cdot v$, then $\mathcal{A}_1 = \mathcal{A}_2$. The same statement can be made for $E_{a_2\bar{a}_1} \cdot v$, and $E_{\bar{a}_2\bar{a}_1}E_{\bar{a}_1\bar{a}_2}E_{\bar{a}_2a_1} \cdot v$. If $\mathcal{A}_1$ and $\mathcal{A}_2$ do not agree on which of the three vertices $E_{a_1\bar{a}_2} \cdot v$, $E_{a_2\bar{a}_1} \cdot v$, or $E_{\bar{a}_2\bar{a}_1}E_{\bar{a}_1\bar{a}_2}E_{\bar{a}_2a_1} \cdot v$ they contain, then $\mathcal{A}_1 \cap \mathcal{A}_2 = v$. To see this note that if $E^i_{a_1\bar{a}_2} \cdot v = E^j_{a_2\bar{a}_1} \cdot v$, $E^i_{a_1\bar{a}_2} \cdot v = E_{\bar{a}_2\bar{a}_1}E_{\bar{a}_1\bar{a}_2}E^j_{\bar{a}_2a_1} \cdot v$, or $E^i_{a_2\bar{a}_1} \cdot v = E_{\bar{a}_2\bar{a}_1}E_{\bar{a}_1\bar{a}_2}E^j_{\bar{a}_2a_1} \cdot v$, then $i = j = 0$. □

Each neighborhood of a vertex intersects at least 3 axes. For example, $\mathcal{I}$ is contained in $\mathcal{A}$, $\tau_1\tau_2\mathcal{A}$, and $\tau_1 E_{\bar{a}_2a_1}\mathcal{A}$. Axes are the notion of straightness mentioned earlier, intuitively if a path λ in $\mathcal{N}$ travels along an axis, it is considered to be straight.

Recall that for a combinatorial map into K_2 a Nielsen point is a vertex that maps to a Nielsen vertex.

Definition 31. *Let λ be an edge loop in $\mathcal{N}$. A Nielsen point $x \in S^1$ is a* corner *if for every neighborhood N of x, $\lambda(N \setminus x)$ intersects more than one axis.*

Note that for each corner, there is a neighborhood N so that $\lambda(N \setminus x)$ intersects only 2 axes, as the interior of each edge is contained in a unique axis by Proposition 7.3.1.

Definition 32. *Let λ be an oriented, basepointed, edge loop in $\mathcal{N}$ whose basepoint maps to $\mathcal{I}$. Let y_1, y_2, ..., y_m be the vertices in $\mathcal{N}$ that λ traverses in order starting and ending with $\mathcal{I}$, and consider the consistent lift of λ. Let α_i be the lift of y_i. λ is* restricted *if for all i, $\alpha_i \in \{E_{a_1a_2}\alpha_{i-1}, E_{a_1\bar{a}_2}\alpha_{i-1}, E_{a_2a_1}\alpha_{i-1}, E_{a_2\bar{a}_1}\alpha_{i-1}\}$.*

Let $x_1, x_2, \ldots x_m$ be the points on S^1 so that $\lambda(x_i) = y_i$ and the x_i are traversed in order when traveling around S^1 beginning and ending at the base-

point. Note that in a restricted loop λ, if $i \neq 1$ or m, x_i is a corner if $\alpha_{i+1} \in \{E_{a_2a_1}^{\pm 1} E_{a_1a_2}^{\pm 1} \alpha_{i-1}, E_{a_1a_2}^{\pm 1} E_{a_2a_1}^{\pm 1} \alpha_{i-1}\}$.

Restricted loops will be important in the next chapter as $Aut(F_n)$ translates of these loops enforce structure in simple patched fillings.

Let λ be an oriented, basepointed, combinatorial loop satisfying all of the requirements of a restricted loop except for one. Specifically, suppose that $\alpha_i \in \{E_{a_1a_2}\alpha_{i-1}, E_{a_1\bar{a}_2}\alpha_{i-1}, E_{\bar{a}_2\bar{a}_1}E_{\bar{a}_1a_2}E_{\bar{a}_2a_1}\alpha_{i-1}, E_{\bar{a}_2\bar{a}_1}E_{\bar{a}_1\bar{a}_2}E_{\bar{a}_2a_1}\alpha_{i-1}\}$. Then let $(\tau_2 E_{\bar{a}_1a_2} \cdot \lambda)(x) = \tau_2 E_{\bar{a}_1a_2} \cdot (\lambda(x))$, and note that $\tau_2 E_{\bar{a}_1a_2} \cdot \lambda$ is restricted.

Proposition 7.3.2. *If λ is a restricted loop, then λ has an even number of corners.*

Proof. Assume that λ is restricted and has an odd number of corners, hence λ has at least one corner. Also we assume that the basepoint is a corner and $y_2 = E_{ab}^{\pm 1} \cdot \mathcal{I}$. If this is not the case, the action of $Aut(F_n)$ can shift the image of a corner to $\mathcal{I}$ and the next vertex to $\mathcal{A}$. Then altering the basepoint to be the corner whose image was shifted to $\mathcal{I}$ completes the assumption. Neither of these alterations change the number of corners. The consistent lift of the last vertex y_m is one of three special automorphisms id, $E_{\bar{a}_2\bar{a}_1}^2 E_{a_1\bar{a}_2} E_{a_2a_1}$, or $E_{a_2\bar{a}_1} E_{a_1a_2} E_{\bar{a}_2\bar{a}_1}^{-2}$. Further, the lift of y_m has the form $E_{a_1a_2}^{i_1} E_{a_2a_1}^{i_2} E_{a_1a_2}^{i_3} \dots E_{a_2a_1}^{i_{k-1}} E_{a_1a_2}^{i_k}$. Note that k must be odd because there are an even number of corners that are not the basepoint.

$E_{\bar{a}_2\bar{a}_1}^2 E_{a_1\bar{a}_2} E_{a_2a_1}$ is not in the group generated by $E_{a_1a_2}$ and $E_{a_2a_1}$. To see this, consider the group generated by $E_{a_1a_2}$, $E_{a_2a_1}$, $E_{\bar{a}_2\bar{a}_1}^{-2} E_{a_1a_2} E_{\bar{a}_2\bar{a}_1}^2$. In Appendix 1, MAGMA is used to show that $E_{\bar{a}_2\bar{a}_1}^2 E_{a_1\bar{a}_2} E_{a_2a_1}$ is not in this subgroup.

Hence, the consistent lift of y_k cannot be $E_{\bar{a}_2\bar{a}_1}^2 E_{a_1\bar{a}_2} E_{a_2a_1}$ or $E_{a_2\bar{a}_1} E_{a_1a_2} E_{\bar{a}_2\bar{a}_1}^{-2}$, and id is the consistent lift of y_k. The consistent lift of y_{k-1} must then be $E_{a_1a_2}^{\pm 1}$,

but then there exists a neighborhood N of the basepoint x where $\lambda(N \setminus x) \subset \mathcal{A}$ and is disjoint from all other axes, and x is not a corner which is a contradiction. No such λ exists and all restricted loops must have an even number of corners. $\square$

For a simplex x, let $lk(x)$ be the link of x.

Proposition 7.3.3. *Let λ be the ϕ image of an edge loop in N where N is a connected component of $\mathcal{N}$, and let $v_1, v_2, \dots v_m$ be the Nielsen vertices that λ passes through in order. Suppose that for each Nielsen vertex v_i in the image of λ that there exists a rose vertex R^i with the following properties:*

1. *$R^i \in lk(v_i)$,*
2. *$R^1 = R^m$, and*
3. *there is a length 2 rose path connecting R^i to R^{i+1}, for all $1 \leq i < m$.*

Then there exists $\alpha \in Aut(F_n)$ so that $\alpha \cdot (\phi^{-1} \circ \lambda)$ is restricted, where $\alpha \cdot (\phi^{-1} \circ \lambda)(x) = \alpha \cdot (\phi^{-1} \circ \lambda(x))$.

Proof. Let S be the first shingle that λ passes through after passing through v_1. Note that there exists α such that

1. $\alpha \cdot S = \tau_1\tau_2 \cdot S_2$ or $\tau_1\tau_2 E_{a_1\bar{a}_2} \cdot S_2$,
2. $\alpha \cdot v_1 = \phi(\mathcal{I})$, and
3. $\alpha \cdot R^1 = I$.

Let $y_1, y_2, \dots y_m$ be the vertices in $\mathcal{N}$ that $\alpha \cdot (\phi^{-1} \circ \lambda)$ that traverses in order with multiplicity, and let $\alpha \cdot (\phi^{-1} \circ \lambda)(x_i) = y_i$. Note that $\mathcal{I} = \phi^{-1}(\alpha \cdot v_1) = y_1$ and

consider the consistent lift $\alpha_1, \alpha_2, \ldots \alpha_m$ of $\alpha \cdot (\phi^{-1} \circ \lambda)$. Since $\alpha \cdot v_2$ is the point in $\alpha \cdot S$ opposed to $\phi(\mathcal{I})$, $\alpha_2 = E_{a_1 a_2}$ or $E_{a_1 \bar{a}_2}$. Additionally, $\alpha \cdot R^2$ is $\alpha_2 \cdot I$ since $\alpha_2 \cdot I$ is the only rose in the radius 2 neighborhood of R^1 in K_1 that is also in $lk(\alpha \cdot v_2)$.

Suppose that x_j is the first corner that $\alpha \cdot (\phi^{-1}\lambda)$ passes through. Assume that $\alpha_{j+1} = E_{a_2 a_1}^{\pm 1} \alpha_j$, otherwise $\alpha_{j+1} = (E_{\bar{a}_2 \bar{a}_1} E_{\bar{a}_1 a_2} E_{\bar{a}_2 a_1})^{\pm 1} \alpha_j$ and take α to be $\alpha \tau_2 E_{\bar{a}_1 a_2}$.

From here the proof proceeds by induction. For $j < i$, suppose that $\alpha_j = E_{a_1 a_2}^{\pm 1} \alpha_{j-1}$ or $E_{a_2 a_1}^{\pm 1} \alpha_{j-1}$, and $\alpha \cdot R^j = \alpha_j \cdot I$. Note that $\alpha_{i-1} \cdot I$ and $\alpha_{i-1} \cdot \phi(\mathcal{I})$ are both contained in 4 shingles, the α_{i-1} translates of the two bottommost shingles in Figures 7.7 and 7.8. The points that are opposed to $\alpha \cdot \lambda(x_{i-1})$ in these shingles are $E_{a_1 a_2}^{\pm 1} \alpha_{i-1} \cdot \mathcal{I}$ and $E_{a_2 a_1}^{\pm 1} \alpha_{i-1} \cdot \mathcal{I}$. So, y_i is one of these four points. Also, the only roses in these shingles that are in $lk(\phi(y_i))$ and are distance two from $\alpha_{i-1} \cdot I$ in K_1 are $E_{a_1 a_2}^{\pm 1} \alpha_{i-1} \cdot I$ and $E_{a_2 a_1}^{\pm 1} \alpha_{i-1} \cdot I$ respectively. This completes the induction step. Hence there exists $\alpha \in Aut(F_n)$ so that $\alpha \cdot (\phi^{-1} \circ \lambda)$ is a restricted loop. □

7.4 The General Case

In this section, a map from $\psi : N \to \mathcal{N}_2$ is given where N is a connected component of $\mathcal{N}_n$ and ψ is used to establish Proposition 7.4.2, that each connected component of $\mathcal{N}_n$ embeds in $K_{2,n}$.

Consider a Nielsen vertex (g, θ_n) in $K_{2,n}$. Let (g', θ_n) be a Nielsen vertex opposed to (g, θ_n). Let R denote the subgraph of θ_n consisting of the $n-2$ loops at the basepoint. Note that the group generated by $g^{-1}|_R$ is the same subgroup of F_n as the group generated by $g'^{-1}|_R$. Hence to each connected component of $\mathcal{N}_n$ we

can associate a subgroup of F_n isomorphic to F_{n-2}. For the connected component containing $\mathcal{I}_n$ this subgroup is generated by the last $n-2$ generators.

Definition 33. *Let $\mathcal{F} : F_n \to F_2$ be given by $\mathcal{F}(a_i) = a_i$ for $i = 1, 2$ and $\mathcal{F}(a_i)$ is the empty word otherwise.*

Proposition 7.4.1. *Let $\tilde{S} = \{w_1, w_2 \dots w_n\}$ be a set of generators for F_n so that the group generated by $w_3, \dots, w_n$ is the subgroup of F_n generated by $a_3, \dots, a_n$. Then $\mathcal{F}(w_1)$ and $\mathcal{F}(w_2)$ generate $< a_1, a_2 >$.*

Proof. Note that a_1 and a_2 can be written in terms $\tilde{S}$, for example let $a_1 = w_1^{r_1} w_2^{r_2} \dots w_m^{r_m}$, where $w_i \in \tilde{S}$ for all i. Then without loss of generality note that

$$\begin{aligned} a_1 &= \mathcal{F}(a_1) \\ &= \mathcal{F}(w_1^{r_1} w_2^{r_2} \dots w_m^{r_m}) \\ &= \mathcal{F}(w_{1'}^{r_{1'}} w_{2'}^{r_{2'}} \dots w_{l'}^{r_{l'}}) \\ &= \mathcal{F}(w_{1'})^{r_{1'}} \mathcal{F}(w_{2'})^{r_{2'}} \dots \mathcal{F}(w_{l'})^{r_{l'}}, \end{aligned}$$

where $w_{i'} \in \{w_1, w_2\}$, since $\mathcal{F}(w) = id$ for $w \in \tilde{S} \setminus \{w_1, w_2\}$. □

Let (g, θ_n) be a homotopy marked graph with basepoint v. Further, suppose that $g^{-1}(\pi_1(R))$ is the subgroup of F_n generated by $a_3, a_4, \dots, a_n$. Consider the graph $\theta'_n = \theta_n \setminus (R \setminus v) = \theta_2$ and the map $g' : F_2 \to \pi_1(\theta'_n)$ where $g'^{-1}(w) = \mathcal{F}(g^{-1}(w))$. (g', θ'_n) is a homotopy marked graph for $n = 2$ because $\mathcal{F}(w_1)$ and $\mathcal{F}(w_2)$ generate F_2. Note that this operation does not raise degree, so if $(g, \theta_n) \in K_{2,n}$ then $(g', \theta'_n) = (g', \theta_2) \in K_{2,2}$. Define the map ψ from the component of $\mathcal{N}_n$ containing $\mathcal{I}_n$ to map (g, θ_n) to (g', θ_2) $g^{-1}(\pi_1(R))$ is indeed the subgroup generated by $a_3, \dots a_n$ because this point is in the same connected component of $\mathcal{N}_n$ as $\mathcal{I}_n$. By definition $\psi(\mathcal{I}_n) = \mathcal{I}_2$.

Note if v, v' are vertices in the connected component of $\mathcal{N}_n$ containing $\mathcal{I}_n$ incident to some edge e and $\phi_n(v)$ and $\phi_n(v')$ are opposed in a translate of shingle 1 or shingle 3, then $\psi(v) = \psi(v)'$, and let $\psi(e) = \psi(v) = \psi(v')$. If $\phi_n(v)$ and $\phi_n(v')$ are opposed in a translate of shingle 2, then $\phi_2 \circ \psi(v)$ and $\phi_2 \circ \psi(v')$ are opposed in a translate of shingle 2 because $\mathcal{F}$ is a homomorphism. Hence, $\psi(v)$ and $\psi(v')$ are connected by an edge. Set $\psi(e)$ to be this edge. An example of ψ is shown in Figure 7.10, note that the solid line in the figure maps to $\mathcal{I}_2$, and otherwise lines in the piece of $\mathcal{N}_n$ map to the lines with the same pattern in $\mathcal{N}_2$.

Proposition 7.4.2. *ϕ_n restricted to a connected component of $\mathcal{N}_n$ is an embedding.*

Proof. Consider the vertices in $\mathcal{N}_n$ that cross $\mathcal{I}_n$ in translates of shingles 1 and 3. The subgroup associated to such vertices by taking the inverse image of R under the marking associated to their image in $K_{2,n}$ is not the subgroup generated by the last $n-2$ generators. These vertices are not contained in the same connected component as $\mathcal{I}_n$, and hence by the action of $Aut(F_n)$, no pair of crossing vertices whose images are contained in a translate of shingle 1 or 3 are contained in the same connected component of $\mathcal{N}_n$. In order to prove that each connected component of $\mathcal{N}_n$ embeds in $K_{2,n}$, it is left to show that each pair of vertices that cross in a translate of shingle 2 are not contained in the same connected component of $\mathcal{N}_n$. To see this suppose that a path existed between $\mathcal{I}_n$ and $p(E_{\bar{a}_1 a_2}) \in \mathcal{N}_n$ which is such a pair. Then the ψ image of this path would be a path from $\mathcal{I}_2$ to $p(E_{\bar{a}_1 a_2}) \in \mathcal{N}_2$, and by Proposition 7.2.1 no such path exists. By the action of $Aut(F_n)$, each pair of vertices that cross each other in a translate of shingle 2 are in different connected components of $\mathcal{N}_n$, which proves that the restriction of ϕ_n to any connected component of $\mathcal{N}_n$ is an embedding. □

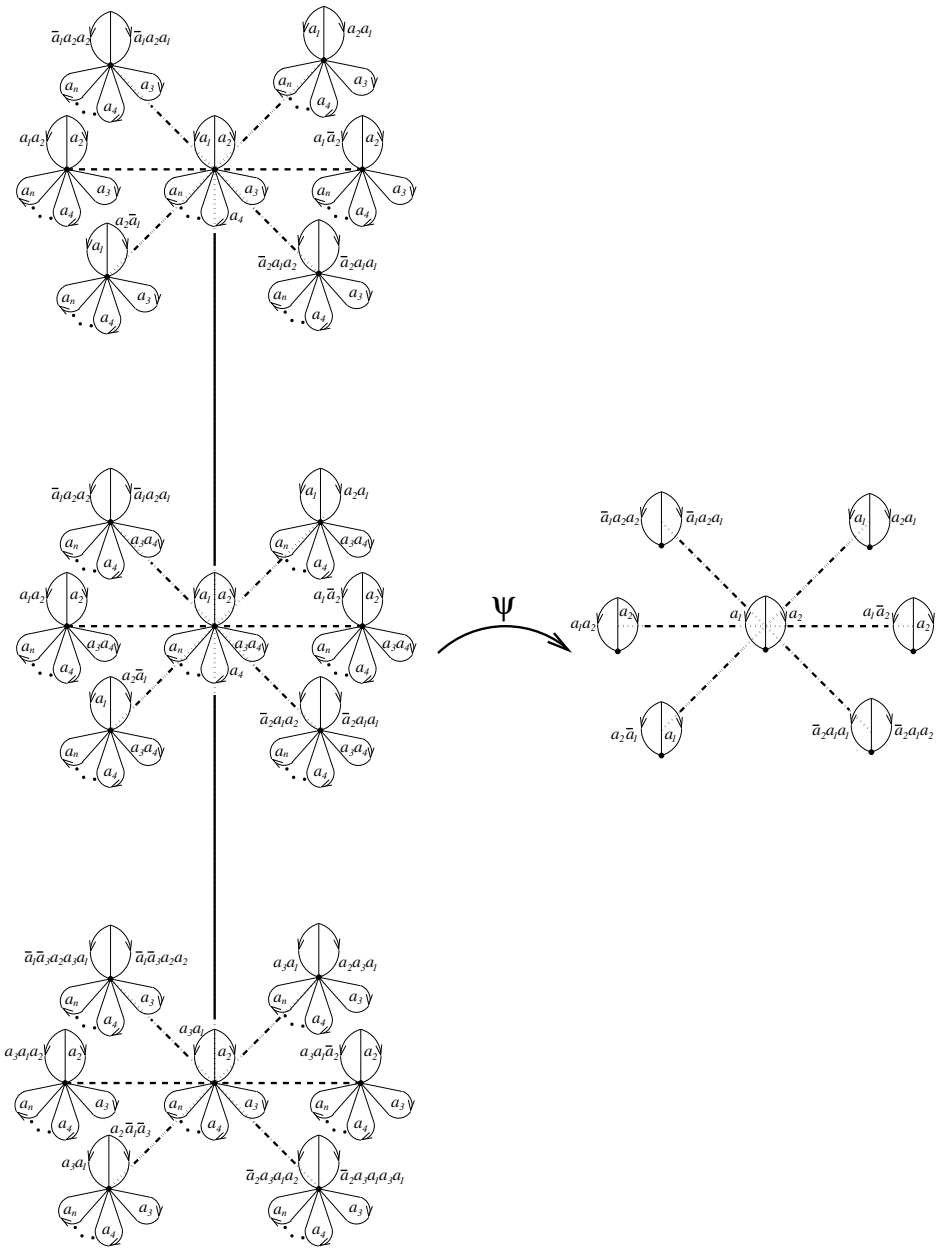

Figure 7.10: Example of ψ

ψ is generalized as follows. Let $\psi_\alpha : N \to \mathcal{N}_2$ be given by $\psi_\alpha(v) = \psi(\alpha \cdot v)$, where $\alpha \in Aut(F_n)$ takes a connected component N of $\mathcal{N}_n$ to the connected component containing $\mathcal{I}_n$. Since for any $x \in \mathcal{N}_n$, there exists α so that $\alpha \cdot x = \mathcal{I}_n$, there are such maps ψ_α for any connected component of $\mathcal{N}_n$.

CHAPTER 8

NIELSEN CORRIDORS AND MINIMALITY

In this chapter we will complete the proof of Theorem 8.5.2 that κ is the minimal simply-connected complex of K_2 that is preserved under the action of $Aut(F_n)$. Most of the chapter will be spent proving Corollary 8.5.1 which states that $Shin_4(id, x)|_{\partial D^2}$ cannot be filled in $K_2 \setminus orbit(\mathsf{F}_4^o)$, $K_2 \setminus orbit(\mathsf{F}_5^o)$, and $K_2 \setminus orbit(\mathsf{F}_6^o)$ by proving Theorem 8.5.1, that every simple patched filling of this loop must use shingle 4. We will assume we have a simple patched filling Δ which does not use shingle 4. Recall $\mathcal{N}$ the Nielsen connection graph defined in chapter 7, and the map $\phi : \mathcal{N} \to K_2$ also defined in chapter 7. For a connected component N of $\mathcal{N}$, $\Delta^{-1}(\phi(N))$ is a disjoint union of graphs embedded in D^2. These graphs are called *Nielsen corridors*, and are central to the proof that $Shin_4(id, x)|_{\partial D^2}$ cannot be filled in $K_2 \setminus orbit(\mathsf{F}_4^o)$. Each Nielsen point, a vertex that maps to a vertex of the form (g, θ_n), in Δ is contained in a unique Nielsen corridor.

Figure 8.1 gives an example simple patched filling of an embedded edge loop in K_1 that uses no patches mapping to translates of shingle 4. Consider the Nielsen point v on the boundary of this filling. Let $\mathcal{N}_v$ be the unique connected component of $\mathcal{N}$ for which $\Delta(v) \in \phi(\mathcal{N}_v)$. Then note that the Δ pre-image of $\phi(\mathcal{N}_v)$ is a graph containing v. This graph is shown in Figure 8.1, and is the Nielsen corridor of v. This graph is one of many Nielsen corridors in D^2 defined by Δ.

In the first two sections of this chapter we prove that for a simple patched filling of $Shin_4(id, x)|_{\partial D^2}$ that does not use patches mapping to translates of shingle 4, the Nielsen corridor containing u in 8.2 is a 1-graph, see section 8.3 for definition. Then in sections 8.3 and 8.4 we prove Proposition 8.3.4, that no 1-graphs exist,

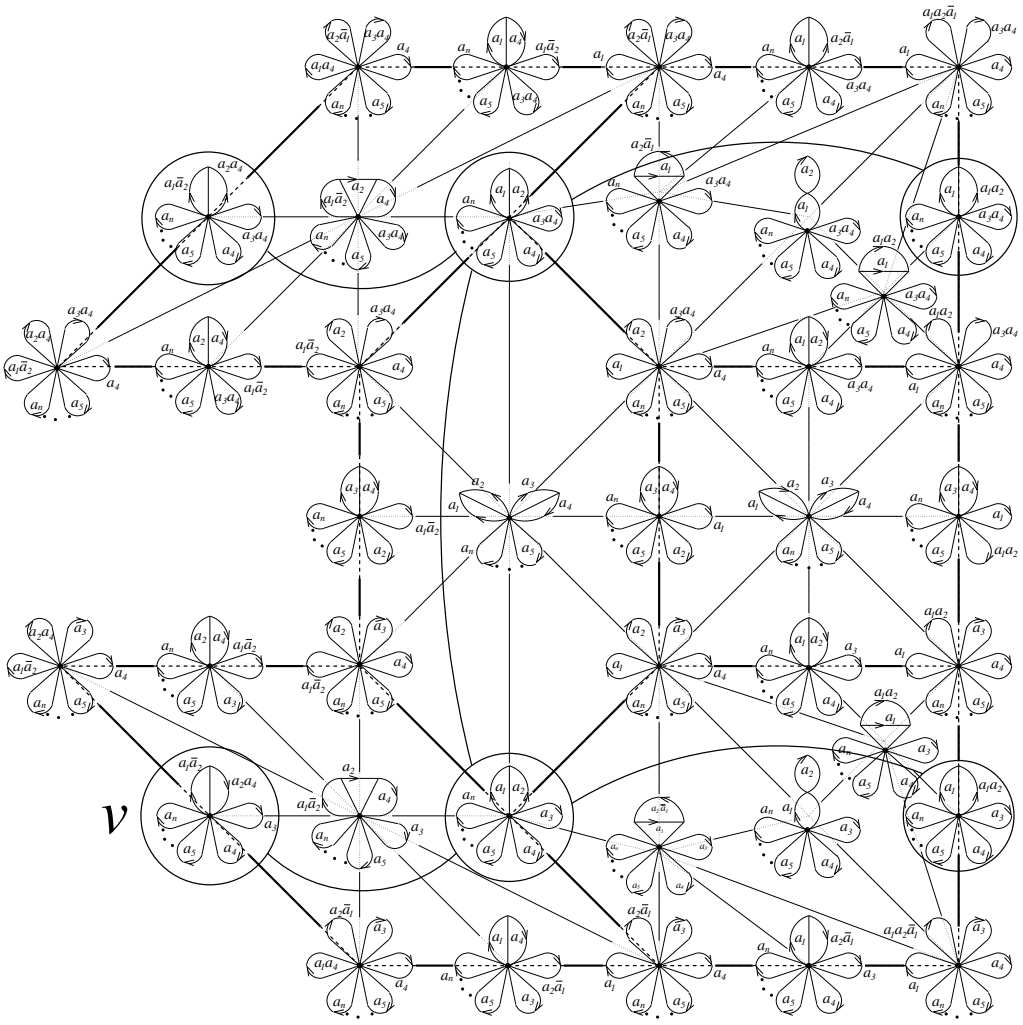

Figure 8.1: Example simple patched filling

completing Theorem 8.5.1.

8.1 Nielsen Corridors

In this section, Nielsen corridors will be defined and the map $\phi_2 \circ \psi \circ \phi_n^{-1} \circ \Delta$ will be examined. This map will be extended to a thickened version of Nielsen corridors. Recall from chapter 7 that while ϕ is not invertible, ϕ is an embedding on each connected component of $\mathcal{N}$. ϕ^{-1} takes as its domain the image of a particular

connected component, the connected component in question is always clear from context.

Let $\rho : S^1 \to K_{2,n}$ be an embedded edge loop with simple patched filling $\Delta : D^2 \to K_{2,n}$. Many of the notions in this chapter can be defined for general simple patched fillings, however since only those that have no patches mapping to shingle 4 are relevant assume for the remainder of the chapter that all simple patched fillings do not use patches mapping to shingle 4. Let $x \in D^2$ be a Nielsen point and consider the connected component of $\mathcal{N}$ containing $\phi_n^{-1}(\Delta(x))$, and call it $\mathcal{N}_x$. The Δ pre-image of $\phi_n(\mathcal{N}_x)$ is a disjoint union of connected graphs by Proposition 7.4.2, let N_x be the connected component of this pre-image containing x.

Definition 34. *N_x is the* Nielsen corridor *of x.*

To motivate studying Nielsen corridors, consider the five Nielsen vertices traversed by $Shin_4(id, x)|_{\partial D^2}$ shown in Figure 3.4.

Proposition 8.1.1. *Let Δ_o be a simple patched filling of $Shin_4(id, x)|_{\partial D^2}$. Consider the five points u, v, w, x, and $y \in \partial D^2$ as shown in Figure 8.2. Then N_u, N_w, and N_y each only contain one point on the boundary of D^2.*

Proof. Recall from chapter 7 that to each connected component of $\mathcal{N}_n$ there is an associated subgroup of F_n given by $g^{-1}(\pi_1(R))$ where $(g, \theta_n) = \phi_n(r)$ for some vertex r in this connected component and R is the subgraph of θ_n consisting of $n-2$ loops at the basepoint. For a Nielsen point s in D^2, $\Delta_o(N_s)$ is contained in the ϕ_n image of a unique connected component of $\mathcal{N}$, the subgroup associated to this connected component can also be associated to N_s. Note that the subgroup can be found by calculating $g^{-1}(\pi_1(R))$ if $\Delta_o(t) = (g, \theta_n)$, for any Nielsen point $t \in N_s$.

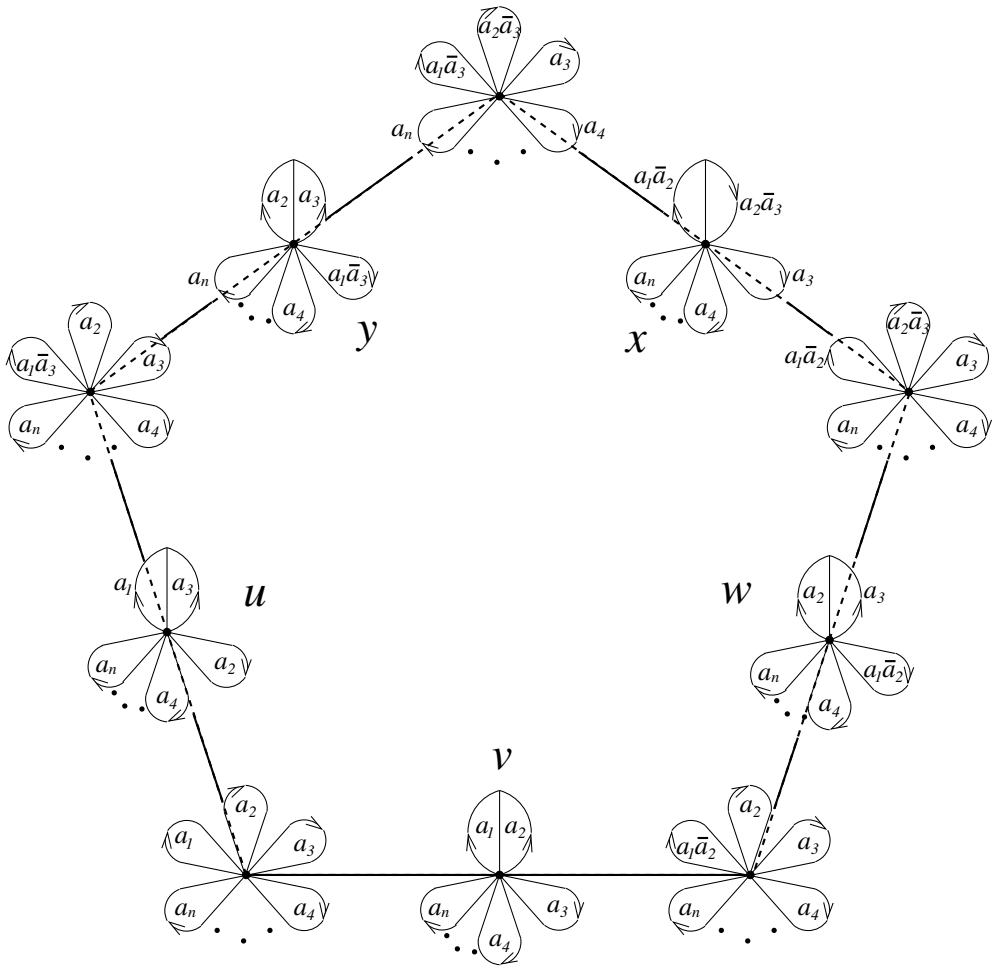

Figure 8.2: Labeling of boundary points in Shingle 4

Let $\Delta_o(i) = (g_i, \theta_n)$, and then note that $g_u^{-1}(R) =< a_2, a_4, a_5, \ldots a_n >$, $g_v^{-1}(R) = g_x^{-1}(R) =< a_3, a_4, a_5, \ldots a_n >$, $g_w^{-1}(R) =< a_1\bar{a}_2, a_4, a_5, \ldots a_n >$, and $g_y^{-1}(R) =< a_1\bar{a}_3, a_4, a_5, \ldots a_n >$.

Hence $v, w, x, y \notin N_u$, $u, v, x, y \notin N_w$, and $u, v, w, x \notin N_y$. □

8.1.1 Definition of Ψ

Let $\alpha \in Aut(F_n)$ be an automorphism so that $\alpha \cdot (\phi^{-1} \circ \Delta(x)) = \mathcal{I}_n$. Let $\Psi_\alpha = \phi_2 \circ \psi_\alpha \circ \phi_n^{-1} \circ \Delta|_{N_x} : N_x \to K_{2,2}$, and since the particular α is usually not relevant, the subscript will be dropped and this map will be called Ψ. The main goal of the remainder of this section is to define Ψ on a thickened version N_x, specifically on the patched neighborhood of N_x.

Definition 35. *Let S be a subspace of D^2. The* patched neighborhood $\tilde{S}$ *of S is the union of the closures of the patches whose interiors have non-empty intersection with S. The* extended patched neighborhood *of S is the union of the closures of the patches whose closures have non-empty intersection with S.*

Let P be a patch in $\tilde{N}_x$. Note that $P \cap N_x$ is an interval and not two intersecting intervals, otherwise ϕ_n restricted to $\mathcal{N}_x$ would not be an embedding. ∂P contains four rose points, removing these points leaves ∂P homeomorphic to the disjoint union of four open intervals. The closure of each of these open intervals will be called a *side* of P. Those sides that intersect N_x are called the vertical sides of P with respect to N_x, while those that are disjoint are called the horizontal sides of P with respect to N_x.

Let y be a Nielsen point in N_x with $\Delta(y) = (g_y, \theta_n)$, and note that $\Psi(y) = ((g_y \circ \alpha)', \theta_2)$. This is well-defined as $(g_y \circ \alpha)^{-1}(\pi_1(R))$ is generated by $a_3, a_4, \ldots a_n$ because $\alpha \cdot (\phi_n^{-1} \circ \Delta(y))$ is in $\mathcal{N}_x$.

Consider a rose point a that is in $\tilde{N}_x$, and note that there exists a Nielsen point $y \in N_x$ so that there is an edge that is incident to both a and y. Let $\Delta(a) = (g_a, R_n)$ and note that there is an edge collapse taking $\Delta(y)$ to $\Delta(a)$. Since R is unaffected by this edge collapse, $g_y^{-1}(\pi_1(R)) = g_a^{-1}(\pi_1(R))$. This makes

$\Psi(a) = ((g_a \circ \alpha)', R_2)$ well-defined. Further, $\Psi(a)$ can be obtained by a forest collapse on $\Psi(y)$ by construction, so Ψ maps the edge incident to y and a to the edge incident to $\Psi(a)$ and $\Psi(y)$.

Note that if z is a Nielsen point in N_x so that there is an edge incident to a and z then $\Delta(y) = \Delta(z)$. To see this, consider the Nielsen vertices in the link of I and the intersection of this link with the ϕ_n image of the connected component of $\mathcal{N}_n$ containing $\mathcal{I}_n$. Specifically, $\phi_n(\mathcal{I}_n)$ is the only point in the intersection. There are only 4 Nielsen vertices in the link of I for which $\pi_1(R)$ under the inverse image of the marking is $< a_3, a_4, \ldots a_n >$. One of these points is $\phi_n(\mathcal{I}_n)$ and the other three cross $\phi_n(\mathcal{I}_n)$ specifically in the shingles $\tau_1\tau_2 \cdot S_2$, $\sigma_{12}\tau_1\tau_2 \cdot S_2$, and $\tau_1 E_{a_1\bar{a}_2} \cdot S_2$. By the action of $Aut(F_n)$, the intersection of the link of $\Delta(a)$ and $\phi_n(\mathcal{N}_x)$ is $\Delta(y)$, and since $\Delta(N_x) \subset \phi_n(\mathcal{N}_x)$, $\Delta(y) = \Delta(z)$. Since y and z map to the same point, the edge collapse taking $\Delta(z)$ to $\Delta(a)$ is the same as the collapse taking $\Delta(y)$ to $\Delta(a)$ and $\Psi(a)$ is well-defined.

This completes the definition of Ψ on all vertical sides of patches in $\tilde{N}_x$ with respect to N_x. It remains to define Ψ on the horizontal sides and on the interiors of the patches in $\tilde{N}_x$. This will be done based on which shingle the patch maps to.

Let P be a patch in $\tilde{N}_x$ that maps to a shingle of type 1 or 3. Let y and z be the Nielsen points in $P \cap N_x$, and let a_y, b_y, a_z, and b_z be the rose points of this patch, with a_y and b_y in the same vertical side as y, a_z and b_z in the same vertical side as z, a_y and a_z in the same horizontal side, and b_y and b_z in the same horizontal side. Figure 8.3 illustrates this notation, where N_x is dotted line. Note that $\Psi(y) = \Psi(z)$, $\Psi(a_y) = \Psi(a_z)$ and $\Psi(b_y) = \Psi(b_z)$. Hence, the edges incident to a_y and y, and incident to a_z and z have the same image under Ψ, the same is also true for b_y and b_z. Define Ψ to map the horizontal side containing a_y

and a_z to $\Psi(a_y)$, and the horizontal side containing b_y and b_z to $\Psi(b_y)$. Further, collapse P to the image of the vertical side containing y in a continuous way so that $\Psi(N_x \cap P) = \Psi(y)$. Figures 8.4 and Figure 8.6 show examples of Ψ on patches that map to shingles 1 and 3 respectively.

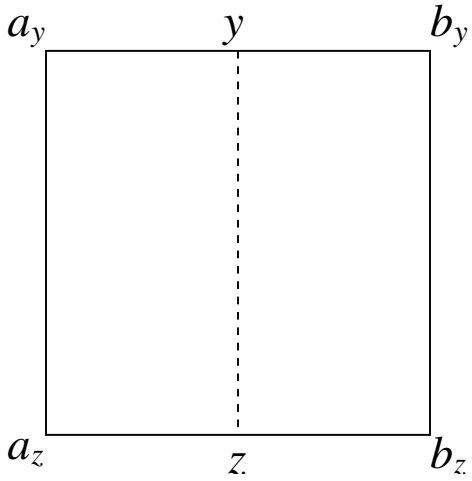

Figure 8.3: Notation for patches in patched neighborhood of a Nielsen corridor

Suppose now that P maps to a translate of shingle 2. Then for all vertices in the image of P, the subgraph R of each graph can be defined so that R is unaffected by the forest collapse maps that relate vertices in $\Delta(P)$. Hence, for all vertices $v \in P$ where $\Delta(v) = (g, \Gamma)$, $(g \circ \alpha)^{-1}(\pi_1(R))$ is the subgroup generated by $a_3, a_4, \ldots a_n$. Recall from chapter 7 that $\mathcal{F} : F_n \rightarrow F_2$ takes the identity map on the first two generators and takes all others to the empty word. Let $\Gamma' = \Gamma \setminus (R \setminus v)$ and $(g \circ \alpha)' : F_2 \rightarrow \pi_1(\Gamma')$ where $(g \circ \alpha)'^{-1}(w) = \mathcal{F}((g \circ \alpha)^{-1}(w))$. By Proposition 7.4.1 $((g \circ \alpha)', \Gamma)$ is a homotopy marked graph in $K_{2,2}$. Let $\Psi(v) = ((g \circ \alpha)', \Gamma')$ and note that Ψ takes the 0-skeleton of P bijectively to the 0-skeleton of a shingle in $K_{2,2}$. This extends to the entire shingle in the natural way, if a simplex in P is spanned by the 0-simplices w, y and z, Ψ maps this simplex to the simplex spanned by $\Psi(w)$, $\Psi(y)$, and $\Psi(z)$. The face relations are preserved because none of the edges

collapsed in the forest collapses used in $\Delta(P)$ are in R, so the images under Ψ are related by the same forest collapses. This takes P combinatorially and bijectively to a shingle in $K_{2,2}$. Figure 8.5 shows an example of Ψ on a patch that maps to shingle 2.

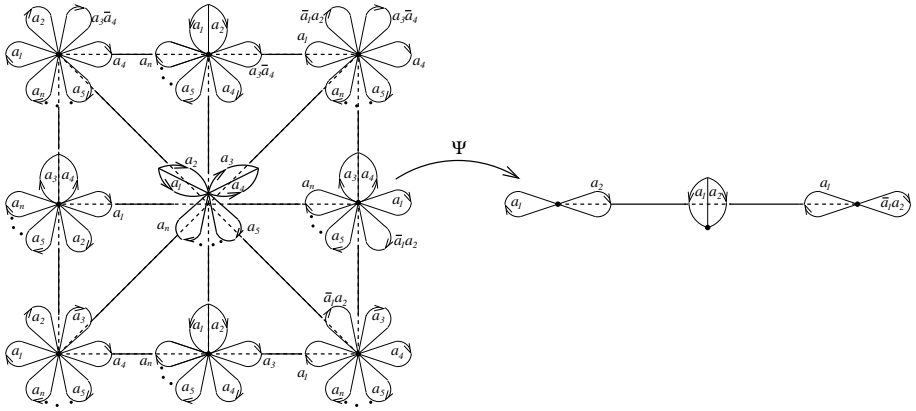

Figure 8.4: Example of Ψ on a patch with Shingle 1 Δ image

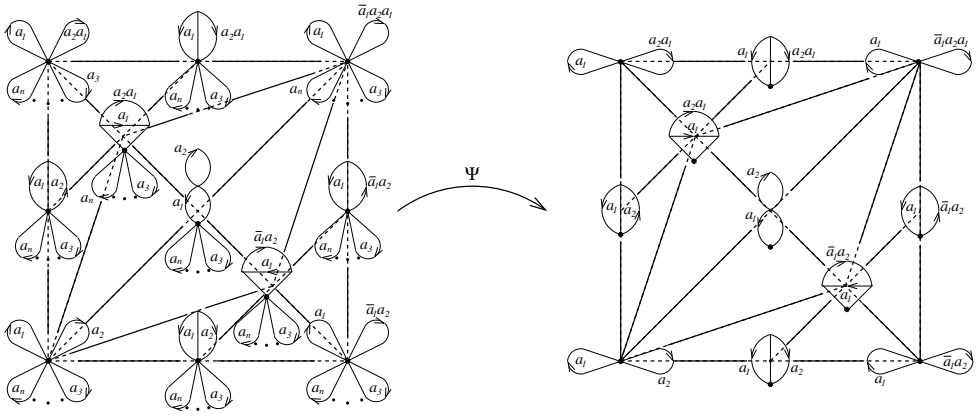

Figure 8.5: Example of Ψ on a patch with Shingle 2 Δ image

It remains to be seen that Ψ is well-defined on horizontal sides of patches in $\tilde{N}_x$. In particular, let v be the Nielsen point in a horizontal side of P_1 and P_2 patches in $\tilde{N}_x$. Let $\Delta(v) = (g_v, \theta_n)$, and observe that if $g_v^{-1}(\pi_1(R))$ is the subgroup of F_n associated to N_x, then P_1 and P_2 map to shingles of type 2. Otherwise P_1

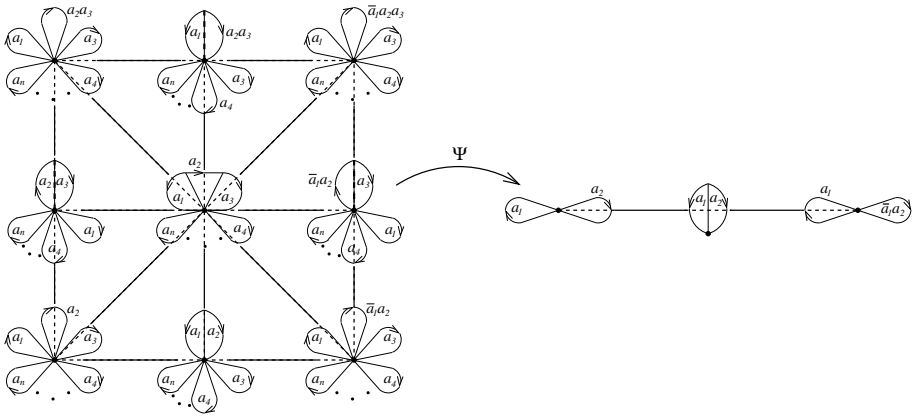

Figure 8.6: Example of Ψ on a patch with Shingle 3 Δ image

and P_2 map to shingles of type 1 or 3. Let a be a rose point in P_1 and P_2 so that there is an edge between v and a. Then if P_1 and P_2 are of type 2, since Ψ is well-defined on a and $\Psi(v)$ is obtained by $\Psi(a)$ by performing the same edge collapse in the case of each patch, $\Psi(v)$ is well-defined. If P_1 and P_2 are of types 1 or 3, $\Psi(a) = \Psi(v)$ and $\Psi(v)$ is well-defined. Hence, Ψ is well-defined on the edge connecting a and v, and on all horizontal edges. This completes the definition of $\Psi : \tilde{N}_x \to K_{2,2}$.

Note that the following diagram commutes:

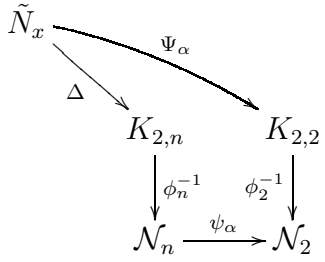

In particular, let $\lambda : S^1 \to N_x$ be an embedded edge loop. Consider the loops $\Psi \circ \lambda : S^1 \to K_{2,2}$ and $\psi \circ \phi_n^{-1} \circ \Delta \circ \lambda : N_x \to \mathcal{N}_2$. These loops are simplicial but are not in general combinatorial as they map edges in S^1 that map to shingle 1 or 3 under $\Delta \circ \lambda$ to points. Let Ψ' and λ' be slightly altered versions of $\Psi \circ \lambda$ and

$\psi \circ \phi_n^{-1} \circ \Delta \circ \lambda$ respectively. Specifically, let $c : S^1 \to S^1$ collapse all edges in S^1 that $\Delta \circ \lambda$ maps to shingles 1 or 3, and note that $\Psi \circ \lambda$ and $\psi \circ \phi_n^{-1} \circ \Delta \circ \lambda$ factor through c. Let $\Psi' \circ c = \Psi \circ \lambda$ and $\lambda' \circ c = \psi \circ \phi_n^{-1} \circ \Delta \circ \lambda$. If $\Delta \circ \lambda(S^1)$ is contained in translates of shingles 1 and 3, then c does not exist in which case set $\Psi' = \Psi \circ \lambda$ and $\lambda' = \psi \circ \phi_n^{-1} \circ \Delta \circ \lambda$. Hence, $\Psi' : S^1 \to K_{2,2}$ and $\lambda' : S^1 \to \mathcal{N}_2$ are either both combinatorial or both constant maps. Further, $\phi_2 \circ \lambda' = \Psi'$.

8.2 Loops and Corners in Nielsen Corridors

In this section we will consider the structure of loops in Nielsen corridors. More specifically, we will study basic loops in Nielsen corridors, those loops whose interiors are disjoint from the corridor. For such a loop λ, we will show that λ' is restricted and use this to show that λ has an even number of corners, where in this context a corner is a Nielsen point in the corridor whose link contains three rose points.

The proof of Theorem 8.5.1 which states that there is no simple patched filling of $Shin_4(id, x)|_{\partial D^2}$ will proceed in future sections as follows. Ignoring bivalent vertices in a Nielsen corridor leaves the corridor with only univalent and trivalent vertices. For a simple patched filling of $Shin_4(id, x)|_{\partial D^2}$ containing no patches mapping to shingle 4, the Nielsen corridor of u shown in Figure 8.2 has only one univalent vertex u. Note that basic loops do not traverse univalent vertices. Since each basic loop has an even number of corners, basic loops must traverse an even number of vertices. A planar graph satisfying these conditions is a 1-graph, and in Proposition 8.3.4 we show that no 1-graphs exist, yielding a contradiction.

Definition 36. *Let N be a Nielsen corridor. A Nielsen point $y \in N$ in the interior*

of D^2 is a corner *of N if y is contained in three patches. A Nielsen point $y \in N$, $y \in \partial D^2$ is a* corner *of N if y is contained in two patches. For an embedded edge loop $\lambda : S^1 \to N$, if $y \in Im(\lambda)$ is a corner of N, then $\lambda^{-1}(y)$ will be called a* corner *of λ.*

Let $\lambda : S^1 \to N$ be an embedded edge loop into a Nielsen corridor of a simple patched filling. Recall that λ^o the interior of λ is the connected component of $D^2 \setminus Im(\lambda)$ that is disjoint from ∂D^2.

Definition 37. *For $\lambda : S^1 \to N$, an embedded edge loop, if $\lambda^o \cap N = \emptyset$, then λ is a* basic loop *of N.*

For the remainder of this section, the following notational conventions are adopted. N is a Nielsen corridor, and $\lambda : S^1 \to N$ is a basic loop. y is a Nielsen point in the image of λ with $\lambda(x) = y$, and when indices are required $\lambda(x_i) = y_i$ for all i.

Proposition 8.2.1. *Let $\lambda : S^1 \to N$ be a basic loop. If λ' is not constant, then there exists $\alpha \in Aut(F_n)$ so that $\alpha \cdot \lambda'$ is restricted.*

Proof. The plan of this proof is to apply Proposition 7.3.3 to Ψ'. Specifically, let $v_1, v_2, \ldots, v_{m-1}, v_m = v_1$ be the Nielsen vertices passed through by Ψ'. We will construct rose vertices $R^1, R^2, \ldots, R^m$ so that:

1. $R^i \in lk(v_i)$,
2. $R^1 = R_m$, and
3. there is a length 2 rose path connecting R^i to R^{i+1} for all $1 \leq i \leq m$.

There rose vertices can be found by considering the loop in the inner boundary of the patched neighborhood of the image of λ. This is an edge loop in D^2 that maps by Ψ to an edge loop in $K_{1,2}$. The rose vertices traversed by this loop are the required vertices. It suffices to find rose points so that

1. $r_i \in lk(y_i)$,
2. $r_1 = r_k$, and
3. there is a length 2 path in the horizontal side of a patch connecting r_i and r_{i+1} for all i, $1 \leq i \leq m$.

This suffices because Ψ maps $r_1, \ldots r_k$, to $R^1, \ldots, R^m$. Note that this map is not injective on the rose points, r_i and r_{i+1} map to the same rose vertex under Ψ if r_i and r_{i+1} are contained in a patch mapping to a translate of shingle 1 or 3 under Δ.

Consider the rose points that are in the link of y_i. Note that this set has two or three points, and that only one of them can be in λ^o. To see this, first suppose that y_i is not in ∂D^2 and note that intersection of N and the extended patched neighborhood of y_i is homeomorphic to an m-pod where m is the number of rose points in the link of y_i. Further, λ traverses two of the m segments making up the m-pod. N separates the extended patched neighborhood of y_i into connected components so that each component contains exactly one of these rose points, and hence if two of the rose points are in λ^o, then N is also in λ^o which contradicts the fact the λ is basic. If $y_i \in \partial D^2$, then two of the rose points must also be in ∂D^2 and not be in λ^o, leaving only one rose point that can be in λ^o.

Further, there must be one rose point in the intersection of the link of y_i and λ^o. This is because the image of λ disconnects the extended patched neighborhood

of y_i, and at least one of the connected components must be in λ^o since λ is a loop. Hence, there is a unique rose point in the intersection of the link of y_i and λ^o. Let r_i be the unique rose point in the intersection λ^o and link of y_i. Note that by definition r_i is in the link of y_i and $r_1 = r_m$.

For each i there exists a patch P_i containing y_i, y_{i+1}, r_i, and r_{i+1} for all i. The unique rose point is contained in the same horizontal side of P_i as r_i is in λ^o since N does not intersect this side, and this rose point is in $lk(y_{i+1})$. Since r_{i+1} is the unique rose point satisfying thee two conditions, it is connected to r_i by a length 2 path in the horizontal side of a patch in $\tilde{N}$, proving the proposition. □

Corollary 8.2.1. *If λ is restricted, λ' has an even number of corners.*

Proof. By Proposition 7.3.2 and Proposition 8.2.1, there exists $\alpha \in Aut(F_n)$ so that $\alpha \cdot \lambda'$ has an even number of corners. The action of $Aut(F_n)$ preserves the number of corners, so λ' has an even number of corners. □

Definition 38. *Let $\lambda : S^1 \to N$ be the basic loop of N passing through y, a Nielsen point in D^2. Then P_1 be the patch λ passes through just before y and P_2 be the patch λ passes through just after y. The unique rose point in $lk(y) \cap (D^2 \setminus \lambda^o) \cap P_1$ is the initial rose point of y. The unique rose point in $lk(y) \cap (D^2 \setminus \lambda^o) \cap P_2$ is the terminal rose point of y.*

Remark: x is a corner if and only if the initial rose point of y and the terminal rose point of y are distinct.

Rose points, initial rose points, and terminal rose points are useful because they encode which axis λ' is traversing, recall that the axes of $\mathcal{N}_2$ are translates of the subgraph shown in Figure 7.9. More specifically let P be a patch mapping

to shingle 2 that λ traverses and let y_1 and y_2 be the points at which λ enters and leaves P respectively. Consider a small neighborhood of $\psi \circ \phi_n^{-1} \circ \Delta \circ \lambda(x_1)$ in $\mathcal{N}_2$, and note that this neighborhood intersects 3 axes. Let U_1 be the intersection of the interior of $\lambda^{-1}(P)$ and a small neighborhood of x_1. $\psi \circ \phi_n^{-1} \circ \Delta \circ \lambda(U_1)$ is contained in one of the three axes that intersect at $\psi \circ \phi_n^{-1} \circ \Delta \circ \lambda(x_1)$. Each of the three axes corresponds to a pair of rose vertices in the link of $\Psi \circ \lambda(x_1)$. Specifically, $\phi_2 \circ \psi \circ \phi_n^{-1} \circ \Delta \circ \lambda(U_1)$ is contained in the same shingle as $\Psi(R_{x_1})$ and the Ψ image of the terminal rose point of x_1. Since only one of the three axes that pass through $\psi \circ \phi_n^{-1} \circ \Delta \circ \lambda(x_1)$ maps to that shingle, the rose point and terminal rose point of x_1 determine which axis contains $\psi \circ \phi_n^{-1} \circ \Delta \circ \lambda(U_1)$. If U_2 is defined analogously, $\phi_2 \circ \psi \circ \phi_n^{-1} \circ \Delta \circ \lambda(U_2)$ is in the same shingle as $\Psi(R_{x_2})$ and the Ψ image of the initial rose point of x_2. Since only one of the three axes that pass through $\psi \circ \phi_n^{-1} \circ \Delta \circ \lambda(x_2)$ maps to that shingle, the rose point and initial rose point of x_2 determine which axis contains $\psi \circ \phi_n^{-1} \circ \Delta \circ \lambda(U_2)$.

Definition 39. *Each point $x \in S^1$ for which the intersection of the patched neighborhood of $\lambda(S^1)$ and the extended patched neighborhood of $\lambda(x)$ contains a patch mapping to shingle 2 and a patch mapping to shingle 1 or shingle 3 is called a* transition point *of λ. Removing the transition points from S^1 disconnects S^1 into open intervals, each of which either maps to patches mapping to shingle 1 or 3 or patches mapping to shingle 2. The closures of these intervals that map to shingle 1 or shingle 3 will be called* trivial *and those that map to shingle 2 will be called* non-trivial.

Remark: Note that if λ has a non-trivial interval, then λ' is not constant.

Recall the map $c : S^1 \to S^1$ that collapses edges that $\psi \circ \psi^{-1} \circ \Delta \circ \lambda$ maps to vertices, so that $\lambda' \circ c = \psi \circ \psi^{-1} \circ \Delta \circ \lambda$. This map is defined if λ is a non-trivial

interval.

Proposition 8.2.2. *If x is a corner of λ and in the interior of a non-trivial interval, then $c(x)$ is a corner of λ'.*

Proof. Note that the initial and terminal rose points of x are distinct. Let P_1 be the patch λ traverses before y and P_2 the patch after y, Further, let U be a small neighborhood of x and U_i the intersection of the interior of $\lambda^{-1}(P_i)$ and U. Note that $\psi \circ \phi_n^{-1} \circ \Delta \circ \lambda(U_1)$ and $\psi \circ \phi_n^{-1} \circ \Delta \circ \lambda(U_2)$ are in different axes. Since x is in the interior of a non-trivial interval, c is injective in U and this implies that $c(x)$ is a corner in λ'. □

Note that if x_1 and x_2 are corners in a trivial interval the unique rose points in $lk(y_1) \cap \lambda^o$ and $lk(y_2) \cap \lambda^o$ map to the same rose vertex under Ψ. Suppose x_1 and x_2 bound an interval where x_1 is the first point in the interval and x_2 is the last, and that this interval is contained in a trivial straight interval. If this interval contains no corners in its interior, then the terminal rose point of x_1 and the initial rose point of x_2 maps to the same rose vertex under Ψ.

Definition 40. *Consider the image of a small neighborhood of a trivial interval of λ minus the closed trivial interval under $\psi \circ \phi_n^{-1} \circ \Delta \circ \lambda$. If this image intersects more than one axis, it is a* trivial corner interval *and otherwise it is a* trivial straight interval.

Proposition 8.2.3. *Suppose λ' is not constant, then a trivial interval of λ is a trivial straight interval if and only if small neighborhoods of the interval contain an even number of corners.*

Proof. There are only two possible choices for the Ψ image of the initial and terminal rose points of Nielsen points in the trivial interval. More specifically, let

x_1 and x_2 be the endpoints of a trivial interval with x_1 before x_2 in the orientation. Either (1) the image under Ψ of the initial rose point of x_1 is not the same as the Ψ image of the terminal rose point of x_2, or (2) these images agree. Assume (1), then there must be an odd number of Nielsen points in the interval where the initial rose point is not equal to the terminal rose point, and hence there are an odd number of corners in the interval. In this case, the image of a small neighborhood of the interval maps to two axes, and the interval is a trivial corner interval. Now assume (2), then there are an even number of Nielsen points in the interval where the initial rose point is not the same as the terminal rose point and hence there are an even number of corners in the interval. Since the Ψ images of the initial rose point of x_1 and the terminal rose point of x_2 agree, the interval is a trivial straight interval. □

Proposition 8.2.4. *Suppose λ' is constant, then λ has an even number of corners.*

Proof. Note there is only one trivial interval which is a trivial straight interval, and no non-trivial intervals. Fix a Nielsen point x in S^1. Either (1) x is a corner and the images under of Ψ of initial and terminal rose points of x are distinct, or (2) x is not a corner and the images of those rose points are the same. In case (1), there must be an odd number of corners that are not x as there must be an odd number of Nielsen points that are not x in S^1 whose initial and terminal rose points have distinct images under Ψ, and hence λ has an even number of corners. In case (2), there must be an even number of corners that are not x as there must be an even number of Nielsen points that are not x in S^1 whose initial and terminal rose points have distinct images under Ψ, and hence λ has an even number of corners. □

Proposition 8.2.5. *Suppose λ' is not constant. The parity of the number of*

corners in λ is the same as the parity of the number of corners of λ'.

Proof. Consider a small neighborhood of a trivial interval. This neighborhood is contracted to a neighborhood of a point in the domain of λ'. If the original interval is straight, then the image of this neighborhood under λ' intersects one axis, and if the original interval is a corner interval then the image of this neighborhood under λ' intersects two axes by Proposition 8.2.3. Then if U is neighborhood of a trivial interval, the number of corners λ in U has the same parity as the number of λ' corners of $c(U)$.

Let V be the interior of a non-trivial interval. By Proposition 8.2.2, $c(V)$ contains the same number of corners as V. For all such U and V, note that U can be taken small enough so that $U \cap V$ contains no Nielsen points and hence no corners for any choices of U and V. These U and V cover S^1, which finishes the proposition. □

Corollary 8.2.2. *λ has an even number of corners.*

Proof. This is an immediate consequence of Propositions 8.2.4, and 8.2.5, and Corollary 8.2.1. □

8.3 Non-Existence of 1-Graphs

The main objective of the next 2 sections is prove Proposition 8.3.4, that there is no finite connected planar graph with one univalent vertex and all other vertices trivalent in which all basic loops traverse an even number of edges and the univalent vertex is not contained in closure of the interior of any embedded loop. To see the

relevance of such graphs, note that in a simple patched filling of $Shin_4(id, x)|_{\partial D^2}$ that uses no patches mapping to shingle 4 a slight simplification of the Nielsen corridor of u from Figure 8.2 is such a graph. This contradiction proves Theorem 8.5.1, that no such filling exists.

In this section, only planar graphs will be considered and moreover we will assume that each planar graph comes equipped with an embedding into $\mathbb{R}^2$. Recall that an edge loop in a planar graph is basic if $\lambda^o \cap \Gamma = \emptyset$.

Definition 41. *A vertex v in a planar graph Γ is* outside *of Γ if there is no embedded edge loop λ in Γ so that v is contained in $\bar{\lambda}$. Similarly, an edge e of Γ is* outside *of Γ if there is no embedded edge loop λ in Γ so that e is contained in $\bar{\lambda}$.*

Whether or not a particular loop in Γ is basic or a particular vertex or edge is outside of Γ depends on the embedding of Γ into $\mathbb{R}^2$. Recall that a simple graph is a graph where each edge is incident to two distinct vertices, and no pair of vertices are both incident to two distinct edges.

Definition 42. *A finite connected simple planar graph Γ with an embedding into $\mathbb{R}^2$ is an* m-graph *if it satisfies the following conditions:*

1. *all vertices of Γ are either univalent or trivalent,*
2. *Γ has m univalent vertices,*
3. *all basic loops in Γ traverse an even number of edges, and*
4. *all univalent vertices and edges incident to univalent vertices in Γ are outside of Γ.*

The goal in this section is to show that no 1-graphs exist. Figure 8.7 gives an example of a 2-graph.

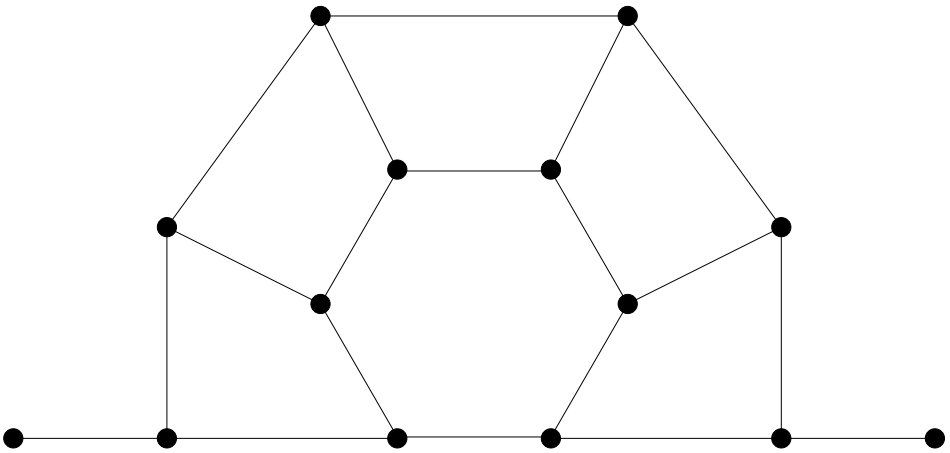

Figure 8.7: Example 2-graph

As a notational convention, the univalent vertices in an m-graph will be labeled $\nu = \nu_1, \ldots, \nu_m$, and the edges incident to these vertices are the *singleton* edges and are labeled $\epsilon_1, \ldots \epsilon_m$. In addition to ν_i, let ϵ_i be incident to μ_i.

If Γ is a 1-graph, we can assume that Γ has no separating as a separating edge creates a new 1-graph. More generally:

Proposition 8.3.1. *Each m-graph Γ contains a m'-graph Γ_o as a subgraph that has no separating edges other than the singleton edges of Γ_o with $m' \leq m$.*

Proof. Let $e \neq \epsilon_i$ for all i be a separating edge of Γ, otherwise take $\Gamma_o = \Gamma$. Let Γ_1 and Γ_2 be the connected components of $\Gamma \setminus e$. Then there is an embedded loop $\rho : S^1 \to \mathbb{R}^2$ so that ρ intersects Γ only once and only on e, and Γ_1 and Γ_2 are in different components of $\mathbb{R}^2 \setminus \rho$. Without loss of generality suppose that $\nu_1 \in \Gamma_1$, then ρ can be chosen such that Γ_2 is in the interior of ρ, otherwise there would be a loop in Γ_2 that contains Γ_1 and hence ν_i, contradicting the fact that Γ is an m-graph.

Suppose that $\nu_2, \nu_3, \ldots \nu_{m'} \in \Gamma_2$. Let $\Gamma_o = \Gamma_2 \cup e$ and let ν' be the vertex in

the intersection of e and the closure of Γ_1. Note that ν' is univalent in Γ_o along with all of the vertices ν_i that are contained in Γ_2, while all other vertices in Γ_o are trivalent. Note that every basic loop in Γ_o is contained in Γ_2. Since Γ_2 is in the interior of ρ, every basic loop in Γ_o is a basic loop in Γ, and every basic loop in Γ_o only intersects an even number of edges. Also, ν' and e are on the outside of Γ_o, and hence Γ_o is a m'-graph, where $m' \leq m$.

Γ_o is an m'-graph that contains at least one less edge than Γ, as Γ_o cannot contain ϵ_1. So, an m-graph with a separating edge that is not a singleton edge can be reduced to a subgraph that is an m'-graph with fewer edges, where $m' \leq m$. Eventually, this reduction produces a graph with no separating edges other than singleton edges, proving the proposition. □

Note that if Γ is a 1-graph, removing ϵ from Γ and subdividing μ into two univalent vertices yields a 2-graph. To prove that no 1-graph exists, we will prove that no such 2-graph exists. To this end, it is necessary to investigate 2-graphs. One way to build 2-graphs is by m-graph products:

Definition 43. *Let Γ_1 be an m_1-graph, and Γ_2 be an m_2-graph. Let $\Gamma_1 \# \Gamma_2$ be an $(m_1 + m_2 - 2)$-graph be called the* m-graph product *of Γ_1 and Γ_2 constructed by identifying ϵ_i, ν_i, and μ_i in Γ_1 with ϵ_j, μ_j, and ν_j in Γ_2 respectively for some i and j.*

Figure 8.8 is $\Gamma \# \Gamma_o$ where Γ is shown in Figure 8.7 and Γ_o is a 3-graph.

Proposition 8.3.2. *Each 2-graph either (1) has no separating edges other than singleton edges, (2) contains a 1-graph, or (3) is a finite graph product of 2-graphs where each summand has no separating edges other than singleton edges.*

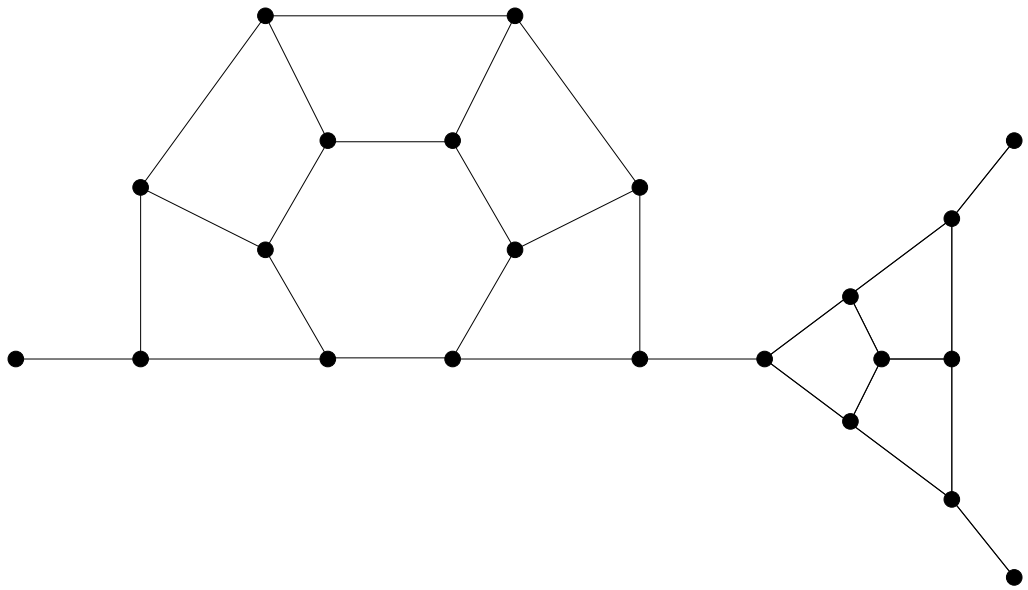

Figure 8.8: Example graph product

Proof. Suppose Γ is a 2-graph with a separating edge e that is not a singleton edge. Let Γ_1 and Γ_2 be the connected components of $\Gamma \setminus e$. If for some i, Γ_i does not contain ν_j for all j, then $\Gamma_i \cup e$ is a 1-graph by the arguments of Proposition 8.3.1. Otherwise, $\Gamma_1 \cup e$ and $\Gamma_2 \cup e$ are 2-graphs by the arguments of Proposition 8.3.1 and $\Gamma = (\Gamma_1 \cup e)\#(\Gamma_2 \cup e)$. Since for each i, $\Gamma_i \cup e$ does not contain ϵ_j for some j, this decomposition can be iterated to produce either a product decomposition of Γ where each summand contains no separating edges other than singleton edges, or a 1-graph is generated. □

Definition 44. *Let Γ be an m-graph with no separating edges that are not singleton edges. The boundary of the union of the closures of the basic loops in Γ is an edge loop called the* outer loop *of Γ, and is denoted ρ_Γ.*

Note that because Γ has no separating edges that are not singleton edges, ρ_Γ is an embedded edge loop. ρ_Γ traverses an even number of edges.

Definition 45. *Let Γ be a 2-graph with no separating edges other than singleton*

edges. Note that ρ_Γ is made up of two paths ρ_1 and ρ_2 from μ_1 to μ_2 that are disjoint except at their endpoints. Since ρ_Γ traverses an even number of edges, each of the two paths from μ_1 to μ_2 traverse the same parity of edges. Γ *is* even *if these paths traverse an even number of edges, and is* odd *if these paths traverse an odd number of edges.*

Note that the graph in Figure 8.7 is an odd 2-graph.

If Γ is a 1-graph, the 2-graph constructed by deleting ϵ and subdividing μ contains an even 2-graph. This is discussed in more detail in Corollary 8.3.4. However, the next step in the proof that no 1-graph exists is to show that no even 2-graphs exist. To see this, a simplification of m-graphs is needed.

Definition 46. *Let $\bar{\Gamma}$ be a graph defined from an m-graph Γ as follows: Delete all edges ϵ_i, and vertices ν_i. Remove the vertices μ_i and if there were edges other than ϵ_i incident to μ_i, join these two edges as one single edge.*

Figure 8.9 shows $\bar{\Gamma}$ for Γ shown in Figure 8.7.

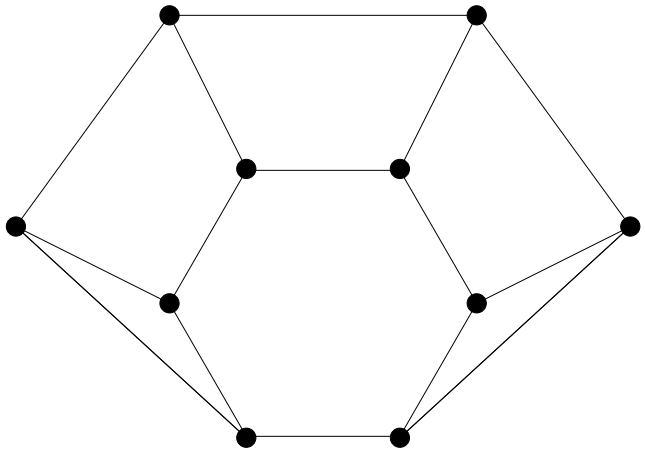

Figure 8.9: $\bar{\Gamma}$ for Γ shown in Figure 8.7

Proposition 8.3.3. *No even 2-graph exists.*

Proof. Let Γ be such a graph, and suppose that there is no pair of edges that separate $\bar{\Gamma}$. Consider the dual graph $\bar{\Gamma}'$ of $\bar{\Gamma}$, and note that this dual is simple. $\bar{\Gamma}'$ is planar, with two vertices of odd valence x and y each of which is incident to an edge that is incident to the vertex v corresponding to the area outside of Γ. All other vertices have even valence and all basic loops traverse three edges. Delete the edges that connect x and y to v, and note that $\bar{\Gamma}'$ remains connected otherwise it would not be simple. All of vertices now have even valence.

Suppose that ρ_i traverses 2 edges for some i, and note that this can only be true of one of the ρ_i as otherwise $\bar{\Gamma}'$ would not be simple. Then $\bar{\Gamma}'$ has one basic loop that traverses 5 edges, and all others traverse 3. By performing a transformation that moves the basic loop that traverses five edges to the outside, observe that it is sufficient to show that there is no finite triangulation of a pentagon so that each vertex has even valence. By Proposition 8.4.7, no such triangulation exists contradicting the existence of Γ.

If ρ_i traverses more than 2 edges for each i, then there are two basic loops traversing four edges while all others traverse three. Note that the valence of v is a multiple of four because Γ is even. v can be divided into two vertices v_1 and v_2 where edges passing through ρ_i are incident to v_i. The valence of v_i is even for each i since Γ is even, and non-zero since each ρ_i traverses more than 2 edges. This vertex subdivision leaves all vertices in the graph with even valence, one basic loop that traverses 8 edges, and all other basic loops traversing 3 edges. By performing a transformation that moves the basic loop that traverses 8 edges to the outside, observe that it is sufficient to show that there is no finite triangulation of a octagon so that each vertex has an even valence. By Proposition 8.4.7, no

such triangulation exists contradicting the existence of Γ.

Hence, for any even 2-graph Γ, there must be a pair edges e_1, e_2 that separate $\bar{\Gamma}$. Note that Γ also has a pair of edges that separate Γ. More specifically, this pair of edges can be found by mapping $\bar{\Gamma}$ onto Γ in the canonical way and choosing the edges in the image of the separating pair of $\bar{\Gamma}$ as the separating pair of Γ. Note that some edges in $\bar{\Gamma}$ map to multiple edges in Γ, if this is the case for one of the separating edges, choose any of the edges in its image. Also observe that the edges in a separating pair of Γ that was defined in this way do not include singleton edges and are not each incident to μ_i for some i. By abuse of notation let e_1 and e_2 also refer to this pair of separating edges in Γ and consider the connected components of $\Gamma \setminus (e_1 \cup e_2)$ where e_1 and e_2 are their images in Γ. If there is a connected component that does not contain μ_1 or μ_2, then the union of this component, e_1, and e_2 is a 2-graph denoted $\tilde{\Gamma}$. By Proposition 8.3.2, (1) either $\tilde{\Gamma}$ has no separating edges other than singleton edges, (2) $\tilde{\Gamma}$ contains a 1-graph, or (3) $\tilde{\Gamma}$ is a finite graph product of 2-graphs where each summand has no separating edges other than singleton edges. Consider these cases in order:

1. If $\tilde{\Gamma}$ has no separating edges other than singleton edges, then it is either even or odd. If it is even, Γ has been reduced to an even 2-graph with fewer edges and this analysis begins anew with $\tilde{\Gamma}$. If it is odd, then replace $\tilde{\Gamma}$ in Γ with an edge, and note that this new Γ is an even 2-graph with fewer edges than Γ.
2. If $\tilde{\Gamma}$ contains a 1-graph, then Γ has a separating edge, which is not permitted as Γ is even.
3. If $\tilde{\Gamma}$ is a finite graph product of 2-graphs where each summand has no separating edges, if any of the summands is even, replace Γ with this summand

which is an even 2-graph with fewer edges than Γ. If all of the summands are odd, then then replace $\tilde{\Gamma}$ in Γ with an edge, and note that this new Γ is an even 2-graph with fewer edges than Γ.

Now assume that there are two components of $\Gamma \setminus (e_1 \cup e_2)$, one containing the image of μ_1, and the other containing the image of μ_2. Taking e_1 and e_2 to be in $\bar{\Gamma}$, consider $\bar{\Gamma} \setminus (e_1 \cup e_2)$. To separate the images of μ_1 and μ_2, e_1 and e_2 must be edges in the paths ρ_i, without loss of generality, assume that e_i is an edge in ρ_i. This means that in $\bar{\Gamma}'$ there is a vertex $w \neq x$ or y such that there are two edges incident to v and w. This also implies that ρ_i traverses more than 2 edges for each i. By the same edge deletion and vertex splitting process described earlier in the proposition, the existence of this graph gives a way to triangulate an octagon where every vertex has even valence, violating Proposition 8.4.7. □

Proposition 8.3.4. *No 1-graph exists.*

Proof. Let Γ be a 1-graph, by Proposition 8.3.1 assume that Γ has no separating edges. Let $\tilde{\Gamma}$ be the 2-graph resulting from removing ϵ from Γ and dividing μ into two univalent vertices. By Proposition 8.3.2 either (1) $\tilde{\Gamma}$ has no separating edges other than singleton edges, (2) $\tilde{\Gamma}$ contains a 1-graph, or (3) $\tilde{\Gamma}$ is a finite graph product of 2-graphs where each summand has no separating edges other than singleton edges. Taking these possibilities in order:

1. If $\tilde{\Gamma}$ has no separating edges, and that makes $\tilde{\Gamma}$ an even 2-graph. By Proposition 8.3.3, no such $\tilde{\Gamma}$ exists.
2. If $\tilde{\Gamma}$ contains a 1-graph, then Γ had a separating edge contradicting the assumption at the start of the proposition.

3. If $\tilde{\Gamma}$ is a finite graph product of 2-graphs, each summand must be odd by Proposition 8.3.3. Then Γ is not a 1-graph since the unique basic loop containing μ traverses an odd number of edges, which is a contradiction.

Hence no such $\tilde{\Gamma}$ exists, and no 1-graph Γ exists. □

8.4 Triangulations of m-gons

Proposition 8.4.7 is the final piece required in the proof of Proposition 8.3.4. Specifically, Proposition 8.4.7 states that for an m-gon where m is not a multiple of 3 and $m > 3$, there is no finite triangulation in which each vertex has even valence.

For the remainder of this section, let M be an oriented basepointed m-gon where $m > 3$ is not a multiple of 3, equipped with a finite triangulation in which each vertex has even valence. M and the triangulation will be used to define a new polygon, the interior neighbor M' of M. The general plan for this proof is to show that M' contains an m'-gon where $m' > 3$ is not a multiple of 3. This creates a list of polygons, one contained in the previous in the triangulation of M that does not terminate, contradicting the existence of the triangulation.

Let $v_1, \ldots, v_{m+1}$ be the vertices of M traversed in the order of this orientation where $v_1 = v_{m+1}$ is the basepoint. Choose v_1 so that v_m, v_1, and v_2 are not the 0-dimensional faces of 2-simplex in the triangulation. Also, let $e_1, e_2, \ldots e_m$ be the edges of M so that e_i is incident to v_i and v_{i+1}.

Definition 47. *Let T be a 2-simplex that contains an edge in M as a 1-dimensional face. The union of the edges in T that are not contained in M is the* interior boundary *of T.*

The interior boundary is connected and can be regarded as a path by ordering the 0-cells that are contained in edges in $T \cap M$. The first and last vertices in this order are the endpoints of the interior boundary, and the path given by traversing the interior boundary of T from the first vertex in this order to the last will be called the *interior path* of T.

The orientation of M fixes an order on the 2-simplices that contain edges in M. Specifically, let $T_1, T_2, \ldots, T_{k'}$ be these 2-simplices listed in increasing order with respect to the total order $T_i < T_j$, if T_i contains $e_{i'}$ and $i' < j'$ for all $e_{j'}$ contained in T_j.

Definition 48. *The* interior neighbor M' *of* M *is the edge loop determined by traversing the interior paths of the* T_i *in increasing order.*

Definition 49. *The union of the 2-simplices* T_i *for* $1 \leq i \leq k'$ *is the* simplicial neighborhood U *of* M*.*

Figure 8.10 illustrates M, M', and U for a fragment of a possible triangulation of an octagon, where M is shown as solid lines, M' is shown as dotted lines, and U is shown as shaded regions.

Note that ∂U is covered by $M \cup M'$. M' is indeed a loop since v_m, v_1, and v_2 are not the 0-dimensional faces of 2-simplex in the triangulation. M' may not be an embedded loop, as M' may traverse an edge or vertex multiple times.

Definition 50. *If* M' *is an embedded loop, then* M' *is* non-degenerate*. If* M' *traverses some vertex more than once but does not traverse an edge more than once, then* M' *is* vertex degenerate*. If* M' *traverses some edge more than once, then* M' *is* edge degenerate*.*

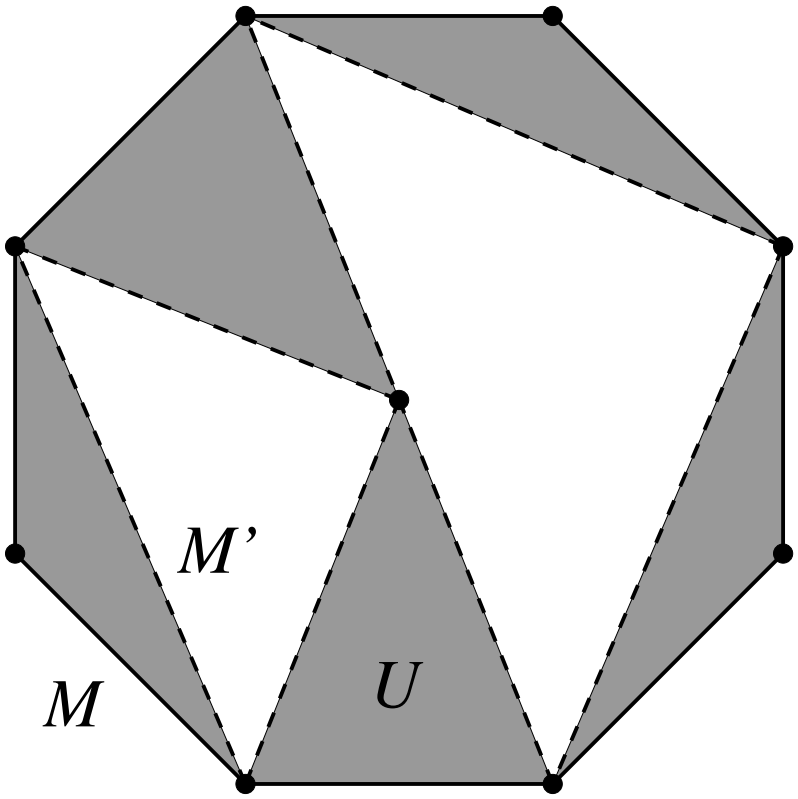

Figure 8.10: Example of M, M', and U

Note that because each vertex v has even valence, if $v \in M$ then v is a 0-dimensional face of an odd number of 2-simplices. Hence, for all v in $M' \cap M$ after traversing v, M' cannot backtrack along the same edge that it used to reach v, as otherwise v would only be contained in two 2-simplices.

Proposition 8.4.1. *Suppose M' is non-degenerate or vertex degenerate, then M' contains an m'-gon where $m' > 3$ is not a multiple of 3.*

Proof. Note that each 2-simplex T_i has either 1 or 2 edges in M. Let $Q_1, Q_2, \ldots Q_j$ be the 2-simplices with one 1-dimensional face in M, and $R_1, R_2, \ldots R_k$ be the 2-simplices with two 1-dimensional faces in M. Consider the ordering $Q_1, R_1, Q_2, R_2, \ldots$, and let P_i be the polygon obtained by passing the edges of

M through the first i simplices in this list. Figure 8.11 shows a possible labeling for the 2-simplices in Figure 8.10 in terms of this notation.

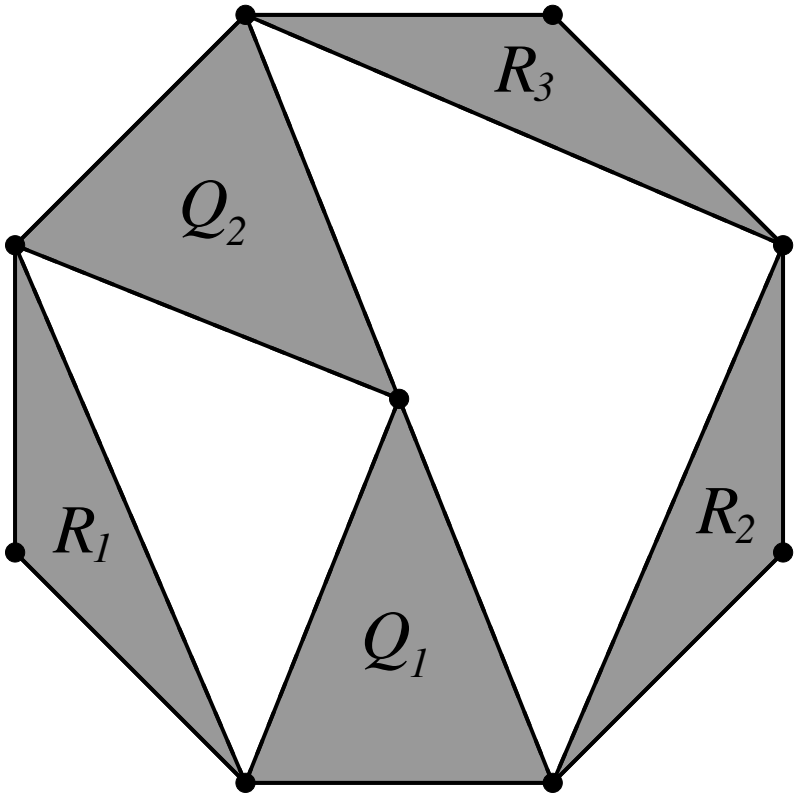

Figure 8.11: Labeling for Figure 8.10

Note $P_0 = M$, and $P_{j+k} = M'$. Consider two cases, (1) $j > k$ and (2) $j \leq k$. In case (1) P_{2k} has the same number of edges as P_0, and note that there are $m - 3k$ edges in M that are not in P_{2k}. For each pair of edges in M that are not in P_{2k} there is one edge in P_{j+k}. The number edges in P_{j+k} is the sum of the number of edges in $P_{j+k} \cap P_{2k}$ and the number of edges in P_{j+k} that are not in P_{2k}. This sum is $3k + \frac{m-3k}{2}$ which is not a multiple of 3. In case (2) P_{2j} has the same number of edges as P_0, and note that there are $m - 3j$ edges in M that are not in P_{2j}. For each edge in M that is not in P_{2j} there are two edges in P_{j+k}. The number edges in P_{j+k} is the sum of the number of edges in $P_{j+k} \cap P_{2j}$ and the number of edges

in P_{j+k} that are not in P_{2j}. This sum is $3j + 2(m - 3j)$ which is not a multiple of 3.

If M' is non-degenerate, then M' is an m'-gon where m' is not a multiple of 3. Note that $m' \geq \frac{m}{2} \geq 2$, but since bi-gons are not allowed in triangulations, $m' > 3$.

If M' is vertex degenerate, M' is a wedge product with polygonal summands. Since M' is not edge degenerate, and bi-gons are not allowed in triangulations, the fewest sides permitted in the polygonal summands of M' is 3. Since the total number of sides of M' is not a multiple of 3, one of the summands has m' sides, where $m' > 3$ and m' not a multiple of 3. □

In order for the process of creating m'-gons in M to continue, the new m'-gon must take the place of M. In other words, it needs to be shown that when the triangulation of M is restricted to the m'-gon, all vertices in the m'-gon must have even valence.

Proposition 8.4.2. *Suppose M' is non-degenerate or vertex degenerate, then each vertex in U has even valence in U. Each vertex in U is incident to an even number of edges that are not in U.*

Proof. Note that since M' is not edge degenerate, M' traverses edges at most once. For $v \in U$ there are an even number of edges incident to v that are in M'. If $v \in M$, the valence of v in M is 2, and otherwise the valence of v in M is 0. So for all $v \in U$, v has even valence in U. Further, since each vertex in U has even valence in the triangulation, each is incident to an even number of edges not in U. □

Let M' be vertex degenerate, and let P be an m'-gon contained in M' with $m' > 3$ not a multiple of 3. It is left show that when the triangulation of M

is restricted to the interior of P that the valence of the vertices in P is even. Proposition 8.4.2 tells us that when the triangulation of M is restricted to the interior of M' that the vertices of P have even valence. Hence it is necessary to investigate vertex degenerate M' further.

Recall from chapter 5 that a disk tree is a CW-complex where the boundary of each 2-cell embeds into the 1-skeleton and the intersection of the images of the boundaries of any two 2-cells is either empty or a point.

Proposition 8.4.3. *If M' is vertex degenerate, M' is the 1-skeleton of a disk tree.*

Proof. Let $\lambda_1, \lambda_2, \ldots \lambda_m$ be the basic loops of M'. Note that if $i \neq j$, and $\lambda_i \cap \lambda_j \neq \emptyset$ then $\lambda_i \cap \lambda_j$ is connected. Otherwise, M would not be connected. If for all $i \neq j$, $\lambda_i \cap \lambda_j$ is empty or 0-dimensional, then M' is a disk tree. Suppose otherwise and let T be a simplex containing an edge in $\lambda_i \cap \lambda_j$. Then $T \setminus T \cap M'$ is in the interior of M', and note that $T \setminus T \cap M'$ contains the interior of an edge in M. But M is disjoint from the interior of M', yielding a contradiction. □

Definition 51. *An edge path given by a basic loop in M' is called a* polygon *of M'.*

Let $\Gamma_{M'}$ be the bipartite graph with a vertex for each polygon of M', a vertex for each vertex that M' traverses multiple times and an edge connecting polygon P to vertex v if $v \in P$. Note that $\Gamma_{M'}$ is a tree by Proposition 8.4.3. Further the vertices that M' traverses multiple times are exactly those that are contained in multiple polygons. For example, for M' shown in Figure 8.10 $\Gamma_{M'}$ is a tree with 2 edges.

Proposition 8.4.4. *If the triangulation of M is restricted to the interior of a polygon P of M', then each vertex of P has even valence in the restriction.*

Proof. Let P be a polygon of M' and suppose that for all vertices of P except v that the vertices have even valence in the triangulation of M restricted to the interior of P. Then v also has even valence in this restriction, as otherwise the restriction gives a triangulation of P where all vertices other than v have even valence. This is not possible since the sum of the valences of vertices in a graph must be even.

Note that if P is a polygon corresponding to a leaf of $\Gamma_{M'}$, all vertices of P except one have even valence in the interior. To see this, let v be the vertex corresponding to the unique vertex in the link of P in $\Gamma_{M'}$. Note that for all vertices in P other than v, the number of edges that are not in U that are incident to the vertex is the valence of the vertex in the restriction of the triangulation to the interior of P. By Proposition 8.4.2, this valence is even for all vertices in P other than v. By the remark above, all vertices of P must have even valence in P. Pruning $\Gamma_{M'}$ of two levels of leaves yields new polygon leaves in which all vertices contained in the polygon with one exception have even valence in the interior of the polygon. Repeated pruning of $\Gamma_{M'}$ in this way completes the proposition. □

For non-degenerate and vertex degenerate M', we have produced an m'-gon where $m' > 3$ is not a multiple of 3, and when the triangulation of M is restricted to the polygon all vertices have even valence. It is only left to show that M' cannot be edge degenerate.

Proposition 8.4.5. *Suppose that M' is edge degenerate, and passes over the edge e twice. If T_i and T_j contain e, then T_i and T_j each contain a unique edge in M,*

$e_{i'} \neq e$ and $e_{j'} \neq e$ respectively, and $e_{i'}$ and $e_{j'}$ are not incident to a common vertex.

Proof. Note that e is not in M as M' does not traverse edges in M. By definition T_i and T_j both must include at least one edge in M. Suppose T_i includes two edges in M, $e_{i'}$ and $e_{i'+1}$. Then e is incident to $v_{i'}$ and $v_{i'+2}$. Note that T_j must contain either $e_{i'+2}$ or $e_{i'-1}$. This means that $v_{i'}$ or $v_{'i'+2}$ has odd valence, contradicting an assumption of the triangulation.

Now, let $e_{i'}$ and $e_{j'}$ be the unique edges in M contained by T_i and T_j respectively. Suppose that these edges are incident to a common vertex. Then that vertex has odd valence, contradicting an assumption of the triangulation. □

Proposition 8.4.6. *M' cannot be edge degenerate.*

Proof. Proceeding by contradiction, let M' be edge degenerate. A subpath $\tilde{M}$ of M' can be defined so that $\tilde{M}$ is a loop and does not traverse any edge twice. In particular, let $E_1, E_2, \ldots E_i$ be the edges that M' passes over twice in the order that M' first traverses them. Let T and T' be the 2-simplices that contain E_i and v and v' be the vertices incident to E_i where M' traverses v' before v. Note that $T \cup T'$ disconnects M'. Considering M' as a combinatorial map from S^1 to the triangulation of M, let R_1 and R_2 be the connected components of $S^1 \setminus M'^{-1}(E_i)$. Since for each 2-simplex containing E_l for some l, the 2-simplex only contains one edge in M by Proposition 8.4.5, R_1 and R_2 contain the interiors of at least 3 edges. Without loss of generality, suppose that $v \in M'(R_1)$ and $v' \in M'(R_2)$. Let $\bar{R}_1$ be the closure of R_1 and note that since E_i is the last edge that M' traverses twice, $M'|_{\bar{R}_1}$ does not traverse any edge more than once. Further, $M'|_{\bar{R}_1}$ factors through S^1 by $c : \bar{R}_1 \to S^1$ where c identifies the endpoints of $\bar{R}_1$. Define $\tilde{M}$ by

$\tilde{M} \circ c = M'|_{\bar{R}_1}$. While $\tilde{M}$ does not traverse any edge more than once, it may traverse vertices multiple times. Abusing notation, the image of $\tilde{M}$ will also be referred to as $\tilde{M}$. Figure 8.12 illustrates this terminology, where $\tilde{M}$ is shown as dotted lines and M is shown as dark solid lines.

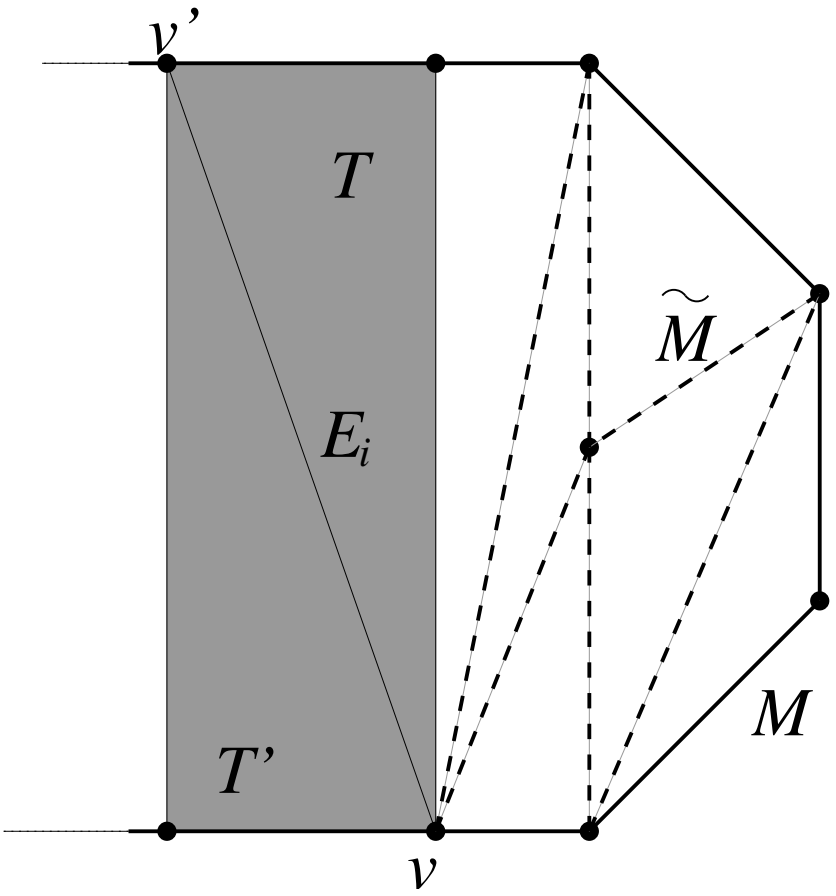

Figure 8.12: Example of edge degenerate M', and resulting $\tilde{M}$

Note that v has odd valence in U. To see this observe that there are an even number of edges in $\tilde{M}$ that are incident to v as $\tilde{M}$ does not traverse any edge more than once. E_i is the only edge in $M' \setminus \tilde{M}$ that is incident to v, and v is incident to two edges in M. Since all edges in U are either in M, $\tilde{M}$, or $M' \setminus \tilde{M}$, v has odd valence in U.

All vertices in $\tilde{M}$ other than v have even valence in U. The difference between these edges and v is that there are no vertices in $M' \setminus \tilde{M}$ that are incident to these vertices. Each of these vertices has even valence in $\tilde{M}$, zero valence in $M' \setminus \tilde{M}$ and valence 0 or 2 in M, and hence even valence in U.

When the triangulation of M is restricted to the closure of the interior of $\tilde{M}$, note that this gives a triangulation of $\tilde{M}$. In order for all vertices in the triangulation of M to have even valence, v must have odd valence in the triangulation of $\tilde{M}$ while all other vertices must have even valence in the triangulation of $\tilde{M}$. This is a contradiction since the sum of the valences of the edges in a graph must be even. Hence, M' cannot be edge degenerate. □

Putting these results together shows that no such triangulation exists.

Proposition 8.4.7. *Suppose $m > 3$ is not a multiple of 3. Then there is no finite triangulation of an m-gon where all vertices have even valence.*

Proof. We will proceed by contradiction assuming that M is such a polygon. Consider the interior neighbor M' of M, and note that by Proposition 8.4.6 that M' is either non-degenerate or vertex degenerate. If M' is non-degenerate then by Proposition 8.4.1 M' is an m'-gon where $m' > 3$ is not a multiple of 3, and by Proposition 8.4.2 all vertices in the closure of M' have even valence in the restriction of the triangulation of M to M'. If M' is vertex degenerate, then by Proposition 8.4.1 M' contains an m'-gon P where $m' > 3$ is not a multiple of 3. By Proposition 8.4.4 all vertices in the closure of P have even valence in the restriction of the triangulation of M to P.

By this method, a list of polygons can be created $M = M_1, M_2, M_3, \ldots$ so that M_i is the m'-gon contained in the interior neighbor of M_{i-1}. This list of does not

terminate, and there is no finite triangulation of M. □

8.5 Simplified Corridors and Proof of Minimality

In this section, the main results of the last 3 chapters are collected to prove Theorem 8.5.2 that κ is the minimal simply-connected complex of K_2 that is preserved under the action of $Aut(F_n)$. More specifically, let Δ be a simple patched filling of $Shin_4(id, x)|_{\partial D^2}$ that does not contain any patches mapping to shingle 4. It is shown in this section that the Nielsen corridor of u from Figure 8.2 in Δ is a 1-graph. Since 1-graphs do not exist, no such Δ exists, proving that $Shin_4(id, x)|_{\partial D^2}$ cannot be filled in $K_2 \setminus orbit(\mathsf{F}_4^o)$, $K_2 \setminus orbit(\mathsf{F}_5^o)$, or $K_2 \setminus orbit(\mathsf{F}_6^o)$.

Definition 52. *For a simple patched filling Δ using no patches mapping to shingle 4, and a Nielsen corridor N in Δ, the* simplified corridor *N' is obtained from N by deleting all bivalent vertices that are not in ∂D^2 and treating the two edges incident to that vertex as a single edge. Each bivalent vertex that is in ∂D^2 is replaced by a trivalent vertex and a new edge the that incident to a new univalent vertex.*

Note that N canonically maps to N'. Further, N' embeds in a neighborhood of D^2 and hence is planar by taking the inverse of the map from N to N' on the image of N, and letting the newly added univalent vertices map to a point outside of D^2 radially outward from the trivalent vertex they are adjacent to. Each vertex in a simplified corridor N' is either univalent or trivalent. Note that the number of univalent vertices in N' equals the number of Nielsen points in N that are in ∂D^2. Let λ be a basic loop in N. Then x is a corner of λ if x maps to a trivalent vertex in N'. Hence every basic loop in N', where the interior of λ is defined by the map of N' into a neighborhood of D^2, crosses an even number of trivalent vertices by

Proposition 8.2.2 and no univalent vertices, and thereby traverses an even number of edges. Additionally, note that univalent vertices and edges that are incident to them are outside of N'.

Theorem 8.5.1. *All simple patched fillings of $Shin_4(id, x)|_{\partial D^2}$ must use at least one patch that maps to a translate of shingle 4.*

Proof. Suppose that there exists a simple patched filling of $Shin_4(id, x)|_{\partial D^2}$ that does not use shingle 4. Then by Proposition 8.1.1, N_u is disjoint from N_z for all Nielsen points z on the boundary where $z \neq u$. Hence N'_u is a 1-graph. By Proposition 8.3.4, no such graph can exist, and no such filling exists. □

Corollary 8.5.1. *There is no nullhomotopy $Shin_4(id, x)|_{\partial D^2} : S^1 \to K_1$ in $K_2 \setminus orbit(\mathsf{F}_4^o)$, $K_2 \setminus orbit(\mathsf{F}_5^o)$, and $K_2 \setminus orbit(\mathsf{F}_6^o)$.*

Proof. Suppose otherwise, then by Corollary 5.4.1, there exists a patched filling for $Shin_4(id, x)|_{\partial D^2}$ that does not use shingle 4. By Proposition 5.5.1, this filling can be assumed to be simple. By Theorem 8.5.1, there is no such simple patched filling, and no such nullhomotopy exists. □

Lemma 8.5.1. *Let K be a simply-connected subcomplex of K_2 that is preserved under the action of $Aut(F_n)$. Then $dim\ K = 2$.*

Proof. $dim\ K > 0$ since K must be connected and preserved under the action of $Aut(F_n)$. $dim\ K \neq 1$ because $Aut(F_n)$ has property FA, and no subcomplex of the 1-skeleton of K_2 has a global fixed point under the action of $Aut(F_n)$. Thus, $dim\ K = 2$. □

Theorem 8.5.2 (Minimality). *For $n \geq 3$, there is no subcomplex of K_2 that is preserved under the action of $Aut(F_n)$ that does not contain κ.*

Proof of Minimality. Suppose that K is a simply-connected subcomplex of K_2 that is preserved under the action of $Aut(F_n)$. Then by Lemma 8.5.1, $dim\ K = 2$. Assume that $n \geq 4$.

If K contains K_1, then K contains $Shin_1(id, x)|_{\partial D^2}$ and $Shin_4(id, x)|_{\partial D^2}$. K must contain $orbit(\mathsf{F}_7)$, since by Theorem 6.5.1 $Shin_1(id, x)|_{\partial D^2}$ cannot be filled in $K \setminus orbit(\mathsf{F}_7^o)$. K must also contain $orbit(\mathsf{F}_4)$, $orbit(\mathsf{F}_5)$, and $orbit(\mathsf{F}_6)$ since by Corollary 8.5.1 $Shin_4(id, x)|_{\partial D^2}$ cannot be filled in $K \setminus orbit(\mathsf{F}_4^o)$, $K \setminus orbit(\mathsf{F}_5^o)$, and $K \setminus orbit(\mathsf{F}_6^o)$. Since $\kappa = \bigcup_{i=4}^{7} orbit(\mathsf{F}_i)$, $\kappa \subseteq K$.

Assume K does not contain K_1. Then since $dim\ K = 2$, there are only three possibilities for K as there are only three 2-dimensional subcomplexes of K_2 that are preserved under the action of $Aut(F_n)$ that do not contain K_1. These subcomplexes are (1) $orbit(\mathsf{F}_1)$, (2) $orbit(\mathsf{F}_4)$, and (3) $orbit(\mathsf{F}_1) \cup orbit(\mathsf{F}_4)$. Consider these three possibilities in order:

Case 1: Let E_1 be a representative of the edge e_1 in $K_2/Aut(F_n)$, and let F_1 be the representative of f_1 containing E_1. See Figure 2.3 for definitions of edges e_i. E_1 is a free face of F_1, and F_1 deformation retracts on to its faces the are representatives of e_2 and e_3. Further the edges in $orbit(\mathsf{E}_1)$ is a union of free faces in $orbit(\mathsf{F}_1)$, and the deformation retraction can be performed on each representative of f_1, and results in a deformation retraction from $orbit(\mathsf{F}_1)$ to $orbit(\mathsf{E}_2) \cup orbit(\mathsf{E}_3)$. Since the action of $Aut(F_n)$ on $orbit(\mathsf{E}_2) \cup orbit(\mathsf{E}_3)$ has no global fixed points, $orbit(\mathsf{E}_2) \cup orbit(\mathsf{E}_3)$ is not simply-connected and hence $orbit(\mathsf{F}_1)$ is not simply-connected.

Case 2: The same argument used in Case 1 applies in Case 2, the only alteration here is that the translates of E_6 are the free faces.

Case 3: The same argument used in Cases 1 and 2 applies in Case 3, the only alteration here is that the translates of both E_6 and E_1 are the free faces.

Since none of the three possible cases are simply-connected, there is no simply-connected subcomplex of K_2 that is preserved under the action of $Aut(F_n)$ that does not contain κ. In this sense, κ is the minimal simply-connected subcomplex of K_2 that is preserved under the action of $Aut(F_n)$.

For the case of $n = 3$, the proof is identical except that F_7 need not be considered as f_7 does not exist in $K_2/Aut(F_3)$. □

CHAPTER 9

DEGREE THEOREM FOR RIBBON GRAPHS

In the study of $Aut(F_n)$, finding inspiration from the study of mapping class groups of orientable surfaces is a standard practice. Tools from the study of mapping class groups have been successfully ported to the study of $Aut(F_n)$ by countless authors. It is impractical to list them all here, however two prominent examples are [3] and [5].

In this chapter and the next we consider the opposite view point, and take inspiration from the study of $Aut(F_n)$ and Auter space to study $MCG_u^{\pm}(\Sigma)$, the mapping class group of an orientable, punctured surface Σ with basepoint u, and $\mathfrak{T}(\Sigma, u)$ the basepointed Teichmüller space of Σ. Analogously to the spine of Auter space, $\mathfrak{T}(\Sigma, u)$ contains a simplicial complex $\mathfrak{R}(\Sigma, u)$ the ribbon graph complex of (Σ, u). Over the next 2 chapters we will use techniques that Hatcher and Vogtmann developed in proving the Degree Theorem for Auter space in [7] to prove the analogous theorem for basepointed Teichmüller space. Specifically we prove Degree Theorem 2 that there exists a sequence of nested simplicial complexes $\mathfrak{J}_0 \subset \mathfrak{J}_1 \subset \ldots \subset \mathfrak{J}_{2n-2} = \mathfrak{R}(\Sigma, u)$ where $\mathfrak{J}_i$ is i-dimensional and $(i-1)$-connected.

9.1 Topological Constructions

We now review the basic definitions and topological constructions regarding basepointed Teichmüller space and the ribbon graph complex. For a more detailed treatment, especially proofs of many facts claimed in this section, see [8] and [9].

Definition 53. *A* ribbon graph *is a finite basepointed connected graph* (Γ, w) *with for each vertex in* Γ *a cyclic ordering of the half edges incident to that vertex. The*

cyclic orderings are together called the ribbon structure *of the ribbon graph and will be notated* $\mathcal{O}(v)$ *where* v *is a vertex of* Γ. Γ *will be referred to as the* underlying graph. *We denote a ribbon graph by the triple* $(\Gamma, \mathcal{O}, w)$.

Notation: $\mathcal{O}$ and w will be dropped from this notation when the ribbon graph structure and basepoint are either implied or irrelevant.

Remark: In most research on ribbon graphs basepoints are not used, but this work utilizes some technical advantages given by the basepoints.

Definition 54. *A* ribbon graph isomorphism *is a graph isomorphism that preserves the ribbon structure at each vertex.*

Given a ribbon graph Γ, we can construct an orientable basepointed surface. Let each directed edge $\overrightarrow{e}$ consist of two ordered half edges e^-, e^+. This construction consists of gluing once punctured disks onto Γ so that the boundary of the disk identifies with a boundary cycle of $(\Gamma, \mathcal{O}, w)$.

Definition 55. *A* boundary cycle *for the ribbon graph* $(\Gamma, \mathcal{O}, w)$ *is a directed, reduced edge cycle,* $(\overrightarrow{e_1}, \overrightarrow{e_2}, \ldots \overrightarrow{e_{l-1}}, \overrightarrow{e_l} = \overrightarrow{e_1})$ *such that for each* i *the half-edges* e_i^+ *and* e_{i+1}^- *are incident to the same vertex, and* e_{i+1}^- *directly follows* e_i^+ *in the ordering at that vertex.*

The surface given by gluing once punctured disks onto Γ in this way is the *ribbon surface* of Γ and is denoted $|(\Gamma, \mathcal{O}, w)|$. For a proof that ribbon surfaces are orientable, see [8]. Note that Γ naturally includes into its ribbon surface.

Definition 56. *For a fixed basepointed punctured surface* (Σ, u), *a* surface marked ribbon graph *is a ribbon graph equipped with a basepoint preserving homeomorphism* $g : \Sigma \to |(\Gamma, \mathcal{O}, w)|$. *Two surface marked ribbon graphs* (g_1, Γ_1) *and* (g_2, Γ_2)

are equivalent *if there exists a ribbon graph isomorphism* $h : \Gamma_1 \to \Gamma_2$ *so that* $\bar{h} \circ g_1 \approx g_2$ *are homotopic by a basepoint preserving homotopy where* $\bar{h}$ *is the homeomorphism induced on the ribbon surfaces.*

The basepointed Teichmüller space $\mathfrak{T}(\Sigma, u)$ for a basepointed punctured surface (Σ, u) is a union of open simplices, and is contractible. The basepoint is usually not relevant and is dropped from this notation. $\mathfrak{T}(\Sigma)$ has an i simplex for each equivalence class of surface marked ribbon graphs with $i+1$-edges, no separating edges, and all vertices other than the basepoint having valence at least 3. The simplex Δ_1 corresponding to (g_1, Γ_1) has simplex Δ_2 corresponding to (g_2, Γ_2) as a face if there exists a forest collapse $h : \Gamma_1 \to \Gamma_2$ so that (g_2, Γ_2) and $(\bar{h} \circ g_1, \Gamma_2)$ are equivalent, where $\bar{h}$ is the homeomorphism induced on ribbon surfaces by h. To see how this definition of the basepointed Teichmüller space relates to more classical definitions, see [9].

Note that collapsing a forest in a ribbon graph defines a canonical ribbon structure on the resulting graph. In particular a forest collapse can be thought of as a sequence of edge collapses, so let e be an edge in Γ that is not a loop. Then Γ/e inherits a ribbon structure from Γ as follows. The set of half-edges not in e but incident to endpoints of e has a cyclic ordering given by $\mathcal{O}$. The half-edges in Γ/e incident to the unique vertex in the image of e are in one-to-one correspondence with these half-edges, and so can be given this same cyclic ordering. For all other vertices in Γ/e, the cyclic ordering is unaffected by the edge collapse. When a forest collapse is performed, the resulting ribbon structure is independent of the order in which the edge collapses are performed, and so this ribbon structure is canonical.

Another description of $\mathfrak{T}(\Sigma)$ is given by considering metrics on ribbon graphs.

Definition 57. *A metric on a finite connected graph is* normalized *if the sum of the lengths of the edges of the graph is 1. A* metric homotopy marked graph *is homotopy marked graph together with a normalized metric.*

For an open simplex Δ in $\mathfrak{T}(\Sigma)$, we can think of Δ as embedded in $\mathbb{R}^{|e|}$ where $|e|$ is the number of edges in Γ. Δ is the subset consisting of points with all positive coordinates of the subspace of $\mathbb{R}^{|e|}$ where the sum of the coordinates is one. Endowing Γ with a normalized metric, the coordinates of $\mathbb{R}^{|e|}$ are regarded as the lengths of the edges in Γ. Each point in Δ represents Γ with the normalized metric given by the coordinates. Hence moving in Δ corresponds to continuously altering the metric on Γ, as shown in Figure 10.1.

Analogously to Auter space, $\mathfrak{T}(\Sigma)$ contains a simplicial complex $\mathfrak{R}(\Sigma)$ that acts as a spine for $\mathfrak{T}(\Sigma)$. The ribbon graph complex $\mathfrak{R}(\Sigma)$ is the geometric realization of the poset of the set of open simplices of $\mathfrak{T}(\Sigma)$ where the order is given by the face relation, $\Delta_1 \geq \Delta_2$ if Δ_2 is a face of Δ_1. $\mathfrak{R}(\Sigma)$ canonically embeds into the barycentric subdivision of $\mathfrak{T}(\Sigma)$, in the same manner as the spine of Auter space embeds in Auter space as described in chapter 2.

The mapping class group $MCG_u^{\pm}(\Sigma)$, the group of homotopy classes of homeomorphisms from Σ to Σ that permute punctures and fix the basepoint, acts on $\mathfrak{T}(\Sigma)$ and $\mathfrak{R}(\Sigma)$. For $\alpha \in MCG_u^{\pm}(\Sigma)$, $\alpha \cdot (g, \Gamma)$ is given by $(g \circ \alpha, \Gamma)$.

Note that an isomorphism $r : F_n \to \pi_1(\Sigma, u)$ defines an embedding of $\mathfrak{T}(\Sigma)$ into Auter space and $\mathfrak{R}(\Sigma)$ into K, by mapping (g, Γ) to $(g_* \circ r, \Gamma)$ where the ribbon structure on Γ is discarded and g_* is the map induced on fundamental groups by g. Further, note that the inverse image of K under this embedding is independent of r. The deformation retraction from Auter space to K restricts to a deformation

retraction of the embedded image of $\mathfrak{T}(\Sigma)$ to the embedded image of $\mathfrak{R}(\Sigma)$ for any r, and so $\mathfrak{R}(\Sigma)$ is contractible.

9.2 Degree Spaces and Subcomplexes

In this section the basic definitions required for the proof of the degree theorem will be given and the overall idea of the proof will be outlined. The techniques used throughout the remainder of this chapter and in the following chapter closely follow the techniques used in [7]. Recall from chapter 2, the degree of a finite connected basepointed graph is:

Definition 58. *The* degree *of a finite connected graph* Γ *with basepoint* w *is:*

$$Deg(\Gamma) = \sum_{x \in V\Gamma,\, x \neq w} |x| - 2,$$

where the sum is taken over all non-basepoint vertices and $|x|$ *denotes the valence of* x*.*

Recall that degree generally corresponds to the amount of branching in a graph that does not occur at the basepoint. This definition extends to ribbon graphs by forgetting the ribbon structure, the degree of a ribbon graph is the degree of its underlying graph. For more discussion about degree, see chapter 2.

Definition 59. *The subspace of* $\mathfrak{T}(\Sigma)$ *consisting of open simplices corresponding to ribbon graphs of degree* i *or less is the* degree i space *of* (Σ, u)*, and is denoted* $\mathfrak{D}_{\Sigma,i}$*.*

The subcomplex of $\mathfrak{R}(\Sigma)$ *that is spanned by* 0*-simplices with underlying graphs of degree* i *or less is the* degree i subcomplex of $\mathfrak{R}(\Sigma)$*, which is denoted* $\mathfrak{J}_{\Sigma,i}$*.*

Note that for any embedding of $\mathfrak{R}(\Sigma)$ into K given by an isomorphism $r : F_n \to \pi_1(\Sigma, u)$, $\mathfrak{J}_{\Sigma,i}$ embeds into K_i, and hence has dimension no greater than i. Further, for every graph Γ so that (g, Γ) is a 0-simplex in K there exists a ribbon structure $\mathcal{O}$ so that $(g', \Gamma, \mathcal{O})$ is a 0-simplex in $\mathfrak{R}(\Sigma)$, so $dim(\mathfrak{J}_{\Sigma,i}) = dim(K_i) = i$.

For the remainder of this work, the degree i space and degree i subcomplex will be in reference to $\mathfrak{T}(\Sigma)$ and $\mathfrak{R}(\Sigma)$ and not in reference to the spine of Auter space. Further, the identity of Σ is usually clear from context, so it does not cause confusion to simplify the subscripts to $\mathfrak{D}_i$ and $\mathfrak{J}_i$. The main result of this chapter and the next is the following theorem and its immediate corollaries.

Theorem 9.2.1. *Every piecewise linear map $f_0 : D^k \to \mathfrak{T}(\Sigma)$ is homotopic to a map $f_1 : D^k \to \mathfrak{D}_k$ by a homotopy f_t during which degree decreases monotonically.*

Corollary 9.2.1. *The pair $(\mathfrak{T}(\Sigma), \mathfrak{D}_i)$ is i-connected. Since $\mathfrak{T}(\Sigma)$ is contractible, $\mathfrak{D}_i$ is $(i-1)$-connected.*

In the deformation retraction of $\mathfrak{T}(\Sigma)$ to $\mathfrak{R}(\Sigma)$, $\mathfrak{D}_i$ deformation retracts to $\mathfrak{J}_i$. The final form of this theorem will be:

Degree Theorem 2. *$\mathfrak{J}_i$ is $(i-1)$-connected and i-dimensional.*

The proof of Degree Theorem 2 will be given in the next chapter. The remainder of this chapter will be spent outlining the main ideas of the proof.

9.3 Degree Theorem Constructions

The constructions in the remainder of this chapter are taken almost identically from [7]. They are repeated here in the spirit of making this work as self-contained

as possible. Further, these constructions were originally developed for graphs while here Γ will denote a ribbon graph. The difference is largely transparent, however some technical issues do arise from the ribbon structure, and these issues will be highlighted. Since we are considering points in $\mathfrak{T}(\Sigma)$, endow Γ with a normalized metric.

9.3.1 Height Functions

Let $\mathcal{H} : \Gamma \to \mathbb{R}$ be the function measuring the distance to w using the metric on Γ. We will refer to and think of $\mathcal{H}$ as a *height function* in the spirit of morse theory and the figures throughout these chapters will also emphasize this point of view. A point $x \in \Gamma$ is called a *critical point* if there are at least two different downward paths leading from x. Again, this notation is motivated by morse theory as the homotopy type of $\mathcal{H}^{-1}([0,t])$ only changes when t passes through a critical value of $\mathcal{H}$. For an example see Figure 9.1.

For Figure 9.1, and all other figures depicting ribbon graphs in this chapter and the next, the following conventions will be used: w is the bottommost point, height denotes the distance from the basepoint, the ribbon structure is given by the numbers in the half-edges at each vertex, and dots denote vertices and critical points.

9.3.2 Cones and Canonical Splitting

Definition 60. *Let x be a critical point of Γ. If x is a vertex then the* cone *of x, C_x, is the union of x and all of the open edges incident to x that proceed downward*

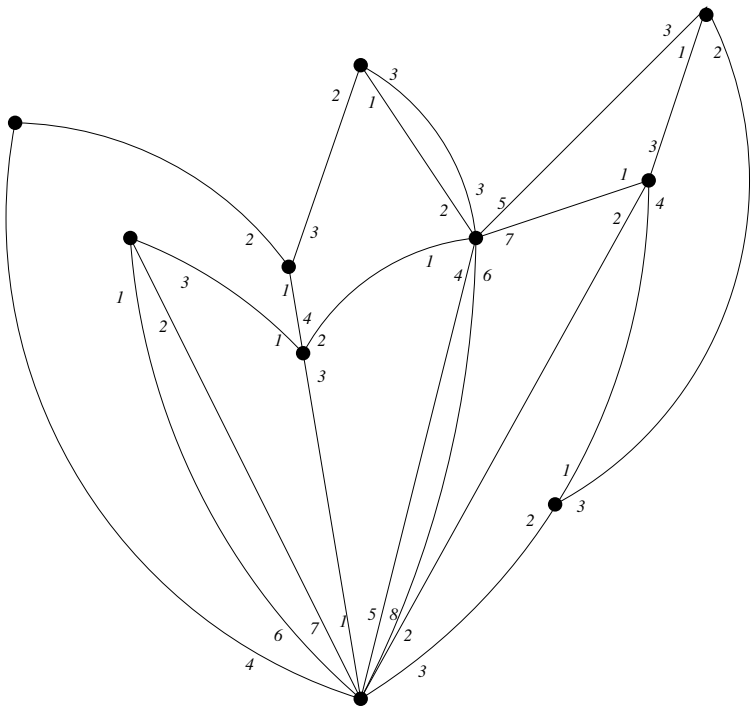

Figure 9.1: Example ribbon graph with height function

from x. If x is not a vertex, let C_x be the open edge containing x. The intersection of C_x and the ε-neighborhood of x is called the ε-cone *of x, and is denoted C_x^ε.*

Definition 61. *The* cone *of x is made of up arcs starting from x and leading downward. These arcs are called the* branches of x. *An* extended branch *of x is a downward path from x that ends at a critical point or at w and that contains no critical points in its interior.*

Note that if x is not a vertex, then x only has 2 branches. If x is a vertex, x may have more than 2 branches and may have edges incident to it that are not branches. Two distinct extended branches can meet up at a non-critical vertex. One operation that will be used in the proof of the degree theorem, called *canonical splitting*, removes these joinings of extended branches from Γ. Informally, Γ is deformed by splitting the non-critical vertex at which the two extended branches

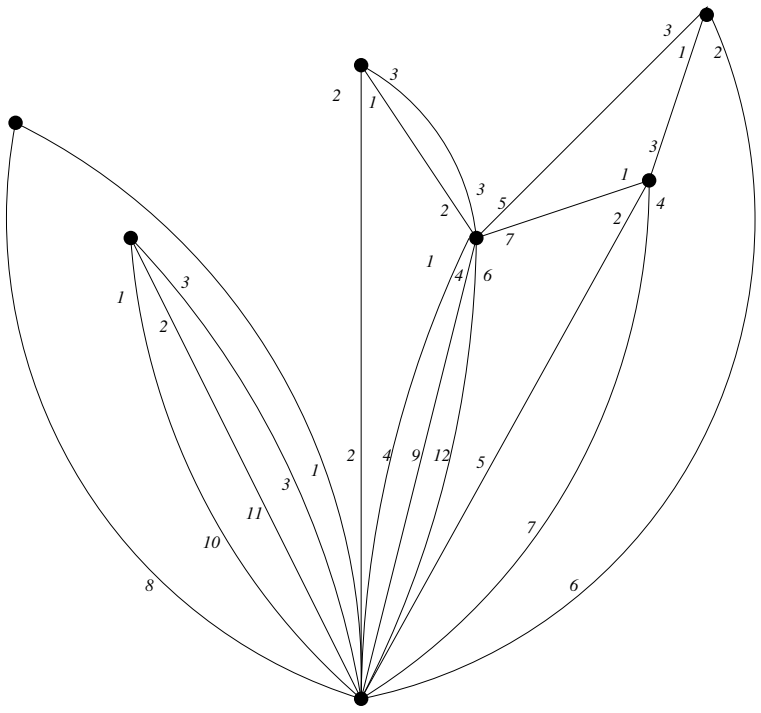

Figure 9.2: Ribbon graph resulting From performing canonical splitting on Figure 9.1

join down to the next critical point or if no critical point is reached all of the way down to the basepoint. Ordering the non-critical vertices of Γ in decreasing order of height, and splitting them in this way one-by-one, a new graph is obtained. This splitting can be accomplished by a sequence of edge collapses, if we are splitting v to v' this is the same operation as collapsing the edge connecting v to v'. Such an edge exists since any non-critical vertex in the interior of the downward path from v to v' would have split previously. The edges collapsed in performing canonical splitting form a forest. To see this note that the interior of each collapsed edge contains no critical points and there is at most one downward edge in the forest incident to each vertex in this subgraph. Since canonical splitting is a forest collapse, the ribbon structure on the resulting graph is determined.

As the name would suggest, this process of removing joinings is canonical. For

an example of the result of this process, Figure 9.2 is the graph resulting from performing canonical splitting on the graph in Figure 9.1. Canonical splitting will decrease the degree of the graph if there are extended branches that split all of the way down to the basepoint, and otherwise does not alter degree. Note that after Γ has been canonically split, Γ is the union of the extended branches of critical points and the basepoint.

9.3.3 Sliding in ε-cones

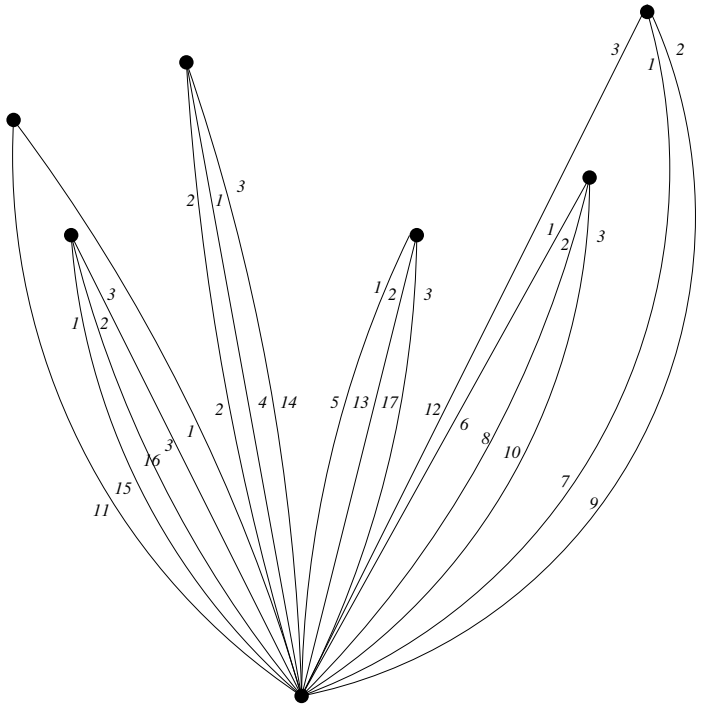

Figure 9.3: Ribbon graph that can be obtained from Figure 9.3 by sliding in ε-cones and canonical splitting

After canonically splitting Γ, we will be perturbing the attaching points of the extended branches within the ε-cones of the critical points that they were previously attached to. This perturbation can be viewed as putting the attaching

points in "general position" with respect to the critical points, though the sense in which this is related to general position theory will be made clear in the next chapter. This perturbation will yield a ribbon graph from which a local forest collapse where no edges collapse to w can recreate Γ, hence this perturbation will not increase degree. Also, the perturbation does not alter the ε-cones of the critical points. Canonically splitting the perturbed Γ will decrease degree as long as the perturbed Γ is not Γ. For an example, see Figure 9.3 which is the graph in Figure 9.2 after this perturbation and a canonical splitting. Note that the underlying graph obtained after sliding in ε-cones and canonically splitting is canonical, but the ribbon structure is not. Figure 9.3 depicts one possible resulting ribbon graph.

CHAPTER 10

PROOF OF DEGREE THEOREM

There are two main stages of the proof of Theorem 9.2.1. In the first stage, the critical points are simplified by a perturbation that changes only the metric on the ribbon graph and does not alter the combinatorial structure nor the ribbon structure of the ribbon graph, and hence does not alter degree. In the second stage, the degree is monotonically reduced while not altering the ε-cones by a combination of sliding in ε-cones and canonical splitting. Much of the discussion in this chapter is taken from [7]. Since ribbon graphs are being considered in this work, our discussion sometimes diverges from [7] in order to work with ribbon structures. The arguments that arise from dealing with ribbon graphs will be highlighted.

10.1 Codimension, Critical Planes, and Stratification

Definition 62. *For a critical point $x \in \Gamma$, if x is a vertex, the* codimension of x *is number of branches of x minus one, and if x is not a vertex the* codimension of x *is 0. The codimension of Γ is the sum of the codimensions of its critical points.*

The motivation for this terminology can be seen by considering an open simplex Δ corresponding to Γ. The set of points in this simplex with underlying graph of codimension i is a subspace of the simplex of codimension i. More specifically, if x is a critical point in the interior of an edge then small perturbations in the lengths of the edges of Γ keep the critical point in the interior of the edge, and the subspace of Δ that has a critical point in the interior of this edge has codimension 0.

If x is vertex with b branches, then these branches are the initial segments of b descending edge paths from x to w of equal length. Recall that we can view Δ as the subspace of $\mathbb{R}^{|e|}$ and note that the subspace of $\mathbb{R}^{|e|}$ made up of graphs where these b paths have equal length is defined by setting b linear equations equal to each other. These equations are linear as they are sums of lengths of edges. They are independent as each contains a variable that none of the other does, the length of the first edge the path traverses. The solution space is a linear subspace $\mathbb{R}^{|e|}$ of codimension $b-1$, and the intersection of this subspace with Δ is a linear subspace with codimension $b-1$ in Δ. See Figure 10.1 for an example 2-simplex illustrating this discussion. The codimension 1 subspaces given this way are depicted by the dotted lines.

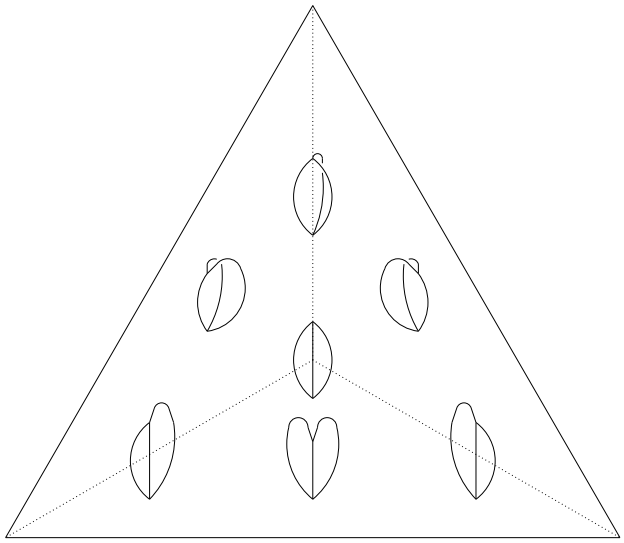

Figure 10.1: Example 2-simplex in $\mathfrak{T}(\Sigma)$ With points of codimension 1 highlighted

The goal of the first simplification is to put $f_o : D^k \to \mathfrak{T}(\Sigma)$ into general position with respect to the sets of points with codimension i or greater. More specifically, f_o will be perturbed so that the inverse image in D^k of points with codimension i or greater has codimension i or greater. The sets of codimension i defines a

stratification of $\mathfrak{T}(\Sigma)$ which is described below.

Definition 63. *A* preferred path *in* Γ *is a path from a vertex* x *to* w *that traverses each edge at most once. Let* l_γ *be the length function of a path* γ *in* Γ*. Setting the length functions of two distinct preferred paths to be equal defines a subspace of* $\mathbb{R}^{|e|}$*, such subspaces are called* critical hyperplanes*. The intersection of a set of critical hyperplanes is called a* critical plane*.*

Note that the minimum length path from x to w is a preferred path. Further, l_γ is a linear function for each γ in Γ.

The critical hyperplanes determine a stratification on $\mathbb{R}^{|e|}$ which induces a stratification on Δ. The strata are defined by lists of equalities and strict inequalities on the length functions of preferred paths, and hence are open convex polyhedra. As we move within a stratum to a codimension 1 face of Δ, an edge e in Γ collapses. Let Γ' be the graph associated to this face, so $\Gamma' = \Gamma/e$, and note that quotient map $q : \Gamma \to \Gamma'$ takes preferred paths to preferred paths. Specifically, the critical hyperplane in Δ defined by $l_{\gamma_1} = l_{\gamma_2}$ meets the face of Δ corresponding to Γ' in the critical hyperplane determined by $l_{q(\gamma_1)} = l_{q(\gamma_2)}$. Hence this is a stratification for all of $\mathfrak{T}(\Sigma)$.

The following proposition shows that within each stratum in an open simplex, the ε-cones of critical points remain unchanged.

Proposition 10.1.1. *Let* $(\Gamma, \mathcal{O}, w)$ *be a point in* Δ*, as we let this point vary within a stratum in* Δ*:*

1. *Each critical point that is a vertex of* Γ *remains a critical point throughout the stratum and the homeomorphism type of its* ε*-cone does not change.*

2. *A critical point that is not a vertex varies continuously within the edge containing it as we move in the stratum.*

3. *Codimensions of critical points are constant in the stratum, and hence the codimension of* Γ *is constant.*

4. *If* Γ *has codimension* i*, the stratum that contains* Γ *is contained in a critical plane of codimension* i*.*

Proof. (1) Let x be a vertex and critical point of Γ. Each branch in C_x^ε is the initial segment of a preferred path from x to w with minimum length. By definition, such paths are part of a collection of preferred paths from x to w all of which have the same length and whose lengths are smaller than the length of any other preferred path from x to w. As we move through the stratum this collection of minimal preferred paths from x to w is unchanged, and hence the topological type of C_x^ε must also be unchanged, and x remains a critical point.

(2) For the critical point x in the interior of e, let v_1 and v_2 be the endpoints of e. If the critical point x moved to v_i then it would create a new minimal path from v_i that begins by traversing e. Since the identity of the minimal paths cannot be altered within a stratum, x remains in the interior of e.

(3) Given by (1) and (2).

(4) Note that since the length functions of preferred paths from x to w with distinct initial segments are independent, the stratum containing Γ is contained in a hyperplane with the same codimension as Γ. □

Remark: Based on Proposition 10.1.1 critical points of regions in $\mathfrak{T}(\Sigma)$ will be used if the region is contained in a single stratum.

10.2 Stage 1: Simplifying Critical Points

Let Ψ_i be the subspace of $\mathfrak{T}(\Sigma)$ made of points with underlying graphs of codimension at least i. Note that this yields a decreasing filtration $\mathfrak{T}(\Sigma) = \Psi_0 \supset \Psi_1 \supset \ldots$. Proposition 10.1.1 implies that Ψ_i is made up of strata of that have codimension i or more in each open simplex. Observe also that Ψ_i is closed since passing to the boundary of a stratum cannot decrease codimension.

Relabel the map f_0 as f and let $(\Gamma_s, \mathcal{O}_s, w_s, g_s)$ be the image of $s \in D^k$ under f. By passing to a homotopic map that does not increase degree, assume that f is piecewise linear. In the description of the homotopies to follow, it is clear how to alter w_s and g_s and usually clear how to alter $\mathcal{O}_s$, as Γ_s is altered. In the situations where the alterations to $\mathcal{O}_s$ are not clear, they will be specified explicitly.

Proposition 10.2.1. *f can be homotoped without altering degree to a piecewise linear map so that for all i, $f^{-1}(\Psi_i)$ has codimension at least i in D^k.*

Proof. Since f is piecewise linear, there is a triangulation of D^k that linearly maps each simplex into a closed simplex of $\mathfrak{T}(\Sigma)$. By taking the barycentric subdivision of this triangulation assume that the image of each simplex in D^k meets no more than one codimension one face of the closed simplex. The images of the vertices will be homotoped within the open simplices that contain them, which preserves the combinatorial structure of Γ_s and the ribbon structure $\mathcal{O}_s$.

To begin, f is homotoped by moving the images of the vertices so that the image of each simplex in D^k has maximal dimension, either the dimension of the simplex in D^k or the dimension of $\mathfrak{T}(\Sigma)$, whichever is smaller. This is an open condition and will be preserved by all other homotopies performed on f.

Consider an open simplex Δ of $\mathfrak{T}(\Sigma)$ as a subspace of $\mathbb{R}^{|e|}$, and let σ be a simplex in D^k that maps to the closure of Δ. The goal of this proposition is to put $f(\sigma)$ into general position with respect to certain critical planes H in Δ. By general position we mean that if L is the subspace spanned by $f(\sigma)$, then either L and H span $\mathbb{R}^{|e|}$ or $L \cap H = \emptyset$. Being an open condition, general position is preserved by small perturbations on the vertices.

A collection of preferred paths is *compatible* if no two paths in the collection traverse an edge in opposite directions. We would like to put $f(\sigma)$ in general position with respect to critical planes defined by setting pairs of lengths of paths from a compatible collection equal to each other. Note that $\Delta \cap \Psi_i$ is contained by a union of critical planes of this type of codimension i. Putting f into general position with respect to such H will imply the proposition because the codimension of $f(\sigma) \cap H$ in $f(\sigma)$ for such H is at least as large as the codimension of $f(\sigma) \cap \Psi_i$ in $f(\sigma)$, and pulling back with a piecewise linear map f preserves codimension.

If $f(\sigma) \subset \Delta$ then standard general position theory completes this proposition. However, f can take the vertices of σ to faces of Δ and then these vertices can only be homotoped within these faces. For this case, consider an open face Δ' of Δ represented by Γ' and the subspace $\mathbb{R}^{|e'|}$ of $\mathbb{R}^{|e|}$ where there are $|e'|$ edges in Γ'. We will show that the codimension of H in $\mathbb{R}^{|e|}$ is the same as the codimension of $H \cap \mathbb{R}^{|e'|}$ in $\mathbb{R}^{|e'|}$. Each of the critical hyperplanes whose intersection defines H is given by an equality $l_{\lambda_1} = l_{\lambda_2}$ for two preferred paths from a compatible collection. Since the collection is compatible, the edges of Γ can be oriented in agreement with the collection. For each critical hyperplane in the intersection defining H, assign a cellular one chain $\lambda_1 \lambda_2^{-1}$. These cellular one chains span a subspace of $H_1(\Gamma, \mathbb{R})$ that has the same codimension in $H_1(\Gamma, \mathbb{R})$ as H has in $\mathbb{R}^{|e|}$. The set of paths λ_i

maps to a collection of compatible preferred paths λ'_i in Γ' via the quotient map $q : \Gamma \to \Gamma'$. Considering the critical hyperplanes in $\mathbb{R}^{|e'|}$ whose intersection defines the critical plane $H \cap \mathbb{R}^{|e'|}$, these planes are defined by the analogous equalities in the $l_{\lambda'_i}$'s. The cellular one chains associated to these critical hyperplanes similarly determine a subspace of $H_1(\Gamma', \mathbb{R})$ with codimension equal to the codimension of $H \cap \mathbb{R}^{|e'|}$ in $\mathbb{R}^{|e'|}$. Since q is a homotopy equivalence, $q_* : H_1(\Gamma, \mathbb{R}) \to H_1(\Gamma', \mathbb{R})$ is an isomorphism, and note that this isomorphism takes the subspace generated by the one chains associated to the critical hyperplanes defining H to those associated to the critical hyperplanes defining $H \cap \mathbb{R}^{|e'|}$, showing that the codimension of H in $\mathbb{R}^{|e|}$ is the same as the codimension of $H \cap \mathbb{R}^{|e'|}$ in $\mathbb{R}^{|e'|}$.

The proof now proceeds by induction, in particular $f(\sigma)$ is contained in set of faces of Δ, $\Delta_1, \Delta_2, \ldots \Delta_p = \Delta$, where Δ_{i-1} is a face of Δ_i. Let V_i be the subspace of $\mathbb{R}^{|e|}$ spanned by Δ_i, H_i be $H \cap V_i$, σ_i be the face of σ that maps into the closure of Δ_i, and L_i be the subspace of $\mathbb{R}^{|e|}$ spanned by $f(\sigma_i)$. Take the statement "L_i is in general position with respect to H_i" as the induction hypothesis. By the comments above, L_1 can be put into general position with respect to H_1 by perturbing the images of the vertices in σ_1 by standard general position theory, completing the base case. Assuming the induction hypothesis and noting that by the argument above the codimension of H_i in V_i is constant over i, we see that L_i is in general position with respect to H_{i+1}. The images vertices of $\sigma_{i+1} \setminus \sigma_i$ are in V_{i+1} and hence standard general position theory gives us that these images can be perturbed to put L_{i+1} in general position with respect to H_{i+1}, completing the induction step. Such perturbations are performed for each critical plane H and each simplex σ in D^k, and since general position is an open condition each perturbation does not disrupt the established general position for the other simplices in D^k. $\square$

Note that after establishing the general position in Proposition 10.2.1, all subsequent homotopies will not alter ε-cones and hence will preserve the general position.

10.3 Stage 2: Canonical Splitting and Complexity Reduction

In this section, the homotopy of f is completed. This part of the homotopy proceeds by induction, assume as the induction hypothesis that the degree of all points in a neighborhood of $f^{-1}(\Psi_{j+1})$ have been reduced to k. The homotopy reducing the degree of all points in a neighborhood of $f^{-1}(\Psi_j)$ to k is built in three steps. First a preparatory canonical splitting is performed on these points so that afterword all attaching points are either contained in ε-cones of critical points or at that basepoint. Secondly the *complexity*, the of number of downward paths that begin and end at critical points, of points in this neighborhood is reduced by sliding in ε-cones. After the complexity has been reduced, canonical splitting reduces degree to at most k which completes Theorem 9.2.1, and Degree Theorem 2

10.3.1 Preparatory Canonical Splitting

The filtration Ψ_i of $\mathfrak{T}(\Sigma)$ pulls back to a filtration on D^k, $\varrho_i = f^{-1}(\Psi_{k-i})$, $\varrho_0 \subset \varrho_1 \subset \ldots \subset \varrho_k = D^k$. Note that ϱ_i is a subpolyhedron of D^k and by Proposition 10.2.1 $dim(\varrho_i) \leq i$. Assume as an induction hypothesis, that the degree of Γ_s in a neighborhood of ϱ_{i-1} is at most k.

Take S to be a connected component of $\varrho_i \setminus \varrho_{i-1}$, and further remove from S a small neighborhood of ϱ_{i-1}. This makes S a compact polyhedron and means that for s in a neighborhood of ∂S, Γ_s has degree at most k. As s varies over S the ε-cones are unchanged since the codimension of the critical points of Γ_s are constant.

Definition 64. *A downward path from one critical point to another is called a* connecting path*, and note that connecting paths may contain critical points in their interiors. The number of connecting paths of $f(s)$ will be called the* complexity of Γ_s *and be denoted c_s. The number of connecting paths that contain no critical points in their interior for a point $f(s)$ will be denoted e_s.*

For example, for Γ shown in Figure 9.1, $c_s = 17$ and $e_s = 9$.

Let J be the set of maximal complexity in S, and note that J is a closed subpolyhedral complex since the only way that complexity can decrease is for a connecting path to move off of a critical point. Let J_o be a connected component of J, and note that since complexity does not change as s varies over J_o, the extended branches also do not change, and canonical splitting can be performed.

However, this homotopy needs to be defined in a neighborhood of J_o which can contain points both inside and outside of S. For points inside S, since ε-cones are constant in S the only possible difference from points inside of J_o is that attaching points of some extended branchings may have shifted off of critical points and into the ε-cones of those critical points. We define the homotopy Γ_{st} to fix the position of such attaching points as t varies and shift the point of attachment as s varies from J_o to points in a neighborhood of J_o and in $S \setminus J_o$. In other words, the canonical spitting ignores these extended branches.

For points in a neighborhood of J_o that are not in S, critical points can bifurcate. For a critical point x, let $H_{x,s}$ be its convex hull in Γ_s for s in a neighborhood of J_o but not in S. Let $H^{\varepsilon}_{x,s}$ be the union of $H_{x,s}$ and all points below and within in ε of $H_{x,s}$. For such Γ_s, extended branches may attach within $H^{\varepsilon}_{x,s}$ instead of at x. The attaching points of these extended branches are fixed as t varies but moved along to their new position as s varies.

In both the case where $s \in S$ and $s \notin S$, the ribbon graph structure on Γ_{st} is given by the ribbon graph structure in Γ_{s0} since Γ_{st} is given by performing edge collapses in Γ_{s0}. Near the boundary of the neighborhood of J_o, this homotopy is damped down so that it is defined on D^k but supported only on this neighborhood of J_o. For simplicity, the result of this homotopy is renamed Γ_s.

10.3.2 Complexity Reduction

After the canonical splitting, the attaching points of all extended branches in a neighborhood N_o of J_o in S are either at the basepoint or in the ε-cone of a critical point. We will now define a homotopy that shifts attaching points of extended branches off of critical points and into the ε-cone of the critical point. This shift must agree with the ribbon structure on Γ_s, so we now examine which points in the ε-cone of x the attaching point of an extended branch can shift to. In this restriction, we diverge from the methods of [7].

In the definitions below, x is a critical point and vertex and all upward edges that attach in C^{ε}_x attach at x. However, these definitions can be extended to the case where some upward edges attach in $C^{\varepsilon}_x \setminus x$ by moving all of these attaching points to x.

Definition 65. *Let $e_1, e_2, \ldots e_p$ be the half edges incident to x written in cyclic order. For an upward half edge e_j the* downward directions *of e_j are the downward half edges nearest to e_j in the order that appear before and after e_j. The downward half edge nearest to e_j in the order that appears before e_j is the* negative *downward direction and the downward half edge nearest to e_j in the order that appears after e_j is the* positive *downward direction. The* attaching interval *of e_j, denoted I_j, is the intersection of the ε-cone of x and the union of the downward directions of e_j.*

Note that the attaching interval of such an e_j is isometric to the open interval $(-\varepsilon, \varepsilon)$ in $\mathbb{R}$.

Definition 66. *A subset of the upward half-edges incident to x is an* attaching set *of x if the half edges are successive in the cyclic order at x and the half edges immediately before and after this subset are downward edges.*

Note that if e_i and e_j are in the same attaching set, they have the same attaching interval, positive downward direction, and negative downward direction. In Figure 10.2, the attaching sets of the critical point shown are $\{2, 3\}$, $\{5, 6\}$, and $\{8\}$. Also, the negative downward direction and positive downward direction of 2 and 3 are 1 and 4. For 5 and 6 these downward directions are 4 and 7, and for 8 these directions are 7 and 1.

Definition 67. *For an attaching set of x made up of the half edges $e_1, e_2, \ldots e_q$ incident to x, consider the direct product $\prod_{i=1}^{q} I_i$, and note that this is isometric to the direct product of q copies of $(-\varepsilon, \varepsilon)$. The* attaching space *of this attaching set is the subspace of $\prod_{i=1}^{q} I_i$ that maps to the subspace of the direct product of q copies of $(-\varepsilon, \varepsilon)$ defined by the equations $y_1 \leq y_2 \leq \ldots \leq y_q$ where y_i is the coordinate of the i-th copy of $(-\varepsilon, \varepsilon)$. The direct product of the attaching spaces of the attaching sets of x will be called the* attaching space of x.

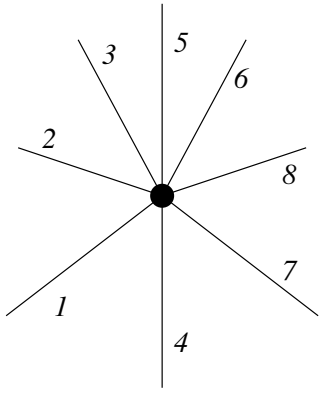

Figure 10.2: Critical point in a ribbon graph

Note that the attaching space of x does not change as s varies in N_o. Hence $\mathbf{C}$, the direct product of the attaching spaces of the critical points of Γ, is constant on N_o and is called the *attaching space of* J_o. Also note that the dimension of $\mathbf{C}$ is equal to e_s for graphs in J_o.

Let α_j be an extended branch in Γ_s for $s \in J_o$, and suppose that this branch attaches at critical point x. α_j can be regarded as a map $\alpha_j : N_o \to I$, where I is the attaching interval of the upward half edge incident to x that α_j traverses, and $\alpha_j(s)$ is the point of attachment of α_j in Γ_s. Note that α_j cannot attach in $C_x^\varepsilon \setminus I$, as the ribbon structure would not be defined. Take the product of these maps $\alpha : N_o \to \prod_j I_j$, where the target product contains a copy of I for each extended branch attaching in C_x^ε for all critical points x. Note that this target space contains $\mathbf{C}$, and that in order to define a ribbon graph $\alpha(s)$ must be in $\mathbf{C}$. Inside of $\mathbf{C}$, let p correspond to the critical point in each summand, and note that $\alpha(s) = p$ for $s \in J_o$. Also note that since complexity is lower in $N_o \setminus J_o$ than in J_o, $\alpha(s) \neq p$ for $s \in N_o \setminus J_o$.

Reducing complexity in J_o corresponds to homotoping α away from p, as com-

plexity decreases when extended branches move off of critical points. Making α disjoint from p means that after the homotopy not every extended branch in Γ_s attaches at a critical point, and thus the complexity of Γ_s will have been reduced for all s in J_o.

We perturb α into general position with respect to p and note that the codimension of $\alpha^{-1}(p)$ in N_o is at least as large as the codimension of p in $\mathbf{C}$. Since $dim(\mathbf{C}) = e_s$, $codim(p) = e_s$. Hence if $dim(N_o) = i < e_s$ the resulting image of α is disjoint from p. Note that general position theory is not necessary to homotope α disjoint from p for points in N_o where e_s is greater than c the number of attaching sets of all vertices in Γ_s. To see this, note that we can define a homotopy on α that perturbs each point toward the point $p' = (p'_1, p'_2, \ldots, p'_c)$ on the boundary of $\mathbf{C}$, where $p'_i = (\varepsilon, -\varepsilon, -\varepsilon, \ldots, -\varepsilon)$ is a point on the boundary of the attaching space of the i-th attaching set. This breaks down when each of the c summands has dimension 1, and hence is only relevant when $e_s > c$. This does not yield a theorem that is stronger than Theorem 9.2.1 because for any fixed n and k there exists a ribbon graph for which $e_s = c$ where F_n is the rank of the fundamental group of Σ. Figure 10.3 depicts such a ribbon graph for $n \leq k$ and Figure 10.4 depicts such graphs for $n > k$. In Figure 10.4, there are $k + 2$ edges connecting the two vertices, $n - k - 1$ loops at the basepoint. Also in Figure 10.4, no ribbon structure is given because any ribbon structure is sufficient. Graphs like those in Figure 10.4 can be drawn in any surface, so Theorem 9.2.1 is the strongest result that can be obtained by this line of investigation for $n > k$. For $n \leq k$, if graphs like those shown in Figure 10.3 can be drawn in Σ, Theorem 9.2.1 is the strongest result. For other surfaces, Theorem 9.2.1 may not be the strongest possible result.

While the homotopy has been defined for a neighborhood N_o of J_o in S, it

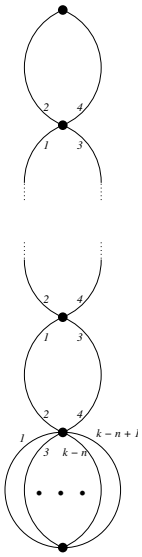

Figure 10.3: For $n \leq k$, ribbon graph with $e_s = c$

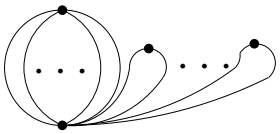

Figure 10.4: For $n > k$, ribbon graph with $e_s = c$

has not yet been defined for points in a neighborhood of J_o in $D^k \setminus S$. For such points, critical points in Γ_s may have bifurcated, and again we construct H_x^ε for such cases. Let $r_x : C_x^\varepsilon \to H_x^\varepsilon$ be the map that takes the endpoints of C_x^ε to the corresponding endpoints of H_x^ε, x to the barycenter of H_x^ε, the paths between x and the endpoints of C_x^ε to the geodesics in H_x^ε between its barycenter and the various endpoints. Precomposing our homotopy with r_x yields a homotopy of Γ_s for s in a neighborhood of J_o in $D^k \setminus S$. Note however that $r_x(\alpha_j)$ need not equal α_j in Γ_s, so we must complete a preparatory homotopy that first moves α_j to $r_x(\alpha_j)$, moving each attaching point at a rate proportional to its distance from $r_x(\alpha_j)$. Near the boundary of this neighborhood of J_o, the homotopy damps down so that outside of the neighborhood of J_o the homotopy is trivial. Hence this homotopy is defined

on all of D^k but only supported in a neighborhood of J_o. After performing the homotopy, the complexity of points in J_o has been reduced. This is done for each connected component of J, and eventually the complexity of all points in S is less than or equal to i.

10.3.3 Degree Reduction

Now that the complexity of all points in S has been reduced, we will see in this subsection that canonical splitting reduces degree below k completing Degree Theorem 2.

Let $SDeg(\Gamma)$ the *split degree* of Γ be the degree the graph obtained by applying canonical splitting to Γ. Further for x a critical point and vertex, let a_x be the number of extended branches that attach at x, and b_x be the number of downward directions of x. Note that $SDeg(\Gamma) = \sum_x (a_x + b_x - 2)$ because the critical vertices of Γ are the only non-basepoint vertices left after canonical splitting. Further,

$$SDeg(\Gamma) = \sum_x (a_x + b_x - 2) \leq \sum_x a_x + \sum_{codim(x)\geq 1} (b_x - 1) = e_s + codim(\Gamma),$$

where $\sum_{codim(x)\geq 1} (b_x - 1) = codim(\Gamma)$ because the number of downward paths from a critical point is unchanged by canonical splitting. On S we have $e_s \leq i$, and $codim(\Gamma) = k - i$ by Proposition 10.2.1. Hence, $SDeg(\Gamma) \leq k$ and all that remains is to pass from split degree to degree.

Consider a refinement of the triangulation on S where split degree is constant over the interior of each simplex Δ. Such a triangulation is possible since split degree only changes when the attaching points of extended branches move off of

critical points. Further, note that points in a neighborhood of Δ not in ϱ_i must have split degree less than or equal to the split degree of Δ.

Assume as an induction hypothesis that the degree has been reduced to be less than or equal to k in a neighborhood of the boundary of Δ, by choosing and reducing lower dimensional simplices first. The discrepancy between degree and split degree occurs when there are extended branches ending at the basepoint with an interior vertex. These branches can be split all the way to the basepoint via canonical splitting. Further, the collection of such extended branches remains unchanged as s varies through Δ as split degree is constant over Δ, so canonical splitting can be applied to Δ. For points in a neighborhood of Δ that are in $S \setminus \Delta$, the attaching points of some extended branches may shift off of critical points. In the homotopy, such attaching points are fixed and only the extended branches that are split in Δ are split in the homotopy.

For points in a neighborhood of Δ that are not in S, recall that critical points may bifurcate and attaching points of extended branches may shift off of critical points. Again, such attaching points are fixed and only those extended branches that split in Δ are split during the homotopy. These attaching points are split down to the convex hulls of the critical points. Points in a neighborhood of Δ that are in $S \setminus \Delta$ either already have degree at most k or have split degree less than or equal to the split degree of Δ and have the same set of branches split as Δ, so these points now have degree at most k. As we approach the boundary of the neighborhood of Δ this homotopy damps down so that the homotopy is constant outside of this neighborhood of Δ. This completes the induction step and sets degree Γ_s to k for all s in a neighborhood of Δ. The result of this induction is that we have reduced the degree of Γ_s to k for s in a neighborhood of S which

completes the original induction argument, and the proofs of Theorem 9.2.1 and Degree Theorem 2.

APPENDIX A

CALCULATIONS IN $SAUT(F_2)$

Via the use of coset enumeration in MAGMA, we investigate a subgroup of $SAut(F_2)$ as described in Proposition 7.2.1. We will use the a presentation of $SAut(F_2)$ given by Appel and Ribnere in [1]. The generators of this presentation are $u = E_{a_1a_2}$, $v = E_{\bar{a}_2\bar{a}_1}$, $x = E_{a_2\bar{a}_1}E_{\bar{a}_2\bar{a}_1}$, and $y = E_{a_1\bar{a}_2}E_{\bar{a}_1\bar{a}_2}$.

Theorem A.0.1. *$SAut(F_2)$ is generated by x, y, u, and v, and presented by the following relations:*

1. $uxu^{-1} = xy$
2. $uyu^{-1} = y$
3. $vxv^{-1} = x$
4. $vxv^{-1} = xy$
5. $vu^{-1}vuv^{-1}u = 1$
6. $(vu^{-1}v)^4 = xy^{-1}x^{-1}y$

Note that this presentation is written opposite of our convention for multiplication of automorphisms. Specifically, $uv = u \circ v$ means apply v first, then apply u. Consider the subgroup K of $SAut(F_2)$ generated by $E_{a_1a_2} = u$, $E_{a_2a_1} = x^{-1}v$, and $E^2_{\bar{a}_2\bar{a}_1} = v^2$. The result of using MAGMA to perform coset enumeration on K as a subgroup of $SAut(F_2)$ is a coset table, a table where the rows correspond to the cosets of K and the columns correspond to the generators and inverses of $SAut(F_2)$. The ij-th entry of this table is the coset resulting from left multiplying the i-th coset by j-th generator. The CosetEnumerationProcess command with strategy = HLT, and workspace = 10^8, yields the following coset table:

	x	y	u	v	x^{-1}	y^{-1}	u^{-1}	v^{-1}
K	xK	yK	K	xK	xK	yK	K	xK
xK	K	xyK	xyK	K	K	xyK	xyK	K
yK	xyK	K	yK	yK	xyK	K	yK	yK
xyK	yK	xK	xK	xyK	yK	xK	xK	xyK

Recall from chapter 7, there are 3 lifts of $p(E_{\bar{a}_1 a_2})$. Specifically, $E_{\bar{a}_1 a_2} = u^{-1}y^{-1}$, $E_{a_1\bar{a}_2}E_{a_2 a_1}E_{\bar{a}_1 a_2}E_{\bar{a}_1 a_2}E_{\bar{a}_1 a_2} = (u^{-1}y^{-1})^3 x^{-1}vu^{-1}$, and $E_{a_2\bar{a}_1}E_{a_1 a_2}E_{\bar{a}_2 a_1}E_{\bar{a}_2 a_1}E_{\bar{a}_1 a_2} = u^{-1}y^{-1}v^{-2}uv^{-1}x$. By the coset table above:

1. $u^{-1}y^{-1}K = yK$,
2. $(u^{-1}y^{-1})^3 x^{-1}vu^{-1}K = yK$, and
3. $u^{-1}y^{-1}v^{-2}uv^{-1}xK = yK$.

Hence, K does not contain any lifts of $p(E_{\bar{a}_1 a_2})$.

Additionally, in Proposition 7.3.2 we claim that $E^2_{\bar{a}_2\bar{a}_1}E_{a_1\bar{a}_2}E_{a_2 a_1} = x^{-1}vu^{-1}v^2$ is not contained in the subgroup J generated by $E_{a_1 a_2} = u$, $E_{a_2 a_1} = x^{-1}v$, $E^{-2}_{\bar{a}_2\bar{a}_1}E_{a_1 a_2}E^2_{\bar{a}_2\bar{a}_1} = v^2uv^{-2}$. The CosetEnumerationProcess command considering J as a subgroup of K with strategy = HLT, and workspace = 10^8, yields the following coset table:

	u	$x^{-1}v$	v^2	u^{-1}	$v^{-1}x$	v^{-2}
J	J	J	v^2J	J	J	$v^{-2}J$
v^2J	v^2J	v^2J	$v^{-2}J$	v^2J	v^2J	J
$v^{-2}J$	$v^{-2}J$	$v^{-2}J$	J	$v^{-2}J$	$v^{-2}J$	v^2J

By this coset table $x^{-1}vu^{-1}v^2J = v^2J$ and $E^2_{\bar{a}_2\bar{a}_1}E_{a_1\bar{a}_2}E_{a_2a_1}$ is not contained in J.

BIBLIOGRAPHY

[1] D. Appel and E. Ribnere *On the Index of Congruence Subgroups of Aut(F_n)*, pre-print, arXiv:0804.2578v1.

[2] H. Armstrong, B. Forrest, and K. Vogtmann *A Presentation for Aut(F_n)*, J. Group Theory, **11** (2008), 267-276.

[3] M. Bestvina and M. Handel *Train Tracks and Automorphisms of Free Groups*, Annals of Mathematics, 2nd. Ser., Vol. 135, No. 1. (Jan. 1992), pp. 1-51.

[4] K. S. Brown, *Presentation for Groups Acting on Simply-Connected Complexes*, Journal of Pure and Applied Algebra **32** (1984), 1-10.

[5] M. Culler and K. Vogtmann *Moduli of Graphs and Automorphisms of Free Groups*, Invent. Math. 84 (1986), no. 1, 91–119.

[6] S. M. Gersten, *A presentation for the special automorphism group of a free group*, J. Pure Appl. Algebra **33**(3) (1984), 269–279.

[7] A. Hatcher and K. Vogtmann, *Cerf Theory for Graphs*, J. London Math. Soc. (2) **58**(3) (1998), 633–655.

[8] M. Horak, *Mapping Class Subgroups of the Outer Automorphism Groups of Free Groups*, Ph.D. Thesis, Cornell University, 2003.

[9] R. C. Penner, *The Poincaré Dual of the Weil-Petersson Kähler Two-Form*, Perspectives in Mathematical Physics, Conf. Proc. Lecture Notes Math. Phys., III, Internat. Press, Cambridge, MA, 1994, pp. 229-249.